ADVANCING SUSTAINABLE MARITIME DEVELOPMENT THROUGH OPERATIONS RESEARCH TECHNIQUES

WANG WEI

PhD

The Hong Kong Polytechnic University

2024

The Hong Kong Polytechnic University

Department of Logistics and Maritime Studies

Advancing Sustainable Maritime Development Through Operations Research Techniques

WANG Wei

A thesis submitted in partial fulfillment of the
requirements for the degree of
Doctor of Philosophy

February 2024

CERTIFICATE OF ORIGINALITY

I hereby declare that this thesis is my own work and that, to the best of my knowledge and belief, it reproduces no material previously published or written, nor material that has been accepted for the award of any other degree or diploma, except where due acknowledgement has been made in the text.

_____(Signed)

WANG Wei (Name of student)

Abstract

Maritime transportation, an indispensable driver of global trade and economic development, faces the imperative of sustainable development amid its pivotal role in international commerce. Despite delivering over 80% of global trade by volume in 2022, the maritime industry grapples with environmental and operational efficiency challenges, necessitating a paradigm shift towards sustainable practices. This thesis delves into three pivotal strategies within the realm of sustainable development: autonomous ships, cleaner energy generation subsidies, and foul cleaning.

Autonomous ships significantly boost maritime sustainability by improving fuel efficiency, cutting emissions, enhancing safety, streamlining operations, optimizing fleet management, reducing human error, and potentially integrating renewable energy sources. Cleaner energy adoption in maritime operations yields benefits such as emissions reduction, regulatory compliance, improved air quality, cost savings, innovation stimulation, and enhanced competitiveness. Foul cleaning, essential for maintaining hull performance and fuel efficiency, reduces drag, lowers fuel consumption, enhances maritime efficiency, and minimizes environmental impact. This practice also extends vessel lifespan, decreases maintenance needs, prevents invasive species spread, and ensures environmental regulation compliance, playing a crucial role in responsible maritime management.

With a dedicated focus on each strategy, we employ operations research techniques to intricately optimize maritime operations. The objective is to navigate towards sustainability with a keen emphasis on cost-effectiveness, striving for a harmonious coexistence between economic benefits and environmental well-being. Through an in-depth exploration of these strategies and the application of advanced operations research methodologies, this study aims not only to reduce the environmental footprint of maritime operations but also to underscore the maximization of benefits at minimized costs.

This thesis makes both theoretical and practical contributions to maritime sustainability. In terms of theoretical advancement, we initially develop models to accurately quantify the problem, enabling the derivation of clear solutions. Subsequently, we refine existing solution methods to expedite computation, rendering large-scale instances solvable within reasonable timeframes. On the practical front, the quantitative analysis yields valuable managerial insights, offering guidance for practical implementation.

Keywords: Maritime Transportation, Sustainable Development, Autonomous Ships, Cleaner Energy Generation Subsidies, Foul Cleaning, Operations Research Techniques, Environmental Efficiency, Economic Viability

Acknowledgements

First and foremost, I extend my deepest appreciation to my supervisor Prof. Shuaian (Hans) WANG, whose generous support has played a pivotal role in both my academic and personal development. I consider myself incredibly fortunate to have such an inspiring supervisor. He has consistently been a source of inspiration, offering guidance even during moments when I struggled to formulate research ideas. His ability to distil information from news and videos into relevant research topics has been particularly admirable. I would like to emphasize Prof. Wang's prompt responsiveness, always addressing my inquiries within a day. This efficiency has significantly expedited the progression of my research outcomes. Beyond academic support, he has generously facilitated opportunities for me to expand my horizons, including conference attendance and participation in attachment programs. Participating in conferences has not only stimulated new ideas for my research but has also allowed me to establish meaningful connections within my research community. Moreover, the experiences gained from visiting other universities have exposed me to diverse research methodologies and deepened my understanding of cultural nuances, contributing to the refinement of my academic and personal objectives.

Next, I extend my heartfelt gratitude to Silong Zhang, a fellow student sharing the same academic office. His profound knowledge in mathematics and expertise in C++ help a lot with my research. Encountering mathematical challenges during my studies was a common occurrence, and he became my go-to person for assistance. His willingness to patiently explain complex theories, coupled with insightful recommendations for relevant books and papers, significantly contributed to my comprehension of challenging concepts. He also played a pivotal role in introducing me to the realm of C++. He emphasized the efficiency of C++ in solving linear and integer problems promptly, motivating me to delve deeper into the language for enhanced problem-solving capabilities.

Then I would express my heartful thanks to my parents, cousin sisters, and friends for their unwavering support and companionship throughout my doctoral journey. My parents have provided me with the freedom to pursue my passions and have consistently shown warmth and concern. Whenever I come home, I can feel their deep love. My cousin sisters have been more than just family but true friends. In moments of joy or hardship, they have been my immediate

point of contact. Their patient listening and willingness to help have been invaluable. Living close to my elder sister during my doctoral studies has allowed us to spend quality time together. We frequently explored new culinary delights and interesting places, creating cherished memories. For my friends, I would like to extend my gratitude for their companionship and assistance. Their presence has been a source of comfort, making the doctoral journey more enjoyable and rewarding.

Finally, I would like to express my heartfelt gratitude to all the staff members at PolyU for their invaluable assistance during my doctoral studies.

Table of Contents

List of Figures

List of Tables

Chapter 1: Introduction

1.1 BACKGROUND

Maritime transportation holds a crucial position in facilitating worldwide trade and promoting economic development, serving as the backbone of international commerce. As per the United Nations Conference on Trade and Development (UNCTAD), maritime shipping is accountable for transporting more than 80% of global trade by volume in 2022. The advantages of maritime transportation are evident in its cost-effectiveness for transporting bulk goods over long distances. The large cargo capacities of vessels enable economies of scale, reducing transportation costs per unit of goods compared to alternative modes. However, the maritime industry is not without challenges. Environmental concerns, including air and water pollution, oil spills, and habitat disturbance, raise questions about the sustainability of current practices. Safety and security risks, such as accidents, piracy, and illegal activities, present ongoing challenges. The industry's reliance on fossil fuels contributes to greenhouse gas emissions, necessitating a transition to more sustainable energy sources.

The maritime industry has been continuously exploring various strategies to address these challenges while preserving and enhancing its operational advantages, aiming to achieve a state of sustainable development. Sustainable maritime development refers to the pursuit of a balanced and harmonious coexistence between maritime economic activities, ecological preservation, and social well-being. Within the framework of sustainable development, efforts are directed towards seeking and adopting methods and technologies that are economically feasible, ecologically sound, and socially conscientious.

This research delves into three methods aimed at achieving sustainable goals: employing autonomous ships, providing subsidies for cleaner energy generation, and implementing foul cleaning. Autonomous ships, characterized by their ability to operate without direct human involvement, utilize advanced technologies, sensors, and artificial intelligence systems to perform tasks traditionally handled by human crews. These vessels contribute significantly to maritime sustainability through enhanced fuel

efficiency, emissions reduction, improved safety measures, and heightened operational efficiency. This technological innovation minimizes the environmental footprint of shipping activities while improving overall operational effectiveness and seafarer wellness. Subsidizing cleaner energy generation incentivizes the adoption of greener energy sources, such as marine diesel oil and electricity, and exhaust gas cleaning equipment in maritime activities. By transitioning towards cleaner energy sources, the maritime industry can significantly reduce its harmful gas emissions, contributing to global sustainability goals. Foul cleaning, involving the removal of fouling organisms from ship hulls, is crucial for maintaining hydrodynamic performance and fuel efficiency. This practice not only reduces drag, leading to lower fuel consumption and operational costs, but also enhances overall maritime efficiency and contributes to environmental sustainability by minimizing the release of harmful anti-fouling chemicals. Foul cleaning additionally extends vessel lifespan, reduces maintenance requirements, prevents the spread of invasive species, and supports compliance with environmental regulations, making it a pivotal aspect of responsible and efficient maritime management.

While these methods offer numerous benefits, they entail additional costs. Therefore, this study aims to maximize efficiency with the least cost through Operations Research methods.

1.2 THESIS OUTLINE

The remainder of this thesis are organized as follows. Chapter 2 review related literature. In Chapter 3, a model is formulated to explore the impact of autonomous ships on maritime operation considering uncertainties. Given the NP-hard nature of the problem, both approximation and exact solution methods are proposed. Additional acceleration strategies are employed to enhance the problem-solving process. Moving on to Chapter 4, a bi-level mixed integer programming model is introduced to optimize a subsidy plan designed to mitigate harmful emissions. The intricacy of the problem arises from the interdependence within the bi-level structure, necessitating the transformation of the model into an equivalent single-level formulation and the use of linearization techniques for effective resolution. Similarly, Chapter 5 presents a bi-level model that concurrently optimizes cleaning equipment deployment by service providers in the upper level and cleaning decisions by shipping companies in the lower

level. To simplify the problem, the bi-level model is converted into a single-level formulation utilizing the big-M method. Finally, Chapter 6 serves as the conclusion, summarizing the thesis's key findings and raising potential avenues for future research.

Chapter 2: Literature review

There are numerous pathways to achieve shipping sustainability, such as the adoption of alternative fuels, implementation of energy-efficient technologies, and optimization of shipping operation. These methods can operate independently or synergistically, complementing one another to enhance overall sustainability efforts. This thesis primarily focuses on three key methods: employing autonomous ships, providing subsidies for cleaner energy generation, and implementing foul cleaning. As a result, the literature review is centered around these three approaches.

2.1 AUTONOMOUS SHIPS

The first research investigates the impacts of autonomous ships. Over the last decade, there has been a notable surge in interest surrounding autonomous vessels. Liu et al. (2016), Schiaretti et al. (2017a, 2017b), Zolich et al. (2018), and Gu et al. (2021) provide comprehensive reviews of autonomous vessels. Besides, there are also many research projects, such as Maritime Unmanned Navigation through Intelligence in Networks (MUNIN[1]), ReVolt[2], and Yara Birkeland[3]. However, since autonomous vessels are in their early stage, these academic research and research projects mainly focus on economic feasibility (Kretschmann et al., 2017; Ghaderi, 2019; Ziajka-Poznańska and Montewka, 2021), safety issues (Wang et al., 2018; Fan et al., 2020; Goerlandt, 2020; Chang, 2021; de Vos, 2021), laws and regulations (Authority, 2017; Cheng and Ouyang, 2021; Zhu and Xing, 2021), vessel design (Jin, Zhang, and Liu, 2018; Makhsoos et al., 2018), etc. There is a dearth of literature that specifically focuses on the operational optimization of autonomous ships, especially when considering the intricate interplay of multiple decisions at both the strategic and the

[1] MUNIN is a collaborative research project, co-funded by the European Commissions under its Seventh Framework Programme. The goal is to verify the concept for autonomous ships and develop technology for unmanned and autonomous vessels.
[2] ReVolt is a concept ship built and tested by classification society DNV GL. This ship is autonomous and fully battery powered. The ship is assumed to be powered by a 3000 kWh battery and sails at an average speed of 6 knots.
[3] Yara Birkeland is the world's first fully electric and autonomous container vessel built by Yara and Kongsberg. It was put into commercial operation in Porsgrunn in the spring of 2022.

operational levels, such as ship routing, fleet sizing, fleet deployment, and demand fulfillment.

To address this gap, this research delves into the operational challenges faced by shipping companies contemplating the integration of autonomous ships. The problem is formulated as variant of vehicle routing problem (VRP), which refers to the problems involving routing, fleet sizing, fleet deployment, and demand fulfillment. This decades-old classic research question dates back to Dantzig and Ramser (1959), which found the shortest route that passes through all end points. The most studied variant is the classical capacitated VRP (CVRP) where all vehicles are identical and have the same capacity. The first important variant is called heterogeneous fleet VRP (HFVRP) where multiple types of vehicles are used to fulfill distribution. Branchini, Armentano, and Morabito (2015) solve the integrated problem of ship routing, scheduling, and fleet deployment to serve all contractual voyages and at the same time serve profitable spot voyages if there is room to spare. They consider different ship types that are restricted by the cargoes that can be loaded, the ports that can be visited, and also client contracts. Fadda et al. (2023) design an optimal maritime network considering draft limits, where ship draft is determined by ship type and cargo weight. A second variant is the multi-trip VRP (MTVRP) that extends the classical VRP by allowing vehicles to execute more than one trip during a predetermined service time (Taillard, Laporte, and Gendreau, 1996). In the MTVRP, the limited carrying capacity reduces the number of customers served on a trip and thus some vehicles need to perform several trips during a workday. When solving the last-mile delivery problem, Şahin and Yaman (2022) exploit service route design for a fleet under time window constraints, considering the compatibility of different vehicle types to different routes in a heterogeneous fleet and multi-trip service for each vehicle. A third variant relaxes constraints that each customer must be visited exactly once. This variant is called split delivery VRP (SDVRP). Archetti, Savelsbergh, and Speranza (2008) prove that demand split is most beneficial when demand mean is slightly above half the vehicle capacity and the variance is relatively small. Yoshizaki (2009) solves a distribution problem of a major Brazilian retail group, determining the best route, distribution schedule, vehicle allocation, and delivery amount for each customer. A fourth variant considers uncertainties in the problem, which leads to a version called stochastic VRP (SVRP). Gutierrez et al. (2018) determine schedule and routes for a group of

technicians to execute repairing tasks within given time windows. Travel time and service time in the research are assumed to be stochastic and identically gamma and log-normal distributed, respectively.

A single variant usually cannot fully capture the essence of real-life transportation problems, so that multiple variants are often combined. Coelho et al. (2016) and Despaux and Basterrech (2016) investigate good delivery from a central depot to geographically scattered customers, simultaneously considering heterogeneous fleet and multi-trips. Wang, Kinable, and Van Woensel (2020) solve a fuel replenishment problem where tanker trucks carry different types of petrol to refuel petrol stations. Stations that have larger demand than the vehicle capacity may need to be refueled several times. Yang (2022) directs a fleet of identical capacitated vehicles to complete package deliveries. To fully utilize the vehicle mobility during working hours, vehicles are allowed to perform multiple trips.

The VRP problem is strongly NP-hard, and various solution techniques have been proposed, including metaheuristics and exact algorithms. Here are the most commonly used metaheuristics: iterated local search (Coelho et al., 2016; Accorsi, and Vigo, 2021), memetic algorithms (Mendoza et al., 2010; Gutierrez et al., 2018), large neighborhood search (François et al., 2016; Wang, Kinable, and Van Woensel, 2020). Exact algorithms include column generation (Jin, Liu, and Eksioglu, 2008; Paradiso et al., 2020), branch-and-cut (Archetti, Bianchessi, and Speranza, 2014; Bianchessi, and Irnich, 2019), branch-and-price (Şahin, and Yaman, 2022; Torres, Gendreau, and Rei, 2022), and branch-and-price-and-cut (Desaulniers, 2010; Poggi, and Uchoa, 2014; Pecin et al., 2017; Gschwind, Bianchessi, and Irnich, 2019; Pessoa et al.,2020).

2.2 SUBSIDIES FOR CLEANER ENERGY GENERATION

The second study shifts its focus towards the adoption of alternative fuels and sustainable shipping practices. The improvement of environmental awareness has made scrubber and shore power hot topics. There are many studies discussing their economic feasibility as well as environmental benefits. Panasiuk and Turkina (2015) uses cash flow model to compare the profitability of scrubber and low sulphur fuel under IMO emission requirements. It mentions that investment in scrubber is an effective choice. Lindstad, Rehn, and Eskeland (2017) explores the ways to abide by IMO Sulphur regulations. It recommends scrubber for ships with the highest fuel

consumption, diesel for smaller vessels when price of crude oil is lower than $50 per barrel, and desulphurised HFO for less fuel-guzzling ships. Andersson, Jeong, and Jang (2020) compares two different types of wet scrubber via life cycle assessment technique. Closed loop scrubber is preferred when environment is the priority while open loop scrubber is better if payback time is more important. Zis, Cullinane, and Ricci (2022) investigates economic and environmental impacts under a series of sulfur reduction regulations. The quantitative analysis confirms that scrubber is more suitable when fuel price is high and ships sail longer time. Similar research can be found on shore power. Yu, Voß, and Tang (2019) studies whether it is beneficial to install shore-side electricity equipment and the best time to invest. A case study of Dalian port indicates that ships with higher visiting frequency are more suitable to be equipped with shore power devices; It is more cost-effective for domestic and near-sea shipping to use alternatives to shore power, such as LNG or scrubber; Larger ships are more environmentally beneficial. Lathwal, Vaishnav, and Morgan (2021) investigates cost and emission reduction when ships switch from high-sulfur fuel to shore-based electricity. Results show that using shore power could reduce 88% PM2.5, 39% SO2, 85% NO (x), $73 million for high-sulfur fuel, and $370 million for low-sulfur fuel, but increases CO2 emissions by 17%. Stolz et al. (2021) also quantifies emission reduction when ships switch from fossil fuels to shore side electricity. It uses Automatic Identification System (AIS) and Monitoring, Reporting and Verification (MRV) scheme data to estimate the auxiliary power demand and emissions at berth for ports in the European Economic Area (EEA) and the United Kingdom (UK). Sun et al. (2022) studies the emission reduction effect of ship berthing using shore power. It finds that using shore power requires specific conditions and only a few cities are suitable for using shore power.

The environment protection of scrubber and shore power has been widely recognized, but the investment for these technologies is expensive (Acciaro et al. 2014; Yin et al. 2022). To promote the use of scrubber and shore power and to protect environment, the government usually adopts subsidies. Wang, Qi, and Laporte (2022) designs shore power price and subsidy to use shore power. The research finds that pricing and subsidy are effective ways to drive shore power usage, while setting an unreasonably high shore power utilization rate has a negative impact on total profit of ports. Song et al. (2022) uses game theory to discuss the influences of government

subsidy plan on the usage of shore power between two shipping companies. Compared to other interventions (e.g., environmental taxes and requirements to improve marine oil specifications), subsidies are proved to be better for satisfying multiple participants. Wang, Jiao, and Peng (2023) also uses game theory to investigate the impact of government subsidy on shipping company's choice of powering method under different power structures. By comparing the profits with and without government subsidy, it concludes that whether governmental subsidy will have impact on shipping company's choice of shore power or lower sulfur fuel oil depends on carbon price. Lu and Huang (2021) optimizes the deployment of shore power considering government subsidy. It finds the optimal conditions for different subsidy strategies.

When considering subsidy, usually multiple parties are involved. Bi-level optimization is a common method for solving multi-party problem (Liu, Wilson, and Luo 2016; Cai et al. 2020). Feng, Pang, and Lodewijks (2015) develops a bi-level model to solve hinterland barge transport planning problem involving both terminal and barge operators. The lower level minimizes turn-around time for barge agent, while the upper level makes sure more requests could be handled at terminal. Chang et al. (2019) redesigns maintenance grouping strategies considering interactions between original equipment manufacturer (OEM) and service providers. The upper-level OEM simultaneously minimizes total maintenance service cost, downtime profit loss, and customer dissatisfaction, while all service providers at lower level could select their service components and corresponding service time. Yang, Luo, and Shi (2020) solves problems caused by uncoordinated subsidies for rail transportation of containers in different regions. It develops a bi-level model with network planner in the upper level to decide the optimal subsidy and shippers in the lower level to optimize cost.

2.3 FOUL CLEANING

Further analysis was conducted to identify the causes of unsustainability, revealing that fouling not only reduces vessel efficiency but also imposes negative impacts on the environment and ecosystems. Consequently, the third study explores measures for fouling removal. Research on ship fouling has garnered attention for more than 40 years. Evans (1981) summarized important findings on the biology of fouling algae, which have proven valuable for the advancement of antifouling

technologies. Additionally, Callow (1990) provided comprehensive information on various solution methods to combat fouling, encompassing both traditional and modern approaches. These methods include the use of antifouling paints, copper, organotin, tributyltin, and fluoropolymers of silicones. Since ship fouling has significant negative impacts on vessel performance and environmental sustainability, there are many studies aimed at quantifying these effects. Townsin (2003) elucidated ship speed and power performance penalties caused by slime, shell, and weed separately. Monty et al. (2016) assessed the ship drag penalty caused by light calcareous tubeworm fouling. Demirel et al. (2017) analyzed the effect of barnacle fouling on ship resistance and powering. Coraddu et al. (2019) developed a data-driven digital twin of the ship using information collected from on board sensors to predict the speed losses caused by fouling. Demirel et al. (2019) investigated frictional resistance coefficients under a range of representative coating and fouling conditions. Farkas et al. (2020) and Song et al. (2020) carried out simulations to investigate the impacts of different fouling conditions on different ship types. The results show that the influence can vary significantly amongst different ship types. Farkas, Degiuli, and Martić (2020) divided biofouling into soft and hard fouling, where the latter has greater impact. To quantify the influence of hard fouling, they developed a roughness function through simulation to measure the resistance caused by fouling. Erol, Cansoy, and Aybar (2020) used data collected from all automation systems instead of noon reports to improve the measurement accuracy of the relationship between fouling and ship performance. In addition to quantifying the impacts, there are also studies investigating the effectiveness of different cleaning methods. Tribou and Swain (2015) assessed the effectiveness of grooming with a five-headed rotating brush to clean biofouling. Experiments show that the effectiveness of the tool depends on the fouling condition. Oliveira and Granhag (2020) investigated the maximum wall shear stress and jet stagnation pressure that do not cause damage or wear to antifouling coatings. Zhong et al. (2022) conducted experiments to verify the feasibility of ultrasonic-enhanced submerged cavitation jets in the cleaning of ship fouling. Given the importance of determining the optimal timing for cleaning methods, several researchers have contributed to this field. Farkas, Degiuli, and Martić (2021a) address the challenge of rapidly predicting propeller performance with fouled surfaces when making maintenance schedules. Farkas, Degiuli, and Martić (2021b) also developed a model

to rapidly predict the effect of biofouling on a ship's hydrodynamic performance during maintenance schedule optimization. Georgiev and Garbatov (2021) performed conceptual multipurpose vessel design and fleet sizing considering hull form, resistance and propulsion, and other dimensions crucial to vessel design. Degiuli et al. (2023) optimized the maintenance schedule for containerships considering fouling penalties under real environmental conditions. While the literature has extensively examined the effects of fouling, cleaning methods, and cleaning schedules, there remains a gap in comprehensive research that simultaneously addresses the optimal locations and timing for ship cleaning, as well as the appropriate number of devices to be deployed.

The problem in this study is formulated as a bi-level model. Bi-level optimization involves two levels of optimization interacting with each other (typically involving a leader in the upper level and a follower in the lower level), where the decisions made in the upper level affect the solution of the lower level and the solution of the lower level in turn influences the objective function or constraints of the upper level. Bi-level programming problems arise in many different applications, such as transportation management (Chang, and Mackett, 2006; Stoilova, and Stoilov, 2022), facility location (Gang et al., 2015; Abareshi, and Zaferanieh, 2019; Casas-Ramírez et al., 2020), and logistics optimization (Camacho-Vallejo et al., 2015; Lee et al., 2015). In the shipping industry, many problems are also formulated as bi-level models. Qi, Wang, and Psaraftis (2021) conducted a comprehensive review of bi-level optimization models for air emission management in the shipping industry. Wang et al. (2020) proposed a novel bi-level model aimed at optimizing the energy consumption of a fleet. The upper-level optimization model determined the loading and speed of each ship, taking into account relevant factors such as port information, the navigational environment, time requirements, and ship parameters. The lower-level problem was formulated as a dynamic model, optimizing energy consumption by considering varied environmental factors and port information. Zhu, Shen, and Shi (2023) developed a bi-level multi-objective model for the allocation of carbon emission allowances. In this model, the government acted as the leader initiating the allocation process, while shipping companies served as followers and made decisions regarding carbon emissions within their operations. Yang, Pan, and Wang (2018) reconstructed liner shipping networks considering the impacts of two new railway

systems built under the one belt one road policy. The upper-level liner shipping company decided shipping routes while the lower-level shippers decided delivery amounts along the routes. Zhuge et al. (2021) investigated the effects of different policies regarding vessel speed reduction in a port area. Four policies were compared and two bi-level subsidy design models were formulated. Ziar et al. (2023) designed an environmentally friendly intermodal transportation network. The government in the upper level decided the location of dry ports, while the freight carriers in the lower-level optimized shipping routes. Wang, Wang, and Zhen (2023) optimized the subsidy plan for scrubbers and shore power through a bi-level mixed-integer programming model, where the government at the upper level minimized the total subsidy amount while ship operators at the lower level chose the most cost-effective energy supply. Cai et al. (2020) used a bi-level mixed-integer programming model to determine the type and amount of search and rescue equipment allocated to activated stations. Although bi-level models have been widely used in maritime operation optimization involving two decision parties, no research has been conducted to explore ship fouling cleaning when cleaning service providers and ships interact with each other.

Chapter 3: The impact of autonomous ships in regional waterways[4]

This chapter examines the influence of autonomous ships on the operations of shipping companies. It addresses a scenario wherein a container liner shipping company manages a fleet of diverse vessels, incorporating both traditional manned ships and autonomous vessels, operating within national waterways. A model is developed to calculate the total profits under optimal ship routing, fleet sizing, fleet deployment, and demand fulfillment before and after introducing autonomous ships. Given the NP-hard nature of the problem, two solution methods, i.e., sample average approximation and a two-phase Benders-based branch-and-cut algorithm, are proposed to solve the problem with acceleration strategies, including column generation and variable fixing. The performance of several solution techniques is tested through numerical experiments using real-world data. Besides, sensitivity analyses are conducted to further discuss the influence of key factors and derive constructive managerial insights for shipping companies.

3.1 INTRODUCTION

Technological innovation continues to improve people's lives and solve problems in all walks of life. In marine shipping, researchers and practitioners have become increasingly interested in autonomous vessels over the past two decades (Gu et al., 2021). Autonomous ships, also known as unmanned or crewless vessels, operate without onboard human intervention for their navigation and control. These ships rely on advanced technologies such as artificial intelligence, sensors, cameras, radar, and satellite communication systems to perceive their surroundings, make decisions, and navigate safely. In 2021, over 1,000[5] maritime autonomous surface ships were in

[4] Wang, W., Wang, S., Zhen, L., & Laporte, G. (2023). The impact of autonomous ships in regional waterways. Transportation Research Part B: Methodological, 178, 102851.
[5] https://maritime-executive.com/editorials/autonomous-vessels-are-becoming-a-commercial-reality.

operation worldwide, managed by more than 53 organizations. By 2023, the market size had reached $7.34[6] billion, with predictions indicating continuous growth in the years to come.

The popularity of autonomous vessels can be explained by multiple reasons. First, the removal of the deckhouse and accommodation structure provides additional space for cargoes, which means that autonomous ships can carry more cargoes than conventional ships of the same size. Second, reduced light displacement (LDT) and air resistance save fuel consumption, thus making autonomous ships more environmentally friendly. Third, autonomous ships are immune to the rising labor costs and the lack of workforce in the industry. Last, autonomous vessels could avoid some human errors, making them safer than conventional ones (Yang et al., 2023).

Although autonomous ships have multiple advantages, regulatory constraints and high manufacturing costs are impeding their application. To overcome regulatory challenges, one could experiment with autonomous ships on national waterways which are more flexible than transnational waterways. For the cost problem, one could redesign the shipping network according to the characteristics of autonomous ships, which may make the shipping network more profitable than with the exclusive use of conventional ships. For example, due to larger capacity, an autonomous ship may visit more ports on a route, hence reducing the number of ships deployed, and ultimately saving operational costs. Therefore, we develop a model to investigate the impact of autonomous ships on shipping company operations.

We consider a problem setting where a container liner shipping company operates a fleet of heterogeneous vessels that consist of both conventional manned ships and autonomous ships on national waterways. Containers are transported along a feeder network with a hub port and many feeder ports, as shown in Figure 3-1. Due to waterway restrictions on feeder ports, such as draft and width constraints, the types of ships that can travel on this network are limited (Lin et al., 2020). Autonomous ships, as mentioned above, have the advantage of carrying more cargoes while consuming less energy compared to conventional ships of the same size. In this context, "size" refers to the physical dimensions of the vessels, i.e., draft and beam. As

[6] https://www.thebusinessresearchcompany.com/report/autonomous-ships-global-market-report.

a result, ports inaccessible to conventional ships may allow access by autonomous ships of the same size.

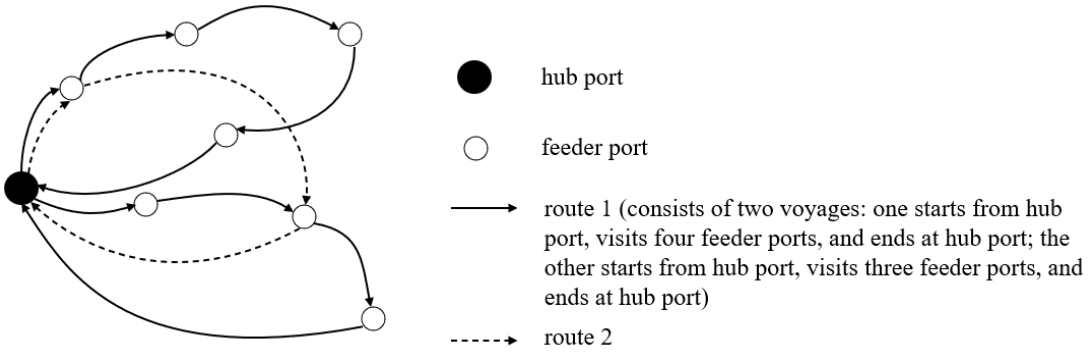

Figure 3-1: An example of feeder network

Within this problem setting, we calculate the total profits before and after introducing autonomous ships, which involves freight revenue, handling costs, ship operating costs (including labor costs, maintenance costs, insurance, etc.), bunkering costs, and capital costs. Cargo handling profits are determined by the volume of cargoes carried on the network. Ship operating and bunkering costs are influenced by routing and vessel assignment decisions. Capital costs are closely related to the number and the types of ships deployed.

Therefore, we develop in this research a model to simultaneously optimize ship routing, fleet sizing, fleet deployment, and demand fulfillment. We consider heterogenous fleet that contains both autonomous and conventional ships. Besides, due to waterway restrictions, small vessels may be used for cargo delivery, which has two main implications. First, cargo transportation demand at a port may be greater than ship capacity, causing demand to be split and fulfilled by multiple voyages. Second, ships are allowed to sail multiple voyages during the fixed service frequency, which is the time interval between two consecutive visits to the same feeder port. For example, a ship spends three days traveling on the voyage Shanghai–Nanjing–Shanghai, but the service frequency is seven days, which means that there are four days until the next visit to Nanjing. To better utilize the shipping capacity, this ship could make another voyage of at most four days. In addition, shipping demand is not stable. Therefore, we include demand uncertainty in the model. This model extends classic vehicle routing problem (VRP) model by combining a heterogeneous fleet (i.e., conventional and autonomous ships of different sizes), multi-trips (i.e., a ship can sail multiple voyages),

split deliveries (i.e., the transportation demand of a port can be satisfied by multiple voyages), and demand uncertainty. Hereafter we refer to it as HFMTSDU-VRP. Since this research involves both strategic decisions that are unlikely to be altered in a short term and operational decisions that are adjusted frequently in response to varying demand, the problem is formulated as a two-stage stochastic programming model. In the first stage, optimal routes, fleet composition, and fleet assignment are determined without realization of demand uncertainty. In the second stage, when demand realization is known, the liner company needs to determine the delivery pattern, i.e., the volume of cargo loaded onto each ship at each port of call. The objective is to maximize the expected service profit. To solve this challenging problem, we propose a sample average approximation (SAA) heuristic and an exact algorithm based on Benders decomposition (BD) and branch-and-cut (BC). Hereafter we refer to the exact algorithm as two-phase Benders-based branch-and-cut (TPBBC) algorithm. Besides, acceleration technologies, such as column generation and variable fixing, are proposed to strengthen the formulation and reduce computational times. Numerical experiments based on real-world data are conducted to evaluate the performance of different solution methods, explore the impact of introducing autonomous ships, discuss the influences of key factors, and derive valuable managerial insights for liner shipping companies.

3.2 RESEARCH GAP

Based on the literature review in Chapter 2, we find that although there is a substantial body of literature exploring single and multiple variants of the VRP, it is worth noting that existing studies typically consider the combination of only two to three variants at most. To the best of our knowledge, there is a research gap in the literature regarding articles that simultaneously investigate capacity, heterogeneous fleet, multi-trip, split delivery, and stochastic VRP. Moreover, the integration of multiple variants in the problem formulation leads to increased computational complexity, posing significant challenges for solving the problem. As a result, novel approaches and algorithmic adaptations are necessary to effectively address the intricacies introduced by these combined variants and achieve efficient solutions.

Given the existing literature, the main contribution of this study is fourfold. First, this study originally explores whether autonomous ships will replace conventional

ones in national waterways by simultaneously optimizing ship routing, fleet sizing, fleet deployment, and demand fulfillment. Second, different from previous models on VRP, the model proposed in this study simultaneously considers heterogeneous fleet, multi-trip, split delivery, and uncertainty, which has rarely been explored in the existing literature. Third, to solve the problem, we propose two types of solution algorithms. One is based on the commonly used SAA technique and the other is an innovative TPBBC algorithm. In the first phase of TPBBC, we relax integer constraints to add as many Benders cuts as possible, which accelerates convergence and computation speed. In the second phase, we restore integer constraints and take advantage of BC and generic callback to speed up the computation process. The TPBBC can be formulated in two ways, which are compared to find the best fit for the problem. Besides, several acceleration strategies are used, including column generation and variable fixing. Fourth, numerical experiments based on real-life data are conducted to yield managerial insights for shipping companies.

3.3 PROBLEM DESCRIPTION AND FORMULATION

We consider a feeder network with a hub port p_0 and a set P of feeder ports, where $P = \{1, \dots, |P|\}$. The ships visiting these ports are heterogenous with a type set V. Due to the port restrictions, such as draft and berth constraints, a feeder port $p \in P$ can only be visited by vessels of certain types, denoted by V_p. While hub port p_0 is accessible to all ship types in V, because the hub port usually has deep water and abundant berths of different sizes. Ships sailing on a feeder network usually follow a fixed service frequency α (days), i.e., the time interval between two consecutive visits to the same feeder port. A closed-loop visiting sequence (hereinafter referred to as sequence), denoted by s, is a voyage from hub port to feeder ports and then back to hub port. It is port set made up of a hub port p_0 and a set $P_s \subseteq P$ of feeder ports and is ordered as a vector according to the visiting sequence, such as $(p_0, p_1, p_2, p_3, p_0)$, where $p_1, p_2, p_3 \in P_s$. Since only ships from certain types, namely V_p, are allowed to visit feeder port p, ship types that are allowed to travel on sequence s are denoted by $V_s = \cap_{p \in P_s} V_p$. The time taken to complete the sequence s, denoted by T_s, is the sum of sailing time and dwell time at ports. The sailing time is determined by the sailing distance and the speed. Since the speed of ships is assumed to be a constant, ship sailing time only depends on the travel distance. The dwell time, denoted by t_p, $\forall p \in$

$\{p_0\} \cup P$, is the time a ship spends at port securing the vessel, discharging or loading cargo, and other activities. The set of feasible sequences, denoted by S, consists of those sequences that satisfy $V_s \neq \emptyset$ and $T_s \leq \alpha$. Since some sequences may have a short duration, a ship is allowed to travel several sequences as long as the total duration does not exceed a predetermined service frequency. Therefore, we define route r as a set of sequences, which contains one or more than one sequence. All the sequences belonging to route $r \in R$ constitute a sequence set $S_r \subseteq S$. The set of ship types that are allowed to be deployed on route r is denoted by $V_r = \cap_{s \in S_r} V_s$. The duration of route r is represented by $T_r = \sum_{s \in S_r} T_s$. A route r is feasible only if $V_r \neq \emptyset$ and $T_r \leq \alpha$. All the feasible routes form a set R. An example in Figure 3-2 is used to illustrate port, sequence, and route. The solid and hollow circles represent hub port and feeder ports respectively. The capital letters are the names of the ports. The letters in parentheses indicate the ship types that are allowed to visit the corresponding port. Ships from three types, namely $\{a, b, c\}$, are available. The numbers on the arcs are the required travelling time (days). The dwell time at each port is assumed to be 0. All sequences of this example are shown in Table 3-1. *Ship type* represents the types of ships that are allowed to travel on this sequence. *Duration* is the amount of time to complete this sequence. *Feasible* indicates whether this sequence is feasible or not considering ship type and duration constraints. Table 3-1 indicates that eight out of 15 sequences are infeasible because no available ship can get access to all ports in each of the eight sequences. Table 3-2 shows all the feasible routes. As we mentioned, a route consists of one or more than one sequence. Thus, in addition to all the feasible single sequences, the combination of feasible sequences can also be regarded as a feasible route if the sequences in this combination can be visited by the same ship and the duration of this combination does not exceed the preset duration requirement (seven days). *Ship type* in Table 3-2 represents the ship types that can get access to all ports on the sequences making up this route. *Duration* is the amount of time it takes for a ship to complete this route. If the route is made up of several sequences, the duration is the sum of the sequences' durations. In total, we have 11 feasible routes.

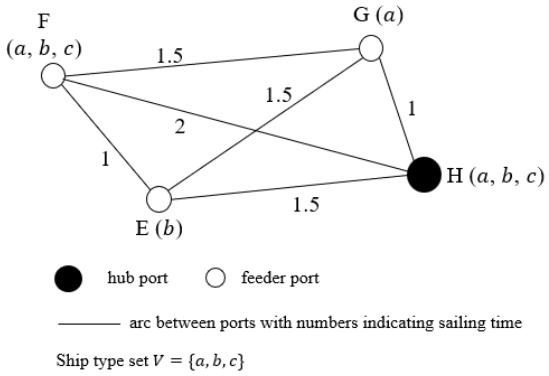

Figure 3-2: An example to illustrate port, sequence, and route

Table 3-1: All sequences of the example feeder network

No.	Sequence	Ship type	Duration	Feasible when $\alpha = 7$
1	(H, E, H)	b	3	Yes
2	(H, E, G, H)	-	4	No
3	(H, E, G, F, H)	-	6.5	No
4	(H, E, F, H)	b	4.5	Yes
5	(H, E, F, G, H)	-	5	No
6	(H, G, H)	a	2	Yes
7	(H, G, E, H)	-	4	No
8	(H, G, E, F, H)	-	5.5	No
9	(H, G, F, H)	a	4.5	Yes
10	(H, G, F, E, H)	-	5	No
11	(H, F, H)	a, b, c	4	Yes
12	(H, F, G, H)	a	4.5	Yes
13	(H, F, G, E, H)	-	6.5	No
14	(H, F, E, H)	b	4.5	Yes
15	(H, F, E, G, H)	-	5.5	No

Table 3-2: All feasible routes of the example feeder network

No.	Route	Ship type	Duration
1	(H, E, H)	b	3
2	(H, E, F, H)	b	4.5
3	(H, G, H)	a	2
4	(H, G, F, H)	a	4.5
5	(H, F, H)	a, b, c	4
6	(H, F, G, H)	a	4.5
7	(H, F, E, H)	b	4.5
8	(H, E, H, F, H)	b	7
9	(H, G, H, G, F, H)	a	6.5
10	(H, G, H, F, H)	a	6
11	(H, G, H, F, G, H)	a	6.5

The feasible routes are regarded as input when formulating the two-stage stochastic programming model. Given the ship routes R, the voyage cost C_r^v (USD/α days), which includes bunkering cost, labor cost, maintenance cost, etc., of using ship type $v \in V_r$ to serve route $r \in R$ during service frequency α can be obtained. Each ship of type v is associated with an average purchasing cost C_v (USD/α days). When the demand[7] of feeder port p is fulfilled, a handling cost of C_p^h (USD/TEU) will be incurred as well as the freight revenue F_p (USD/TEU). Since demand is uncertain, we use scenarios to represent varying demand, which may lead to different results for demand fulfillment under different scenarios. Hence, we optimize ship routing, fleet sizing, and fleet deployment in the first stage when demand is uncertain. In the second stage, with the realization of demand, the shipping company determines the flow of cargoes. The objective is to maximize expected total profits, i.e., expected revenue minus expected costs. The first stage objective function comprises voyage cost and purchase cost during the service frequency. The second stage objective function equals expected revenue minus handling costs associated with the cargo flow. This research makes three assumptions. First, a sequence can only be contained in one route. Second, a route can be assigned at most one ship and can be travelled at most once during

[7] We only consider export demand of each feeder port, i.e., the demand that needs to be loaded at a feeder port and unloaded or transshipped at a hub port. If other types of demand need to be considered, the model can be easily extended.

service frequency. Third, the number of ships that can be deployed is unlimited. Notations used to formulate the two-stage stochastic programming model are listed in Table 3-3.

Table 3-3: Notations used to formulate the model

Sets	
P	Set of feeder ports to be visited, indexed by p, $p = 1, \dots, \|P\|$
S	Set of sequences, indexed by s, $s \in S$
R	Set of possible shipping routes, indexed by r, $r \in R$
V	Set of ship types, indexed by v, $v \in V$
R_s	Set of shipping routes that contain sequence s
S_p	Set of sequences that contain port p
P_s	Set of feeder ports that are visited by sequence s
V_r	Set of ship types that can be deployed on route r
Ω	Set of demand scenarios, indexed by ω, $\omega \in \Omega$
Parameters	
C_r^v	Voyage cost (USD) of using ship type v to serve route r during the predetermined time interval, including bunkering cost, labor cost, maintenance cost, etc.
C^v	Average purchasing cost (USD) of a ship from type v during service frequency
C_p^h	Handling cost (USD/TEU) of demand at feeder port p, including loading and unloading costs
F_p	Unit revenue of demand fulfillment of feeder port p (USD/TEU)
Q^v	Capacity (TEUs) of ship type v
T_s	Duration (hour) of a sequence s
D^p	Random demand (TEUs) of feeder port p
$D^p(\omega)$	Demand (TEUs) of feeder port p under scenario ω
α	Service frequency
Decision variables	
x_r^v	Binary variable, equal to 1 if a ship of type v is deployed on route r, and 0 otherwise
$y_s^p(\omega)$	The amount of demand of feeder port p that is served by sequence s under scenario ω

The model is given as follows:

$$\text{[RM] maximize } \mathbb{E}_\Omega\left[Q\left(x, D(\omega)\right)\right] - \sum_{r\in R}\sum_{v\in V_r}(C_r^v + C^v)x_r^v \tag{3-1}$$

subject to

$$\sum_{r\in R_s}\sum_{v\in V_r} x_r^v \le 1, \forall s \in S \tag{3-2}$$

$x_r^v \in \{0,1\}, \forall v \in V_r, r \in R$ (3-3)

where the recourse function $Q(x, D(\omega))$ denotes the optimal value of the second stage problem under scenario ω:

$Q(x, D(\omega)) = \text{maximize} \sum_{s \in S} \sum_{p \in P_s} (F_p - C_p^h) y_s^p(\omega)$ (3-4)

subject to

$\sum_{s \in S_p} y_s^p(\omega) \leq D^p(\omega), \forall p \in P$ (3-5)

$\sum_{p \in P_s} y_s^p(\omega) \leq \sum_{r \in R_s} \sum_{v \in V_r} Q^v x_r^v, \forall s \in S$ (3-6)

$y_s^p(\omega) \geq 0, \forall p \in P_s, s \in S.$ (3-7)

The objective function (3-1) maximizes the expected total profit, which is the expected second-stage profit associated with cargo flow, minus the first-stage voyage cost and the average purchasing cost. Constraints (3-2) require that a maximum of one ship of the permitted type can be deployed on each route and each sequence can belong to at most one route. Constraints (3-3) define the domains of first-stage decision variables. Equation (3-4) is the second-stage objective function for one demand scenario. Constraints (3-5) state that the fulfilled demand at each feeder port cannot exceed its total demand. Constraints (3-6) illustrate that the total demand served by a sequence cannot exceed the capacity of the ship deployed to travel along this sequence. Constraints (3-7) are the non-negativity conditions of second-stage decision variables.

3.4 SOLUTION METHOD

In this section, we first introduce label setting algorithm that is used to generate feasible routes. We then apply both SAA and TPBBC to solve the two-stage stochastic programming model. To speed up the computation process, we apply some acceleration techniques.

3.4.1 Generating Feasible Routes

In maritime transportation, the number of ports is limited, especially in a feeder network. Additionally, shipping routes often follow specific directions within a feeder network. For example, the ports along the Yangtze River are almost distributed along a line. Ships usually sail in one direction and then return in the opposite direction. A ship is unlikely to change direction back and forth halfway. It is therefore easy to enumerate all feasible routes as input.

To generate the route set, we use a label setting algorithm to first generate a feasible sequence set and then combine sequences of the same vessel type under the service frequency constraints. The detailed procedure for the label setting algorithm is provided in Appendix A.

3.4.2 Sample Average Approximation

To SAA is often used to solve stochastic programming model by using empirical distribution obtained from samples to approximate the true distribution of the problem. The sample Ω' comprises $|\Omega'|$ scenarios of demand with the same probability of occurrence $\frac{1}{|\Omega'|}$. The SAA formation of the model [RM] is given as follows:

$$\text{[SAA] maximize } \frac{1}{|\Omega'|}\left(\sum_{\omega\in\Omega'}\sum_{s\in S}\sum_{p\in P_s}\left(F_p - C_p^h\right)y_s^p(\omega)\right) - \sum_{r\in R}\sum_{v\in V_r}(C_r^v + C^v)x_r^v \quad (3\text{-}8)$$

subject to (3-2) and (3-3)

$$\sum_{s\in S_p} y_s^p(\omega) \le D^p(\omega),\ \forall p \in P,\ \omega \in \Omega' \quad (3\text{-}9)$$

$$\sum_{p\in P_s} y_s^p(\omega) \le \sum_{r\in R_s}\sum_{v\in V_r} Q^v x_r^v,\ \forall s \in S,\ \omega \in \Omega' \quad (3\text{-}10)$$

$$y_s^p(\omega) \ge 0,\ \forall p \in P_s,\ s \in S,\ \omega \in \Omega'. \quad (3\text{-}11)$$

The sample size $|\Omega'|$ determines the solution quality of SAA. The larger is the sample size, the better is the solution quality, but the longer is the calculation time. To determine the appropriate sample size that could balance between solution quality and computation tractability, we propose Algorithm 1, which calculates confidence intervals (CIs) for lower bound, upper bound, and optimality gap under given sample size. CI is a range of estimates for an unknown parameter. The τ in Algorithm 1 is the level of significance and $1-\tau$ is the confidence level. $|M|$ is the number of samples for CI.

Algorithm 1 Estimate $(1-\tau)$-CI for lower bound, upper bound, and optimality gap under given sample size $|\Omega'|$

1. Generate a set of scenarios Ω'.
2. Solve the SAA with Ω' and obtain the optimal first-stage solution x^*.
3. **for** $m = 1, \dots, M$ **do**
4. Generate a set of new independent scenarios Ω'', $|\Omega''| = |\Omega'|$.
5. Solve SAA with Ω'' and obtain the objective value z_m.
6. Generate a set of new independent scenarios Ω''', $|\Omega'''| \gg |\Omega''|$.
7. Evaluate the quality of the first-stage solution x^* on scenarios in Ω'''. Input x^* into SAA, obtaining cost $z_{x^*}^m$.
8. Let $g_m := z_m - z_{x^*}^m$.
9. **end for**
10. Estimate $(1-\tau)$-CI for the lower bound
11. Let $L := \frac{1}{M}\sum_{m=1}^{M} z_{x^*}^m$ and $S_L := \frac{1}{M-1}\sum_{m=1}^{M}(z_{x^*}^m - L)^2$.
12. The $(1-\tau)$-CI for the lower bound is $\left[L - \frac{t_{M-1,\frac{\tau}{2}}\sqrt{S_L}}{\sqrt{M}}, L + \frac{t_{M-1,\frac{\tau}{2}}\sqrt{S_L}}{\sqrt{M}}\right]$, where $t_{M-1,\frac{\tau}{2}}$ is the t-value obtained from t-distribution with $M-1$ degrees of freedom and confidence level $1-\tau$.
13. Estimate $(1-\tau)$-CI for the upper bound
14. Let U: $= \frac{1}{M}\sum_{m=1}^{M} z_m$ and $S_U := \frac{1}{M-1}\sum_{m=1}^{M}(z_m - U)^2$.
15. The $(1-\tau)$-CI for the upper bound is $\left[U - \frac{t_{M-1,\frac{\tau}{2}}\sqrt{S_U}}{\sqrt{M}}, U + \frac{t_{M-1,\frac{\tau}{2}}\sqrt{S_U}}{\sqrt{M}}\right]$
16. Estimate $(1-\tau)$-CI for the optimality gap
17. Let $G := \frac{1}{M}\sum_{m=1}^{M} g_m$ and $S_G := \frac{1}{M-1}\sum_{m=1}^{M}(g_m - G)^2$.
18. The $(1-\tau)$-CI for the optimality gap is $\left[0, G + \frac{t_{M-1,\tau}\sqrt{S_G}}{\sqrt{M}}\right]$.

3.4.3 Exact Algorithm

Although two-stage stochastic programming problems are notorious for being computationally intractable, Benders decomposition (BD) has been widely used to solve the problems efficiently. The main idea of BD is to use delayed constraint generation algorithm to reduce the number of variables and constraints in the problem. It decomposes the stochastic programming model into a master problem and a number of linear subproblems. These two types of problems are then solved iteratively, adding additional constraints, referred to as Benders cuts, to the master problem. However, traditional BD has an obvious limitation. If the master problem contains discrete variables, it will be very time consuming to solve the master problem with an increasing number of Benders cuts. In order to improve efficiency, we propose a two-

phase Benders-based branch-and-cut (TPBBC) algorithm, which will be elaborated in the following sections.

Benders Decomposition

There are usually two ways to conduct BD for a two-stage model: the first is to regard each scenario as an independent subproblem, as in Peng, Delage, and Li (2020). In this case, many Benders cuts, one for each subproblem, are added at each iteration to accelerate the convergence. The second is to combine all scenarios into a single subproblem, as in Adulyasak, Cordeau, and Jans (2015), to avoid adding too many cuts at each iteration and control the time taken to solve the master problem. The relative performances of these two methods depend on problem structures and numerical instances. In numerical experiments, we will first compare the performances of TPBBC with those of the two BD formulations and then select the better one for the following numerical analysis. The models for these two methods are shown as follows:

$$\text{[MP1] maximize } \frac{1}{|\Omega|}\sum_{\omega\in\Omega}\phi(x,\omega) - \sum_{r\in R}\sum_{v\in V_r}(C_r^v + C^v)x_r^v \tag{3-12}$$

subject to (3-2) and (3-3)

$$\text{[SP1] } \phi(x,\omega) = \text{maximize } \sum_{s\in S}\sum_{p\in P_s}\left(F_p - C_p^h\right)y_s^p(\omega) \tag{3-13}$$

subject to (3-5)–(3-7)

$$\text{[MP2] maximize } \phi(x) - \sum_{r\in R}\sum_{v\in V_r}(C_r^v + C^v)x_r^v \tag{3-14}$$

subject to (3-2) and (3-3)

$$\text{[SP2] } \phi(x) = \text{maximize } \frac{1}{|\Omega|}\sum_{\omega\in\Omega}\sum_{s\in S}\sum_{p\in P_s}\left(F_p - C_p^h\right)y_s^p(\omega) \tag{3-15}$$

subject to (3-9)–(3-11).

MP1 (resp. MP2) and SP1 (resp. SP2) refer to the master problem and subproblem when each scenario is an independent subproblem (resp. when all scenarios are in one subproblem). In the following analysis, for convenience, we refer to both MP1 and MP2 as master problem (MP), and to SP1 and SP2 as subproblem (SP).

There are two types of cuts in BD, that is feasibility cuts and optimality cuts. It is easy to verify that SP is feasible and bounded (see Appendix B), therefore, we only need to consider optimality cuts as shown in (3-16) and (3-17) for independent and aggregated cases, respectively:

$$\phi(x,\omega) \le \sum_{p\in P} D^p(\omega)\,\hat{\lambda}_p + \sum_{s\in S}\sum_{r\in R_s}\sum_{v\in V_r} Q^v x_r^v\,\hat{\mu}_s,\ \forall \omega \in \Omega,\ (\hat{\lambda}_p, \hat{\mu}_s) \in I \quad (3\text{-}16)$$

$$\phi(x) \le \sum_{\omega\in\Omega}\sum_{p\in P} D^p(\omega)\,\hat{\lambda}_{p\omega} + \sum_{\omega\in\Omega}\sum_{s\in S}\sum_{r\in R_s}\sum_{v\in V_r} Q^v x_r^v\,\hat{\mu}_{s\omega},\ \forall(\hat{\lambda}_{p\omega}, \hat{\mu}_{s\omega}) \in I \quad (3\text{-}17)$$

where λ_p and μ_s (resp. $\lambda_{p\omega}$ and $\mu_{s\omega}$) correspond to the dual variables associated with constraints (3-5) and (3-6) (resp. (3-9) and (3-10)) respectively. The dual problem of SP has an extreme point set I. For each extreme point $(\hat{\lambda}_p, \hat{\mu}_s) \in I$ (resp. $(\hat{\lambda}_{p\omega}, \hat{\mu}_{s\omega}) \in I$), Benders cut (3-16) (resp. (3-17)) holds.

There will be an exponential number of Benders cut, which will make the problem intractable. BD effectively handles this problem by employing a delayed constraint generation algorithm, which means that BD relaxes the MP with only a subset of these cuts, resulting in a relaxed master problem (RMP).

Two-phase Benders-based Branch-and-cut Algorithm

Unfortunately, BD converges slowly because RMP is an integer problem whose size keeps growing as the iteration count progresses. For this reason, we integrate BD inside branch-and-cut (BC) to make full use of the advantages of BC for solving mixed integer programming (MIP) problems. The basic idea of BC is to divide the entire solution space into multiple subsets that are not constrained by integers, remove infeasible nodes through boundary constraints, and optimize the solution space by adding cuts.

The innovative method of integrating BD inside BC is called two-phase Benders-based branch-and-cut algorithm. At the first phase, we relax integer constraints on RMP and run BD multiple times until no Benders cuts can be added, which speeds up the convergence and saves computation time for the second phase. We then restore integer constraints and keep all generated cuts at first phase. At the second phase, we use BC at each node to find integer solutions. Once an integer solution is found, we use generic callback to solve SP, add Benders cut, and update boundaries. The detailed procedures of TPBBC algorithm are shown in Algorithm 2. First, we define RMP without integer constraints (3-3) as LRMP. Additional notations for Algorithm 2 are shown in Table 3-4. The set of active nodes in the branch-and-bound (BB) tree is denoted by N. In the initialization process, it contains only the root node. The value of the best-known feasible solution, called incumbent solution, for the original problem is stored as $\underline{r}$ and provides a lower bound. The upper bound of the objective value is

denoted as $\overline{r}$, which is initialized to positive infinity at root node. Each node of the BB tree has an upper bound $ub_n, n \in N$, initialized to the value of the parent node, and will be updated if the value of LRMP is lower than initialization value. The maximum upper bound of all active nodes is denoted by $UB_N = \max\{ub_n : n \in N\}$.

Table 3-4: Additional notations for Algorithm 2

N	Set of active nodes in branch-and-bound (BB) tree, indexed by n, $n \in N$
$\underline{r}$	Incumbent solution for the original problem, which provides a lower bound
$\overline{r}$	Upper bound of the original problem
ub_n	Upper bound of node n
UB_N	The maximum upper bound of all active nodes, where $UB_N = \max\{ub_n : n \in N\}$

Algorithm 2: Two-phase Benders-based branch-and-cut algorithm

1. **Input:** A tolerance $\epsilon \geq 0$, maximum first-phase run time T_1, maximum second-phase run time T_2, and sample Ω
2. **Output:** The optimal solutions $\boldsymbol{x}$ and objective value $\underline{r}$
3. **Initialize** $\overline{r} \leftarrow \infty$, $\underline{r} \leftarrow -\infty$, active node set $N \leftarrow$ {root node}, and $UB_N \leftarrow \infty$
4. First phase:
5. **while** $\overline{r} - \underline{r} > \epsilon$, and first-stage runtime$< T_1$ **do**
6. Solve LRMP: Solve LRMP to obtain optimal solution $\hat{\boldsymbol{x}}$ and optimal objective value is z_n
7. Input $\hat{\boldsymbol{x}}$ to SP to check whether Benders cut is needed
8. **if** needed **then**
9. Add Benders cut (3-16) or (3-17) to LRMP
10. **else**
11. **end while**
12. **end if**
13. Second phase: Restore integer constraints and imbed BD into BC
14. **while** $N \neq \emptyset, \overline{r} - \underline{r} > \epsilon$, and second-phase run time $< T_2$ **do**
15. Node selection: Select a node n from N
16. **if** $ub_n < \underline{r}$ **then**
17. Prune node n (prune by bound)
18. Continue with the next iteration (back to line 15)
19. **end if**
20. Solve LRMP: Solve LRMP to obtain optimal solution $\hat{\boldsymbol{x}}$ and optimal objective value is z_n
21. **if** $z_n < \underline{r}$ **then**
22. Prune node n (prune by bound)
23. Continue with next iteration (back to line 15)
24. **else if** $z_n < ub_n$ **then**
25. $ub_n \leftarrow z_n$
26. Update UB_N
27. Update $\overline{r} \leftarrow UB_N$
28. **end if**
29. **if** $\hat{\boldsymbol{x}}$ satisfies integer constraints **then**
30. Input $\hat{\boldsymbol{x}}$ to SP and obtain optimal solution $\hat{\boldsymbol{y}}$
31. Calculate $lb_n \leftarrow \frac{1}{|\Omega|}\sum_{\omega\in\Omega}\sum_{s\in S}\sum_{p\in P_s}\left(F_p - C_p^h\right)\hat{y}_s^p(\omega) - \sum_{s\in S}\sum_{v\in V_s} C_s^v\,\hat{x}_s^v$
32. $\underline{r} \leftarrow \max\left(\underline{r}, lb_n\right)$
33. **if** add Bender cut **then**
34. Add Benders cut (3-16) or (3-17) to LRMP
35. Back to solve LRMP (line 20)
36. **else**
37. Prune node n (prune by integer)
38. Continue with next iteration (back to line 15)
39. **end if**
40. **else**
41. Branch: add two new nodes into N
42. Remove node n from N
43. **end if**
44. **end while**
45. **Return** $\underline{r}$ and corresponding optimal solution $\boldsymbol{x}$

Since we have already described the procedure of the first phase above, we only introduce the second phase. For the second phase, a node is first selected. It is verified whether the upper bound of the node is less than the lower bound of the original problem. If yes, the node is pruned. Otherwise, solve LRMP to obtain optimal first-stage solutions and objective value. Conduct a bound check again. If the objective value is lower than the inherited upper bound, update the upper bound of the node and at the same time update the upper bound of the problem if the condition is met. Then check whether integer constraints are satisfied. If the solution is integer, solve the subproblems and update the lower bound. Then check whether the optimality constraints are violated. Add Benders cuts once a violation is found. Otherwise, prune the node. If the solution is fractional, branch the node into two new nodes. Repeat the iteration until active node set is empty, the gap between upper and lower bounds is below a predetermined tolerance level, or the time exceeds a preset value.

Acceleration Techniques

With the increase of the number of variables and constraints, the problem will become computationally difficult, and the computer could run out of memory. Therefore, in this section, we propose several acceleration techniques that can greatly reduce the number of variables and constraints, thus speeding up the computation process.

We know that only a small proportion of x_r^v will equal 1 in the optimal solution. Therefore, we apply variable fixing (VF) to assign zero to part of the variables, which can reduce the search space and simplify the computation. To set the value of x_r^v, we make use of Proposition 1.

Proposition 1. *Let* $\boldsymbol{P}$ *be an MIP defined as* $z(\boldsymbol{P}) = \max\{\boldsymbol{cx} + \boldsymbol{dy} | \boldsymbol{Ax} + \boldsymbol{By} \leq \boldsymbol{h}, \boldsymbol{x} \in \{0,1\}^{n_1}, \boldsymbol{y} \in \mathbb{R}_+^{n_2}\}$. *Let* $\boldsymbol{x'}$ *and* $\boldsymbol{y'}$ *be a feasible solution, and* $\boldsymbol{\omega}$ *be a feasible dual solution of the linear relaxation of* $\boldsymbol{P}$. *Any optimal solution* $\boldsymbol{x}^*$ *cannot contain a variable* $x_i^* = 1$ *if the reduced cost* c_i *is less than* $\boldsymbol{cx'} + \boldsymbol{dy'} - \boldsymbol{\omega h}$.

The proof of Proposition 1 is in Appendix C. According to Proposition 1, we need to identify a feasible solution $\boldsymbol{x'}$ and $\boldsymbol{y'}$, and a feasible dual solution $\boldsymbol{\omega}$. Since finding a good feasible solution of MIP is not easy in a large-size problem, we can

exploit the property that column generation (CG) only uses a subset of variables to solve the problem to simply computation process. The CG algorithm will decompose the problem into a master problem and a subproblem. The master problem is MP1 (resp. MP2) with a relaxation of integer constraints (3-3) and only a subset of variables. The subproblem is PP1 (resp. PP2) that is used to identify the variables that could improve objective function. At each iteration, we solve master problem to optimum under the given subset of variables, obtaining optimal solution $\boldsymbol{x}^*$. Then input $\boldsymbol{x}^*$ into SP1 (resp. SP2) to check whether to add Benders cuts. If no Benders cut can be added, run PP1 (resp. PP2) to check whether to add new variables to MP1 (resp. MP2). If new variables could be added, repeat the above process, otherwise, a good subset of variables $\boldsymbol{x}_{sub}$ for feasible solution of original MIP and the optimal dual objective $z(\boldsymbol{\omega})$ of linear relaxation of MIP are obtained, and the CG computes

$$[\text{PP1}]\ \sum_{s\in S_r}\eta_s^* - \sum_{k\in K}\sum_{s\in S_r} Q^v \hat{\mu}_s^k \xi_k^*,\ \forall v \in V_r, r \in R\backslash R' \tag{3-18}$$

$$[\text{PP2}]\ \sum_{s\in S_r}\eta_s^* - \sum_{k\in K}\sum_{\omega\in\Omega}\sum_{s\in S_r} Q^v \hat{\mu}_{s\omega}^k \xi_k^*,\ \forall v \in V_r, r \in R\backslash R' \tag{3-19}$$

where η_s^* is the dual of Constraints (3-2), ξ_k^* is the dual of k^{th} Benders cut added to master problem, $\hat{\mu}_s^k$ (resp. $\hat{\mu}_{s\omega}^k$) is the dual of Constraints (3-6) (resp. Constraints (3-10)) in the k^{th} Benders cut.

Having the subset $\boldsymbol{x}_{sub}$, we restore integer constraints and use procedures in the second phase of TPBBC to generate a feasible objective $z(MIP)$ for original MIP. We then use variable fixing for all $\boldsymbol{x}$. If the reduced cost $c_r^v, \forall v \in V_r, r \in R$ satisfies $c_r^v < z(MIP) - z(\boldsymbol{\omega})$, we have $c_r^v = 0$. Setting part of the variables to 0 and lower bound of MIP to $z(MIP)$, we run the second phase of TPBBC to obtain optimum solution of MIP.

In addition to Proposition 1, we also propose two valid constraints that could strengthen the formulation of the problem and reduce the search space. The first valid constraint (3-20) is based on comparison of cost and profit of using the vehicle type v to serve route r:

$$x_r^v = 0, \forall v \in V_r, r \in R \text{ if } C_r^v + C^v \geq UQ^v \tag{3-20}$$

where $U = \max\{F_p - C_p^h | \forall p \in P\}$. This means that if the cost of using ship type v on route r is no less than the maximum profits can be earned on this trip, the ship type v cannot be deployed on route r.

The second valid constraint is for split delivery. Dror and Trudeau (1990) propose a theorem for split delivery stating that if the costs satisfy triangular inequality, there exists an optimal solution in which no two routes have more than one split customer in common. Inspired by this theorem, Archetti, Bianchessi, and Speranza (2014) propose Corollary 1 that is more suitable for solving our problem.

Corollary 1. *If the costs satisfy triangle inequality, then there exists an optimal solution such that the total number of splits is lower than the number of routes*.

According to Corollary 1, we can obtain the following valid constraint:

$$x_r^v = 0, \forall v \in V_r, r \in R \text{ if } \sum_{p \in P_r} n_{pr} \geq N_r \quad (3\text{-}21)$$

where n_{pr} is the number of splits port p experiences on route r. For example, if two sequences of route r visit port p, then $n_{pr} = 2 - 1$. N_r is the number of sequences route r contains.

3.5 NUMERICAL EXPERIMENTS

In this section, we use real-world data to test the performances of the solution methods. We first use label setting to generate feasible routes. We then compare the performances of solution algorithms mentioned above. We also conduct sensitivity analysis to test the impact of some key parameters, which provides valuable managerial insights for practical implement. All the experiments are carried out on a laptop with i9-12900K CPU, 3.20 GHz processing speed and 32 GB of memory. The model was implemented in C++ programming and solved by CPLEX 12.10.

3.5.1 Parameter Setting

The numerical experiment uses real world data along the Yangtze River, as shown in Figure 3-3. A total of 13 ports are considered where Shanghai port is a hub port while the remaining ports are feeder ports. The distance between ports is given in Table 3-5. The number in each cell represents the distance from the port in the first row to the leftmost port in the first column. For example, it is 53 nautical miles from SH to NT. Six ship types are considered in the numerical experiment, as shown in Table 3-6. Capital letters S, M, and L represent small-, medium-, and large-size ships, respectively. We assume that conventional and autonomous ships of the same size have different capacities because the removal of deckhouse and hotel system in

autonomous vessels leaves more room for cargoes. The same is true for medium- and large-size ships. The ship operational cost includes labor cost, maintenance cost, insurance, etc. The capital cost includes the purchase cost and the cost related to shore control center for autonomous ships (Notteboom and Cariou, 2013; Kretschmann, Burmeister, and Jahn, 2017). Demands of feeder ports are based on data provided by Ministry of Transport of the People's Republic of China. Demand dataset contains 216 scenarios where each scenario contains weekly demand of all feeder ports. The revenue and handling costs for serving a container from a feeder port are the real-time prices obtained from the logistics website. The port dwelling time, including loading, unloading, waiting, etc., is calculated based on Tan et al. (2021). Parameters related to feeder ports are shown in Table 3-7. The symbol "-" in the second and third columns means that the revenue and handling cost of SH are not considered because we do not consider the demand of hub port. Meanwhile, "-" in port dwell time columns means the corresponding ship type is not allowed to berth at the feeder port because of the waterway restrictions, such as draft and width constraints (Li et al., 2019). The service frequency α is set to seven days and the sailing speed is 15 knots.

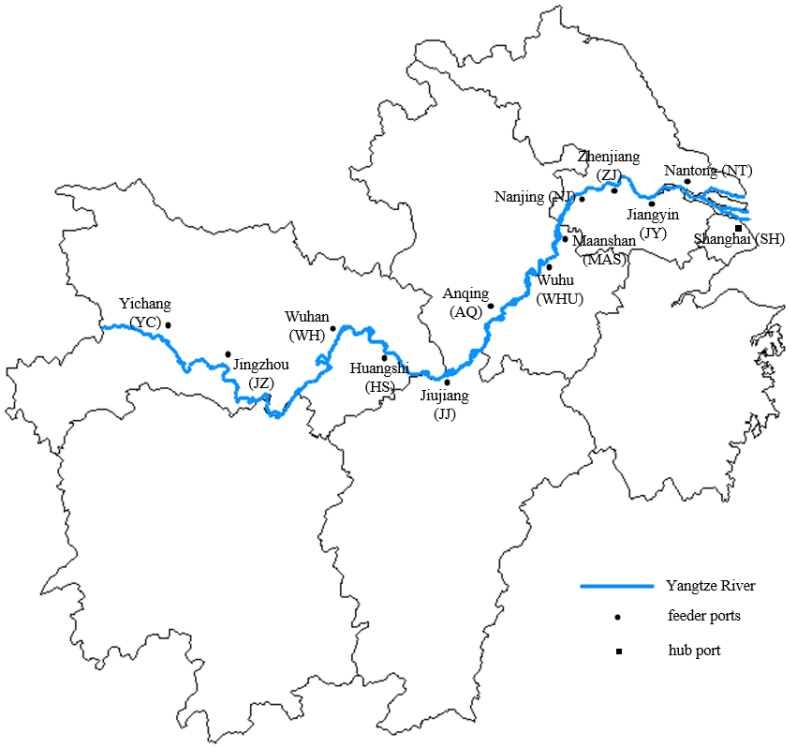

Figure 3-3: Ports along the Yangtze River

Table 3-5: Distance between ports (nautical mile)

	SH	NT	JY	ZJ	NJ	MAS	WHU	AQ	JJ	HS	WH	JZ
NT	53											
JY	85	31										
ZJ	147	94	63									
NJ	187	134	103	40								
MAS	214	160	129	66	26							
WHU	239	186	154	92	52	25						
AQ	345	292	260	198	158	131	106					
JJ	428	375	343	281	241	214	189	83				
HS	492	439	408	345	305	279	253	147	64			
WH	563	510	478	416	376	349	324	218	135	71		
JZ	787	733	702	639	599	573	548	442	359	294	224	
YC	901	848	816	754	714	687	662	556	473	409	338	114

Note: The distance is obtained from the website http://ports.com/sea-route/.

Table 3-6: Ship type information

	Conventional vessels			Autonomous vessels		
	C-S	C-M	C-L	A-S	A-M	A-L
Capacity (TEUs)	300	400	500	420	560	700
Unit bunkering cost (USD/nautical mile)	25	29	33	23	27	31
Ship operational cost (USD/hour)	119	144	160	71	86	96
Capital cost (million USD/year)	1.36	1.64	1.82	1.49	1.80	2.01

Note: The data have been adjusted based on the data used in the studies by Notteboom and Cariou (2013) and Kretschmann, Burmeister, and Jahn (2017).

Table 3-7: Parameters related to feeder ports

Ports	Revenue (USD/TEU)	Handling cost (USD/TEU)	Port dwell time (hours)					
			C-S	C-M	C-L	A-S	A-M	A-L
SH	-	-	8.9	9.4	9.9	8.9	9.4	9.9
NT	154	39	5.2	5.7	6.2	5.2	5.7	6.2
JY	168	28	4.0	4.5	5.0	4.0	4.5	5.0
ZJ	168	37	4.7	5.2	5.7	4.7	5.2	5.7
NJ	154	33	4.2	4.7	5.2	4.2	4.7	5.2
MAS	168	56	6.8	7.3	-	6.8	7.3	-
WHU	168	88	6.7	7.2	-	6.7	7.2	-
AQ	280	74	4.2	4.7	-	4.2	4.7	-
JJ	168	54	6.5	7.0	-	6.5	7.0	-
HS	210	60	6.7	7.2	-	6.7	7.2	-
WH	168	82	5.6	6.1	-	5.6	6.1	-
JZ	168	34	4.1	-	-	4.1	-	-
YC	168	30	3.6	-	-	3.6	-	-

Note: The data have been adjusted based on the data used in the studies by Li et al. (2019) and Tan et al. (2021).

3.5.2 Computational Performances

In this section, we use parameters provided in Chapter 3.5.1 to test the performances of the solution techniques mentioned in Chapter 3.4. We generate test instances of varying sizes by adjusting two parameters: the number of ports and the service frequency. The number of ports ranges from six to 13, while the service frequency is set to three, five, or seven days. To avoid computation burden of large sample size, in this test, we set the sample size to be 10. The influences of sample size will be explored in the following section.

A total of five solution methods, i.e., SAA, TPBBC with each scenario being an independent subproblem (TPBBC-I), TPBBC with all scenarios in one subproblem (TPBBC-A), branch-and-Benders-cut (BBC), and TPBBC-I with CG and VF (TPBBCCGVF-I), were tested. BBC is a commonly used branch-and-cut method that only has the second phase of TPBBC. By comparing the performances of TPBBC and BBC, we can know whether it is necessary to conduct first phase of TPBBC before the classic branch-and-cut method. For TPBBCCGVF-I, we first apply valid constraints before solving the problem to see if some variables can be eliminated. Then in the first phase of TPBBC, we iteratively use CG and add Benders cut to obtain a subset of routes for a feasible solution and an optimal dual solution to the original MIP without integer constraints. Having the subset, we restore the integer constraints, and obtain a feasible solution to MIP. With a feasible solution and a dual solution, variable fixing is applied to assign a value of zero to part of the variables. With reduced variables and constraints, the second phase of TPBBC is conducted.

We first compare performances of TPBBC-I and TPBBC-A. Results are shown in Figure 3-4, where (a), (b) and (c) show the time spent for the first-phase when service frequency is three, five, or seven days, respectively; (d), (e), and (f) show the total time when the service frequency is three, five, or seven days, respectively. The horizontal bar indicates the number of ports considered, while the vertical bar is the solution time. The dashed red horizontal line is the time limit (i.e., 7200s). When the point reaches the line, the computation time of this algorithm exceeds the limit and we thus do not have the exact time for them. The dashed red vertical line represents the turning point when computation time of the algorithm exceeds the time limit. For example, in Figure 3-4 (e), when the number of ports is 10, the total time of TPBBC-

A exceeds 7200s. We can see that TPBBC-I always outperforms TPBBC-A for two main reasons. First, the former adds more Benders cuts and thus makes the computation converge more quickly. Second, we can only obtain at most one Benders cut after solving the subproblem under all scenarios of a sample for TPBBC-A, while for each scenario, we have about one Benders cut for TPBBC-I, which means the time spent for obtaining the Benders cut is much shorter for TPBBC-I. The results mean that TPBBC-I is more suitable for our problem and hence we only consider the case for which each scenario corresponds to an independent subproblem in the following analysis.

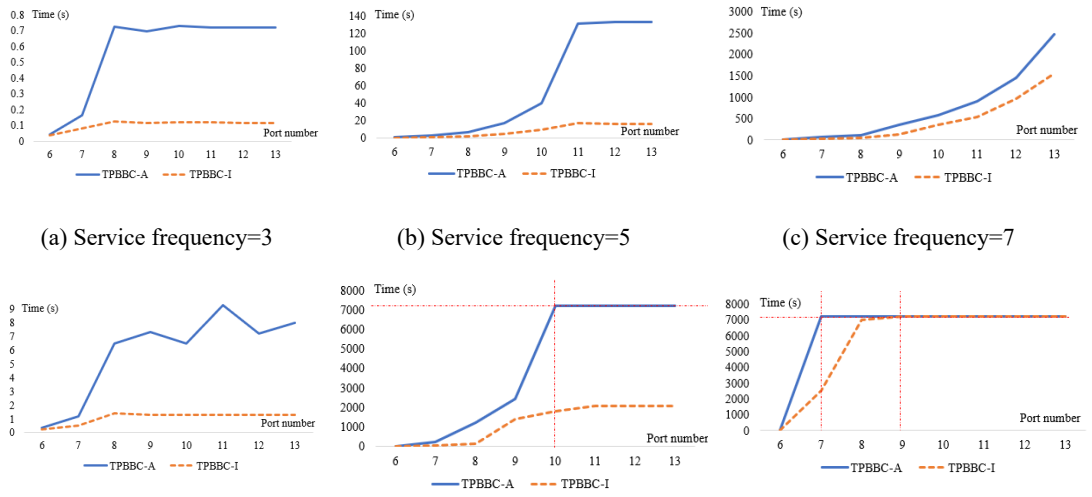

(a) Service frequency=3 (b) Service frequency=5 (c) Service frequency=7

(d) Service frequency=3 (e) Service frequency=5 (f) Service frequency=7

Note: (a), (b) and (c) show the first-phase time when service frequency is three, five, or seven days, respectively. (d), (e), and (f) show total time when service frequency is three, five, or seven days, respectively.

Figure 3-4: Comparison of computational times (second) between TPBBC-I and TPBBC-A under different service frequency and the number of ports.

We then compare TPBBC-I with BBC to determine whether it is more efficient to add some Benders cuts at root node before branch-and-cut process. The results shown in Figure 3-5 indicate that modifying BBC to TPBBC-I speeds up convergence and saves computation time.

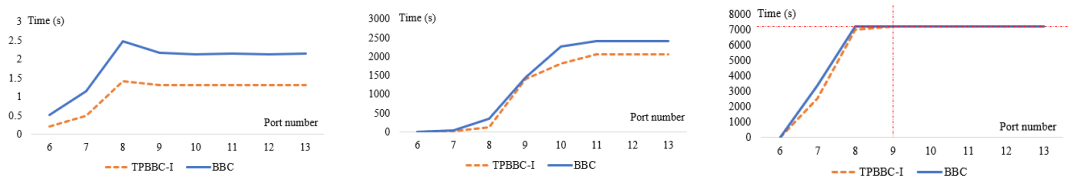

(a) Service frequency=3 (b) Service frequency=5 (c) Service frequency=7

Figure 3-5: Comparison of computational times between TPBBC-I and BBC under different service frequency and the number of ports

Knowing that TPBBC-I outperforms TPBBC-A and BBC in all test instances, we then compare SAA, TPBBC-I, and TPBBCCGVF-I. From Figure 3-6, we can see that TPBBC-I spends less time in small size instances and the gap between these methods is small, while for medium and large instances, there are significant differences between the solution times of these methods. When the service frequency is five days, SAA takes over an hour and a half in 50% of the instances and fails to solve the problem optimally within the time limit for two instances. Meanwhile, TPBBC-I finds an optimal solution for all instances within one hour, and TPBBCCGVF-I does this within three minutes. When the service frequency is seven days, SAA can only obtain an optimal solution for one instance. TPBBC-I can solve the problem to optimality only when the number of ports is less than nine. TPBBCCGVF-I finds an optimal solution for all instances in about one hour. The reason for the high efficiency of TPBBCCGVF-I can be seen from Table 3-8. SF and NP are the service frequency and the number of ports, respectively. Variables and Constraints indicate the number of variables and constraints in the model. For SAA, these are the number of columns and rows after MIP presolve. For TPBBC-I and TPBBCCGVF-I, these are the corresponding values for the second phase after restoration of the integer constraints. Variable fixing shows the number of variables that were set to 0 during variable fixing procedure in TPBBCCGVF-I. Valid 1 and 2 are the number of variables set to 0 by valid constraints (3-20) and (3-21), respectively. Since only TPBBCCGVF-I uses variable fixing and valid constraints, the values for SAA and TPBBC-I are not available in the corresponding columns, so we use "-" instead. At the beginning of TPBBCCGVF-I, some variables were eliminated by valid constraints, which shortens the time for first phase. Then during variable fixing, other variables were set to 0, greatly accelerating the computation at the second phase. This

is particularly significant in large instances where a large number of variables were eliminated in the first phase.

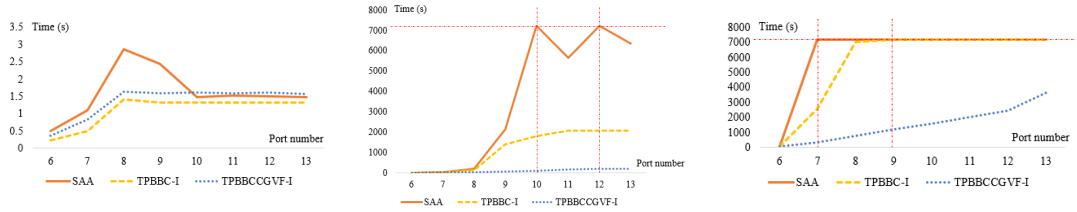

(a) Service frequency=3 (b) Service frequency=5 (c) Service frequency=7

Figure 3-6: Comparison of computational times between SAA, TPBBC-I, and TPBBCCGVF-I under different service frequencies and number of ports

Table 3-8: Comparison of SAA, TPBBC-I, and TPBBCCGVF-I in terms of variables and constraints

SF	NP	Algorithm	Variables	Constraints	Variable fixing	Valid 1	Valid 2
3	6	SAA	958	390	-	-	-
		TPBBC-I	218	89	-	-	-
		TPBBCCGVF-I	217	89	0	0	1
3	7	SAA	2,108	741	-	-	-
		TPBBC-I	341	171	-	-	-
		TPBBCCGVF-I	340	171	0	0	1
3	8	SAA	2,691	1,000	-	-	-
		TPBBC-I	401	208	-	-	-
		TPBBCCGVF-I	400	284	0	0	1
3	9	SAA	2,691	1,000	-	-	-
		TPBBC-I	401	208	-	-	-
		TPBBCCGVF-I	400	284	0	0	1
3	10	SAA	2,691	1,000	-	-	-
		TPBBC-I	401	208	-	-	-
		TPBBCCGVF-I	400	284	0	0	1
3	11	SAA	2,691	1,000	-	-	-
		TPBBC-I	401	208	-	-	-
		TPBBCCGVF-I	400	284	0	0	1
3	12	SAA	2,691	1,000	-	-	-
		TPBBC-I	401	208	-	-	-
		TPBBCCGVF-I	400	284	0	0	1
3	13	SAA	2,691	1,000	-	-	-
		TPBBC-I	401	208	-	-	-
		TPBBCCGVF-I	400	284	0	0	1
5	6	SAA	3,404	391	-	-	-
		TPBBC-I	2,719	89	-	-	-
		TPBBCCGVF-I	688	89	1,376	16	639

5	7	SAA	7,950	753	-	-	-
		TPBBC-I	6,197	190	-	-	-
		TPBBCCGVF-I	1,203	197	3,562	20	1,411
5	8	SAA	12,644	1,467	-	-	-
		TPBBC-I	8,497	271	-	-	-
		TPBBCCGVF-I	2,542	321	4,348	0	1,560
5	9	SAA	19,524	2,885	-	-	-
		TPBBC-I	9,794	410	-	-	-
		TPBBCCGVF-I	3,331	399	4,749	0	1,572
5	10	SAA	33,176	5,692	-	-	-
		TPBBC-I	11,049	699	-	-	-
		TPBBCCGVF-I	3,749	466	5,351	0	1,573
5	11	SAA	52,613	9,819	-	-	-
		TPBBC-I	12,323	1,009	-	-	-
		TPBBCCGVF-I	3,749	495	6,318	0	1,573
5	12	SAA	52,613	9,819	-	-	-
		TPBBC-I	12,327	1,020	-	-	-
		TPBBCCGVF-I	3,749	494	6,321	0	1,573
5	13	SAA	52,613	9,819	-	-	-
		TPBBC-I	12,327	1,020	-	-	-
		TPBBCCGVF-I	3,749	494	6,321	0	1,573
7	6	SAA	25,769	391	-	-	-
		TPBBC-I	25,160	93	-	-	-
		TPBBCCGVF-I	3,031	92	2,506	15,150	4,473
7	7	SAA	92,222	753	-	-	-
		TPBBC-I	90,599	179	-	-	-
		TPBBCCGVF-I	5,624	202	9,724	63,465	11,786
7	8	SAA	167,204	1,467	-	-	-
		TPBBC-I	163,683	283	-	-	-
		TPBBCCGVF-I	27,301	371	64,707	678	70,997
7	9	SAA	231,421	2,885	-	-	-
		TPBBC-I	222,781	425	-	-	-
		TPBBCCGVF-I	37,474	546	95,321	2,394	87,575
7	10	SAA	294,915	5,711	-	-	-
		TPBBC-I	274,567	706	-	-	-
		TPBBCCGVF-I	41,017	668	128,231	6,222	98,848
7	11	SAA	364,565	11,353	-	-	-
		TPBBC-I	316,569	1,229	-	-	-
		TPBBCCGVF-I	49,482	834	152,217	10,028	104,184
7	12	SAA	431,234	22,555	-	-	-
		TPBBC-I	323,515	2,240	-	-	-
		TPBBCCGVF-I	49,482	822	156,579	11,599	104,195
7	13	SAA	521,678	38,763	-	-	-
		TPBBC-I	328,508	3,420	-	-	-
		TPBBCCGVF-I	84,115	1,198	124,477	13,265	104,195

Based on the above analysis, the following conclusions can be drawn within the context of this study: 1) When implementing Benders decomposition, treating each scenario as an independent subproblem proves to be a more efficient approach; 2) The two-phase branch-and-Benders-cut method demonstrates superior performance compared with the classic one; 3) The acceleration techniques significantly enhance computational speed. In summary, the proposed solution algorithm, choosing right Benders decomposition method, modifying existing BBC, and adding acceleration techniques, can efficiently solve the problem within a reasonable amount of time, especially for large-size instances. Therefore, it is suitable for our problem.

3.5.3 Determination of the Sample Size

As we mentioned in Chapter 3.4.2, the larger the sample size, the better the solution quality but the longer the computation time. To identify a sample size that can achieve a balance between solution quality and computation complexity, Algorithm 1 was used in this section under the given parameter setting. From the previous experiments we know that the instance size that SAA can solve to optimality is limited. Considering the computation time, we selected 10 instances shown in Figure 3-7 and Figure 3-8. Each instance was tested under five different sample sizes, i.e., 10, 30, 50, 100, and 150. Figure 3-7 and Figure 3-8 show the ratio between the 95% confidence interval for the optimality gap and a point estimate of lower bound and computation time for 10 test instances under different sample sizes, respectively. The dashed line in Figure 3-7 is the 1% limit. It can be seen that when sample size reaches 100, the ratio falls below 1% in all cases. Although the computation time is slightly longer than for smaller sample sizes, it is acceptable given the size of the instance. Therefore, considering both solution quality and computation time, we set the sample size to 100 for the following analysis.

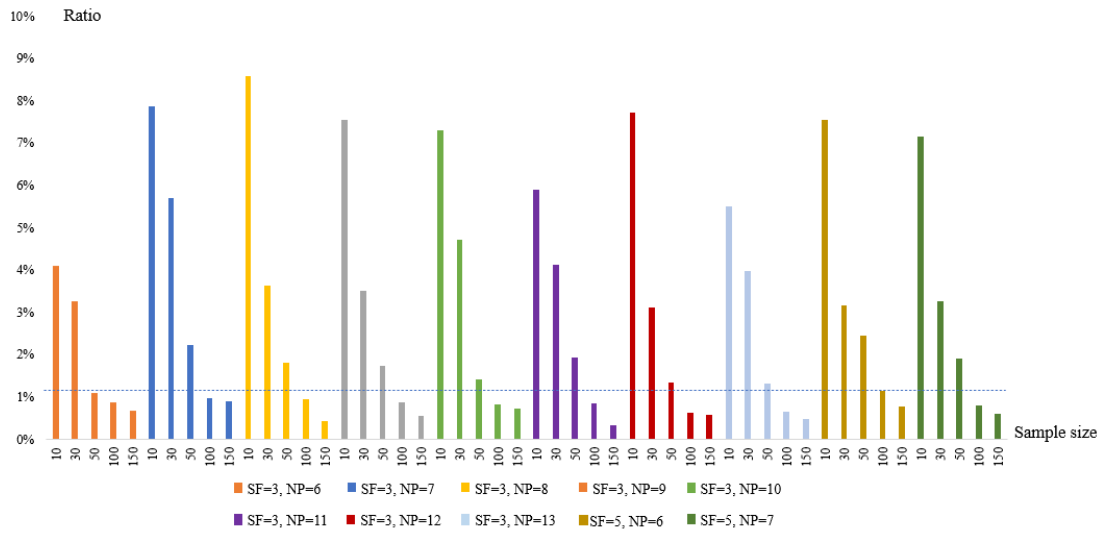

Figure 3-7: Ratio between the 95% confidence interval for optimality gap and the point estimate of lower bound under different sample size and problem setting

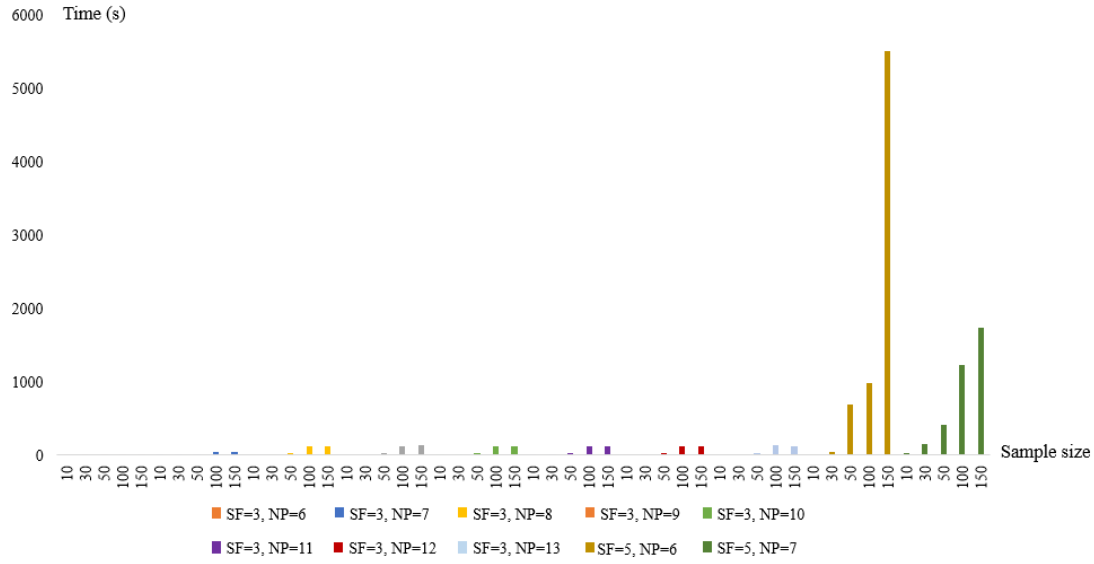

Figure 3-8: Computation time under different sample size and problem setting

3.5.4 Sensitivity Analysis

In this section, we investigate the influence of key factors and derive constructive managerial insights for shipping companies.

The Impact of Autonomous Ships

We design two scenarios where in the first scenario only conventional ships are used, while in the second scenario we consider all types of ships. The comparison between these two scenarios is shown in Table 3-9 and Table 3-10. The ship fleet in

Table 3-9 is the fleet composition under the corresponding scenarios. C and A represent conventional and autonomous ships, respectively. S, M, and L represent small, medium, and large ships, respectively. Route in Table 3-9 provides information on the optimal route, including the number of routes selected, and the number of sequences that make up of each route. The first row of Table 3-10 contains the names of six feeder ports. We find that when autonomous ships are added to the network, profits increase while costs decrease. The increase in profit comes from the larger capacity of autonomous ships to serve more demand, which could be reflected from the demand satisfaction level in Table 3-10. The cost reduction is the result of two main causes. First, ships with larger capacity can visit more or even farther ports in one voyage, thus reducing the number of sequences and reducing voyage cost. Second, more port demands can be fulfilled in one visit, reducing the additional cost of multiple visits to the same port. Therefore, although autonomous ships are more expensive, the benefits far outweigh the costs.

Table 3-9: Comparison between the cases with and without autonomous ships

	Total profit	Voyage cost	Capital cost	Service profit	Ship fleet	Route
Scenario 1	123,959	65,996	4,356	194,312	1 C-S, 1 C-L	two routes: one sequence three sequences
Scenario 2	150,573	42,839	5,219	198,631	1 A-M, 1 A-L	two routes: one sequence two sequences

Note: Scenario 1 denotes the condition where only conventional ships are permissible for use, while Scenario 2 denotes the condition where both conventional and autonomous ships are allowed.

Table 3-10: Port demand satisfaction level under two scenarios

	NT	JY	ZJ	NJ	MAS	WHU
Scenario 1	99.4%	100.0%	100.0%	100.0%	96.0%	79.6%
Scenario 2	100.0%	100.0%	100.0%	100.0%	99.0%	94.9%

Note: Scenario 1 denotes the condition where only conventional ships are permissible for use, while Scenario 2 denotes the condition where both conventional and autonomous ships are allowed.

The Impact of Port Restriction

As mentioned before, due to waterway restrictions on feeder ports, such as draft and width constraints, some ports inaccessible to conventional ships may be visited by lighter autonomous ships of the same size. In this section, we want to check whether the results would change if ports treated both types of ships equally. The results are

shown in Table 3-11 and Table 3-12. We find that port restrictions do not influence the outcome in this research. Because autonomous ships in this research are more advantageous. Even though we relaxed port restrictions, the same ship type was chosen. In a situation where conventional ships would be more beneficial, the port restriction may have impacts on system performance.

Table 3-11: Comparison between the cases with and without port restriction

Restriction	Total profit	Voyage cost	Capital cost	Service profit	Ship fleet	Route
Yes	150,573	42,839	5,219	198,631	1 A-M, 1 A-L	two routes: one sequence two sequences
No	150,573	42,839	5,219	198,631	1 A-M, 1 A-L	two routes: one sequence two sequences

Table 3-12: Port demand satisfaction level with and without port restriction

	NT	JY	ZJ	NJ	MAS	WHU
With restriction	100.0%	100.0%	100.0%	100.0%	99.0%	94.9%
Without restriction	100.0%	100.0%	100.0%	100.0%	99.0%	94.9%

The Impact of Cost Structure

The previous analysis was carried out in the case where autonomous ships are more advantageous. In this section, we explore what happens if the cost advantage of autonomous ships wanes. We scaled the capital cost and operational cost of autonomous ships by different coefficients in Table 3-13 and Table 3-14, respectively. The results in Table 3-13 suggest that autonomous ships will only lose their competitive advantage if their capital costs are sufficiently large. In this research, autonomous ships will partially and completely lose their competitive advantage if the capital cost is four and 10 times the current value, respectively. Table 3-14 suggests that if the operational cost increases to four times its current value, the conventional ships will outperform autonomous ones. The findings from both tables indicate that operational costs have a significant impact on ship operations due to their substantial proportion. If the technology and skilled technicians required for autonomous ships become excessively expensive, shipping companies may opt for conventional ships. However, as technology continues to advance, the cost of autonomous ships is expected to decrease gradually, making them increasingly competitive in the future.

Therefore, once they are allowed to be widely adopted in the maritime industry and their costs become manageable, autonomous ships have the potential to replace traditional ships.

Table 3-13: The impact of capital cost

Coefficient	Total profit	Voyage cost	Capital cost	Profit	Ship fleet
1	150,573	42,839	5,219	198,631	1 A-M, 1 A-L
2	145,353	42,839	10,439	198,631	1 A-M, 1 A-L
4	140,198	43,913	11,726	195,837	1 C-S, 1 A-M
6	135,266	43,913	16,658	195,837	1 C-S, 1 A-M
8	130,335	43,913	21,589	195,837	1 C-S, 1 A-M
10	123,959	65,996	4,356	194,312	1 C-S, 1 C-L

Table 3-14: The impact of operational cost

Coefficient	Total profit	Voyage cost	Capital cost	Profit	Ship fleet
1	150,573	42,839	5,219	198,631	1 A-M, 1 A-L
2	137,724	54,969	5,219	197,912	1 A-M, 1 A-L
3	126,166	62,196	4,795	193,156	1 A-S, 1 A-L
4	123,959	65,996	4,356	194,312	1 C-S, 1 C-L
6	123,959	65,996	4,356	194,312	1 C-S, 1 C-L
8	123,959	65,996	4,356	194,312	1 C-S, 1 C-L

The Impact of Demand Satisfaction

In the previous analysis, we found that in order to maximize total profit, not all demands are satisfied. In this section, we explore the impact of satisfying all demands. Results are shown in Table 3-15. The first column indicates whether the constraints by which all demands should be satisfied are considered. We find that when all demands are required to be fulfilled, the total profit decreases. The reason is that the number of ports that can be served during a voyage is reduced. Therefore, more sequences must be travelled, increasing voyage costs.

Table 3-15: Comparison between the cases with and without constraints of demand satisfaction

All demand	Total profit	Voyage cost	Capital cost	Service profit	Ship fleet	Route
No	150,573	42,839	5,219	198,631	1 A-M, 1 A-L	two routes: one sequence two sequences
Yes	143,933	50,822	5,219	199,975	1 A-M, 1 A-L	two routes: two sequences two sequences

The Impact of technology development and government intervention

The level of automation in autonomous ships is continuously evolving. The IMO has classified them into four levels based on their degree of automation: crewed ship with automated processes and decision support (degree one); remotely controlled ship with seafarers on board (degree two); remotely controlled ship without seafarers on board (degree three); and fully autonomous ship (degree four). Based on whether there are seafarers on board, we can further divide all the ships into two categories: low degree and high degree. For the low degree ships, we assume that they have the same exterior design as the conventional ships, while for high degree ships, we assume that the deckhouse and accommodation structures are removed so that they have greater capacity for cargoes. Table 3-16 and Table 3-17 illustrate the impact of capital and operational costs when considering both conventional ships and low-degree autonomous ships. We assume that low-degree autonomous ships have the same capacity as conventional ships, but their cost structure aligns with that of the autonomous ships discussed in Chapter 3.5.1. The results in Table 3-16 and Table 3-17 align with the trends observed in the impact of cost structure. Since low-degree autonomous ships do not possess a capacity advantage, their adoption will primarily depend on the level of capital and operational costs. Only when these costs are sufficiently low will low-degree autonomous ships be chosen. For high-degree autonomous ships, where autonomous ships have greater capacity, the optimization results align with those discussed in the impact of cost structure.

Table 3-16: The impact of capital cost when both conventional ships and low degree autonomous ships are involved

Coefficient	Total profit	Voyage cost	Capital cost	Profit	Ship fleet
1	136,553	52,964	4,795	194,312	1 A-S, 1 A-L
2	131,758	52,964	9,589	194,312	1 A-S, 1 A-L
3	127,217	56,971	10,123	194,312	1 C-S, 1 A-L
4	124,464	56,971	12,877	194,312	1 C-S, 1 A-L
6	123,959	65,996	4,356	194,312	1 C-S, 1 C-L
8	123,959	65,996	4,356	194,312	1 C-S, 1 C-L

Table 3-17: The impact of operational cost when both conventional ships and low degree autonomous ships are involved

Coefficient	Total profit	Voyage cost	Capital cost	Profit	Ship fleet
1	136,553	52,964	4,795	194,312	1 A-S, 1 A-L
2	123,959	65,996	4,356	194,312	1 C-S, 1 C-L
3	123,959	65,996	4,356	194,312	1 C-S, 1 C-L

Another crucial factor that influences the adoption of autonomous ships is government policies. Government intervention may be driven by objectives such as promoting technological innovation, stimulating economic growth, reducing environmental impact, and enhancing maritime safety. The government can stimulate the adoption of autonomous ships by offering subsidies or establishing regulations on the proportion of autonomous ships owned by shipping companies. Subsidies can effectively reduce either the capital or the operational costs, and their impacts align with those discussed in the impact of cost structure. Setting the proportion of autonomous ships owned by shipping companies can yield different outcomes, as demonstrated in Table 3-18. In the previous analysis, conventional ships were considered only when the operational costs of low-degree autonomous ships and high-degree autonomous ships respectively increased to two and four times their original values. Therefore, we use the results obtained by scaling the operational costs to the corresponding multiples as the reference for comparison. Table 3-18 indicates that when autonomous ships are advantageous, there is no need to set a proportion because the optimal results will not include conventional ships. However, if conventional ships are preferred, setting the proportion will reduce the profits of shipping companies. In such cases, the government would need to provide additional benefits to compensate for the profit losses.

In summary, the level of automation and government policies, such as subsidies and regulations on the proportion of autonomous ships owned by shipping companies, play a significant role in shaping the application of autonomous ships. Higher levels of automation can provide autonomous ships with a capacity advantage. However, when making decisions, shipping companies must also consider the impact of costs. Government intervention can potentially result in reduced profits for shipping companies. Therefore, it is necessary to provide compensation measures to mitigate any financial losses incurred by these companies.

Table 3-18: The impact of setting proportion

Case	Proportion	Total profit	Voyage cost	Capital cost	Profit	Ship fleet
I	none	123,959	65,996	4,356	194,312	1 C-S, 1 C-L
	10%	123,272	66,505	4,534	194,312	1 C-L, 1 A-S
	30%	123,272	66,505	4,534	194,312	1 C-L, 1 A-S
	50%	123,272	66,505	4,534	194,312	1 C-L, 1 A-S
	100%	121,064	68,453	4,795	194,312	1 A-S, 1 A-L
II	none	123,959	65,996	4,356	194,312	1 C-S, 1 C-L
	10%	121,408	65,951	5,000	192,359	1 C-M, 1 A-L
	30%	121,408	65,951	5,000	192,359	1 C-M, 1 A-L
	50%	121,408	65,951	5,000	192,359	1 C-M, 1 A-L
	100%	114,702	73,660	4,795	193,156	1 A-S, 1 A-L

Notes: Case I denotes the condition where conventional ships and autonomous ships with seafarers on board are considered, while Case II denotes the condition where conventional ships and autonomous ships without seafarers on board are considered. The "none" in the "Proportion" column means there is no restriction on the proportion of the autonomous ships.

3.6 CONCLUSIONS

Although autonomous ships may be the future of the shipping industry, they are currently in the early stages. Very little research has been conducted on the influence of autonomous ships on conventional ones in national waterways. In this paper, we have developed a two-stage stochastic programming model to investigate the impact of autonomous ships on shipping company operations. In the first stage, optimal routes, fleet composition, and fleet assignment are determined without the realization of demand uncertainty. In the second stage, when demand realization becomes known, the liner company determines the delivery pattern, i.e., the volume of cargo loaded on each ship from each feeder port. The objective is to maximize the expected total profit. An approximation algorithm SAA and an exact solution method TPBBC were proposed to solve the problem. To speed up the computations, we have used acceleration strategies, such as column generation and variable fixing.

The solution methods were validated by numerical experiments based on real-world data. After comparison, TPBBCCGVF-I was proved to be more suitable and efficient for this research. Sensitivity analyses are conducted to further explore the influences of key factors and derive valuable managerial insights to guide practical implementation in shipping companies. Our results show that autonomous ships are competitive under most of the scenarios considered. Besides, it was proved that the satisfaction of all demands will lead to a decrease in total profits.

Despite the contributions and insights provided by this study, there are certain limitations that should be acknowledged. Firstly, this research assumes full automation of ships that can operate without human intervention. However, in reality, autonomous ship technology is still in the research and development stage, and achieving full automation requires multiple stages of development and testing. Therefore, to better reflect the evolutionary process of autonomous ships, future research can consider developing a multi-period model that incorporates the characteristics of autonomous ships at different stages of development. Secondly, the current study addresses demand uncertainty by using scenarios, which may not capture the full range of demand characteristics. To overcome this limitation, future research can explore the use of advanced data analytics and machine learning techniques to enhance the accuracy of demand modelling.

Chapter 4: Optimal subsidy design for energy generation in ship berthing[8]

This chapter focuses on addressing the challenge of reducing the maximum sulfur content in exhaust gas to comply with maritime regulations. When berthing, three prominent methods are employed for regulatory compliance: marine diesel oil, scrubber, and shore power. While scrubber and shore power possess greater potential for emission reduction, they may incur higher costs compared to marine diesel oil. In an effort to encourage the adoption of scrubber and shore power, the government provides subsidies. Consequently, this chapter introduces a bi-level mixed-integer programming model designed to align with the objectives of both the government and ship operators. Given the intricate interdependence within the bi-level structure, solving the problem poses challenges. An efficient method integrating transformation and linearization is proposed for resolution. Numerous numerical experiments are conducted to assess the model's performance. The results indicate that the promotion of scrubber or shore power should commence with larger ships. Additionally, increasing the number of ships equipped with scrubber or shore power leads to a reduction in subsidies. Furthermore, each subsidy corresponds to a specific utilization range, enabling the government to tailor the subsidy amount according to the targeted utilization level.

4.1 INTRODUCTION

Environment is the foundation for human survival and development, so environmental protection has undoubtedly become the consensus of all walks of life. Shipping, the backbone of economic development, becomes one of the biggest threats to the environment. According to the Fourth IMO GHG Study, shipping emissions, including greenhouse gas (GHG), SOx, and particulate matter (PM), represent a non-

[8] Wang, W., Wang, S., & Zhen, L. (2023). Optimal subsidy design for energy generation in ship berthing. Maritime Policy & Management, 1-14.

negligible percentage of total annual anthropogenic emissions and are increasing every year. These exhaust emissions cause more than 70,000 premature deaths annually all over the world (Huang, et al. 2018). Endresen et al. (2003) show that nearly 70% of ship emissions come within 400 km of land, greatly contribute to air quality degradation in coastal areas. This pollution is of particular concern due to its proximity to the population in coastal areas and its potential to grow continually. If no effective control measures are implemented, problems caused by exhaust emissions will be exacerbated.

To reduce ship air pollution, IMO (International Maritime Organization) enacted MARPOL Annex VI[9] to limit the main air pollutants, SOx and NOx, contained in ships exhaust gas and revised it by reducing the maximum sulphur content in the exhaust gas to 0.1% by 2015 in emission control area (ECA) and globally to 0.5% by 2020. This sulphur content cap could be achieved by using abatement technologies, such as scrubber, or alternative compliant fuels.

According to the Fourth IMO GHG Study, heavy fuel oil (HFO), cheap but high in sulphur, remains the dominant fuel in international shipping, accounting for 79% of total fuel consumption by energy content in 2018. This type of oil, with a sulphur content of up to 3.5%, cannot meet the requirement of IMO and thus needs to use scrubber to clean exhaust gap before emission. Marine diesel oil (MDO) that is more expensive than HFO but can abide by the 0.5% sulphur content regulation has experienced 6% market share growth in recent years. Another emerging and promising energy supply method, shore power, has been successfully implemented in several ports around the world (Qi, Wang, and Peng 2020). All these methods could greatly reduce sulphur emission and comply with IMO regulations, but their efficiency and costs vary significantly. For example, scrubber can reduce 90–99% SOx and 60–85% PM and using shore power will not generate emissions in port areas. About the cost, the acquisition costs of scrubbers for 15,000, 110,000, and 310,000 dwt ships are 2.6, 3.3 and 4.2 million USD respectively (Lindstad, Rehn, and Eskeland 2017). Prices of HFO and MDO change every day. Taking Singapore as an example, prices of HFO

[9] The introduction of MARPOL Annex VI can refer to this website: https://www.imo.org/en/OurWork/Environment/Pages/Index-of-MEPC-Resolutions-and-Guidelines-related-to-MARPOL-Annex-VI.aspx

and MDO were 390 and 648.5 USD/mt respectively on February 7, 2023, but changed to 406.5 and 662.5 USD/mt respectively on the next day. The modification cost of a ship to receive onshore power ranges from 500,000 to 2 million USD (Wang, Mao, and Rutherford 2015). The shore power price ranged between 0.17–0.2 USD/kWh for ports along the coastline of China in 2019 (Wang, Qi, and Laporte 2022). Since ship operators are most concerned with cost, they usually choose the least costly method, which may not be the most ideal approach to environmental protection. Therefore, the government needs to make subsidy plan to reduce the cost born by ship operators to steer them towards efficient green methods.

Therefore, this research involves two decision-making parties: the government aims to achieve the desired utilization level[10] of each method at the lowest subsidy cost, while the ship operators adopt the least costly energy generating method. A bi-level optimization model is developed to formulate this problem, which is difficult to solve due to the interdependence and nonlinearity. We therefore convert the bi-level model into single-level model and linearize the nonlinear components to make it computationally tractable. Several numerical experiments are conducted to evaluate the performance of the model. Valuable managerial insights are also derived from sensitivity analyses.

4.2 RESEARCH GAP

After reviewing literature, we can find that most research considers only one innovative technology to solve environmental problem in maritime industry. However, the proliferation of pollution abatement technologies gives ships at berth more options. Therefore, one contribution of this research is to simultaneously consider three techniques: MDO, scrubber, and shore power. Besides, increasing the number of available techniques does not change the model, which means this model is very flexible for practical policy making. There are price differences between these three technologies, so in order to promote a certain technology, we need to consider subsidy.

[10] Since green technologies such as scrubber and shore power can significantly reduce harmful emissions, to promote the use of these technologies, some governments may set target utilization level. For example, the California Air Resources Board (CARB) requires that every vessel coming into a regulated California port either use shore power (e.g., plug in to the local electrical grid) or a CARB-approved control technology, such as scrubber, to reduce harmful emissions.

Another contribution is that we consider ship type and target utilization level of three techniques when designing subsidy. Under the same subsidy plan, ships in different types will act differently. Different utilization level will influence subsidy plan. Therefore, results obtained from the model considering ship type and target utilization level are more instructive for practical implementation. The third contribution is that we propose a bi-level mixed integer programming model to solve the problem which is rarely used in subsidy design in ship operation management.

4.3 PROBLEM DESCRIPTION AND FORMULATION

4.3.1 Problem Description

This chapter presents a bi-level optimization model involving government and ship operators. The methodological framework is the Stackelberg game where the government is the leader that determines subsidy for each energy generation method, aiming to achieve the desired utilization levels at the lowest cost, while the ship operators are followers that choose the lowest cost energy generation method considering government subsidies.

In this article we consider a port that abides by 0.5% sulphur content regulation and has already installed shore power facilities to provide shore power service to ships. Ships that visit this port can be divided into four types: without scrubber and shore power equipment, with only scrubber, with only shore power equipment, and with both scrubber and shore power equipment. The first type can only use MDO to supply energy while berthing. The second can choose between MDO and HFO. If HFO is used, exhaust gas needs to be cleaned by scrubber. The third can choose between MDO and shore power. The last one can choose among MDO, HFO, and shore power. The energy generation methods while berthing, i.e., MDO, HFO, and shore power, are represented by a set I. It is indexed by i with $i = 0$ indicating a ship uses MDO to generate energy, $i = 1$ indicating a ship uses HFO to provide energy while using scrubber to clean exhaust gas, and $i = 2$ indicating a ship uses shore power to supply energy. Ships visiting this port are represented by a set V. We assume that information about ship set V is known, including total number of ships, equipment that each ship owns, total energy consumption while berthing, and cost of each method to provide required energy. The total number of ships visiting this port is denoted by n. The number of ships equipped with scrubber but not shore power, with shore power but

not scrubber, and with both scrubber and shore power are denoted as n_s, n_p, and n_{sp}, respectively. Since using scrubber and shore power could greatly reduce sulphur emissions, government has set the minimum utilization levels α and β of the two technologies, where $\alpha \leq \frac{n_s+n_{sp}}{n}$, $\beta \leq \frac{n_p+n_{sp}}{n}$, and $\alpha+\beta \leq \frac{n_s+n_p+n_{sp}}{n}$. To achieve these levels, government needs to provide subsidy s_i for a ship that uses energy generation method $i \in I$ to lower the energy cost. The operator of ship $v \in V$ react according to subsidy to make decisions x_i^v on whether to use power generation method i ($x_i^v = 1$) or not ($x_i^v = 0$).

4.3.2 Mathematical Model

Before presenting the mathematical model, we list all the notations in Table 4-1.

Table 4-1: Notations used in this research

Notations	Definition
Sets and Indices	
I	Set of energy supply methods while berthing, where I = {0=MDO, 1=HFO+scrubber, 2=shore power}
V	Set of ships visiting a port
i	Index of energy supply method while berthing, $i \in I$
v	Index of a ship, $v \in V$
Parameters	
C_i^v	Cost of powering ship v using method i (it does not include government subsidy)
K_i^v	Binary parameter, =1 if ship v can be powered by method i, and =0 otherwise
α	The minimum utilization level of scrubber
β	The minimum utilization level of shore power
Decision variables	
x_i^v	Binary variable, =1 if ship v uses method i to generate energy, and =0 otherwise
s_i	Government subsidy for using method i
$\vec{x}^v$	Vector of decision variable x_i^v for ship v, where $\vec{x}^v = (x_0^v, x_1^v, x_2^v)$
$\vec{s}$	Vector of decision variable s_i, where $s_i = (s_0, s_1, s_2)$

Then the problem faced by the government can be described by the following model:

$$\text{Min} \sum_{v\in V} \sum_{i\in I} s_i\, x_i^v \tag{4-1}$$

subject to

$$\frac{\sum_{v\in V} x_1^v}{|V|} \geq \alpha \tag{4-2}$$

$$\frac{\sum_{v\in V} x_2^v}{|V|} \geq \beta \tag{4-3}$$

$$s_i \geq 0, \forall i \in I \tag{4-4}$$

$$\vec{x}^v \in \Phi^v(\vec{s}) \text{ , } \forall v \in V \tag{4-5}$$

where $\Phi^v(\vec{s})$ is determined by the following model:

$$\Phi^v(\vec{s}) = \text{argmin} \sum_{i\in I}(C_i^v - s_i)x_i^v \quad (4\text{-}6)$$

subject to

$$\sum_{i\in I} x_i^v = 1 \quad (4\text{-}7)$$

$$x_i^v \le K_i^v, \forall i \in I \quad (4\text{-}8)$$

$$x_i^v \in \{0,1\}, \forall i \in I. \quad (4\text{-}9)$$

The objective function (4-1) aims to minimize total subsidy. Constraint (4-2) and (4-3) set utilization rate for scrubber and shore power separately. Constraints (4-4) specify the domains of the subsidy decision. Parameters x_i^v depend on decisions of ship operators, which are denoted by $\Phi^v(\vec{s})$.

Since each ship makes decisions independently, we build $\Phi^v(\vec{s})$ for each ship $v \in V$. The objective function (4-6) aims to minimize its energy cost while berthing. Constraint (4-7) requires that each ship must choose one method for energy supply. Constraints (4-8) state that if a ship is to be powered by certain method, it must have corresponding equipment. Constraints (4-9) are domains of decision of ship operators.

4.4 SOLUTION METHOD

The problem is difficult to solve because of the interdependence between bi-level structure. The leader's decisions have an impact on the follower's decisions, which in turn, influence the leader's objective function value. What is more, the problem is non-linear. Therefore, we first convert the bilevel model into an equivalent single-level model, and then reformulate the model by linearization. This new model could be easily solved by an off-the-shelf CPLEX solver.

4.4.1 Single-level Model

Since ship operators are most concerned with cost, they will choose the available and least costly method of energy generation. Therefore, the decision-making process at the ship level can be represented by the following constraints:

$$(C_i^v - s_i) - \left(C_j^v - s_j\right) \le M^v\left(1 - x_i^v + 1 - K_j^v\right), \forall i \in I, j \in I\backslash\{i\}, v \in V \quad (4\text{-}10)$$

where $M^v = \max_{i=0,1,2} C_i^v$.

Constraints (4-10) ensure that ship operator will choose the available and lowest cost method. This transformation is successful because the lower-level problem is a

binary decision problem that does not entail continuous variables or nonlinear constraints.

4.4.2 Model Linearization

The objective (4-1) contains the product of decision variables, namely $s_i x_i^v$. We linearize it by introducing decision variables z_i^v, which means the subsidy for ship v to be powered by method i. Then the objective function is converted to:

$$\text{Min} \sum_{v \in V} \sum_{i \in I} z_i^v \tag{4-11}$$

with four set of constraints:

$$s_i - z_i^v \leq \widehat{M}(1 - x_i^v) \,, \forall i \in I, v \in V \tag{4-12}$$

$$z_i^v \geq 0, \forall i \in I, v \in V \tag{4-13}$$

$$z_i^v \leq s_i, \forall i \in I, v \in V \tag{4-14}$$

$$z_i^v \leq \widehat{M} x_i^v, \forall i \in I, v \in V \tag{4-15}$$

where $\widehat{M} = \max_{v \in V} \max_{i=0,1,2} C_i^v$.

The bilevel model is therefore converted into an equivalent single-level model with objective function (4-11) and constraints (4-2)–(4-4), (4-7)–(4-9), (4-10), (4-12)–(4-15).

4.5 NUMERICAL EXPERIMENTS

In this section, we conducted multiple numerical experiments to validate the model and derive managerial insights. These experiments have different values of crucial parameters, including C_i^v, K_i^v, α, and β. All the experiments were carried out on a Dell XPS 15 9500 laptop with i7-10750H CPU, 2.60 GHz processing speed and 16 GB of memory. The model was implemented in C++ and solved by CPLEX 12.10.

4.5.1 Parameter Setting

The parameters were based on existing studies and reports. The Port of Shanghai (POS) is selected to test subsidy plan under different experiments. Dai et al. (2019) divide container ships visiting POS into 4 categories according to their capacities, i.e., 0–4000 TEU, 4000–8000 TEU, 8000–12000 TEU and 12000+ TEU. For each category, ships fall into this category are the same, which means that these ships have the same capacity, power consumption at berth, and gross tonnage that are set to the

average values of this category. The total annual energy consumption for ships that belong to category t while berthing is calculated by following equations:

$$E_t = N_t \times AP_t \times T_t \quad (4\text{-}16)$$

$$AP_t = W_t \times R \times L \quad (4\text{-}17)$$

where E_t is the total annual energy consumption at berth (kWh); N_t is the total number of annual ship calls; AP_t is average power consumption at berth (kW); T_t is the average berthing time for each ship call (h). Since when ships use shore power, it takes an average of 2 hours to connect devices, we added 2 hours to T_t for ships using shore power. W_t is the gross tonnage of the ships in category t (ton). R is the ratio of power consumption by tonnage, set to 0.2 kW/t, and L (set to 0.17) is load factor that measures the utilization rate of power consumption. The values of parameters related to energy consumption are shown in Table 4-2.

Table 4-2: Parameter values related to the ship category

	Ship category			
	I	II	III	IV
Average capacity (TEU)	2,000	6,000	10,000	15,000
Average gross tonnage (ton)	20,000	60,000	100,000	150,000
Total ship calls	6,612	2,628	1,608	1,152
Average time at berth (h)	33.2	19.8	24.8	28.9

To calculate cost for each energy supply method per ship call, we first calculate energy consumption of each energy supply method. For MDO and HFO, we need to multiply energy conversion rate. As shown in Wild (2005), it takes an average of 244g MDO or 260.5g HFO to generate 1 kWh energy. We then multiply energy consumption by the corresponding energy price. The price information is obtained from Lindstad, Rehn, and Eskeland (2017) and Yu, Voß, and Tang (2019). The prices for MDO, HFO, and shore power are 644 USD/mt, 491 USD/mt, and 0.12 USD/kWh. Having cost and energy consumption information, the energy cost using different energy supply methods for a ship call can be calculated. The results are shown in Table 4-3.

Table 4-3: Costs (dollar) of energy supply methods per ship call

	Ship category			
	I	II	III	IV
MDO	3,548	6,347	13,250	23,160
HFO	6,299	7,607	14,182	23,306
Shore power	6,489	8,024	14,606	23,673

Table 4-2 shows ship category according to average gross tonnage. We also mentioned in Chapter 4.3.1 that ships visiting a port can be divided into four types: without scrubber and shore power equipment, with only scrubber, with only shore power equipment, and with both scrubber and shore power equipment. Therefore, we have 16 ship types and we use parameter r_c^t to represent the ratio of ships that are equipped with t devices, where $t = \{\text{neither, scrubber, shore power, both}\}$, in category c, where $c = \{\text{I, II, III, IV}\}$. For example, if $r_I^{scrubber} = 5\%$, it means that the number of ships that are equipped with scrubber in category I is 331 ($6612 \times 5\%$). We set 6 scenarios for the ratio which are shown in Table 4-4. We assume that the proportion of ships equipped with a certain device is equal in different ship categories.

Table 4-4: Scenarios for type ratio

	Neither	Scrubber	Shore power	Both
Scenario 1	85%	5%	5%	5%
Scenario 2	70%	10%	10%	10%
Scenario 3	55%	15%	15%	15%
Scenario 4	40%	20%	20%	20%
Scenario 5	25%	25%	25%	25%
Scenario 6	10%	30%	30%	30%

4.5.2 Computational Performance

We set both α and β to 5% under 6 scenarios. The computational results under 6 scenarios are shown in Table 4-5. The second column is the total subsidy for all ship calls. The third column is the subsidy for each energy supply method for one ship call, where the first number is the subsidy for using MDO, the second one is the subsidy when powering ships with HFO and cleaning exhaust gas with scrubber, and the last number is the subsidy for using shore power. The last column is the running time.

Table 4-5: Results for 6 scenarios

	Objective (USD)	Subsidy for Methods (USD)	Time (s)
Scenario 1	3,415,200	{0, 2751, 2941}	2.75
Scenario 2	1,762,200	{0, 1260, 1677}	14.3
Scenario 3	1,372,800	{0, 932, 1356}	37.02
Scenario 4	1,372,800	{0, 932, 1356}	121.27
Scenario 5	1,372,800	{0, 932, 1356}	109.94
Scenario 6	-	-	>7200

Note: "-" means results cannot be obtained within 7200s.

Table 4-5 shows that under the same value of α and β, increasing the proportion of ships equipped with scrubber and shore power devices could reduce total subsidy. Because both shore power and scrubber have scale economy, which means it is more beneficial for large-size ships. With the increase of ship size, the cost gap between energy supply methods becomes smaller and thus the subsidies for energy supply methods decrease. From scenario 1 to 6, the ratio of ships equipped with scrubber, shore power devices, and both increase from 5% to 30%, which means more large ships have the mentioned equipment. Since the subsidy for larger ships is cheaper and the requirements for ships using scrubber and shore power remain the same, more large-size ships will be subsidized and thus the total subsidy reduces.

The subsidy for each energy supply method will also reduce. As ships will choose the cheapest available supply method (i.e., MDO), to make ships use scrubber, the subsidy for using scrubber should be at least the cost gap between MDO and scrubber. It is the same for shore power. Since we set requirements for both scrubber and shore power, the cost for these three methods should be equal for at least one category. The cost gaps decrease as ship size increases. With more large ships being able to use scrubber and shore power, the subsidies for these two methods decrease.

Solution time increases with scenario and for scenarios 6, results even cannot be obtained within 7200s. Because as the ratio increases, the constraints become more and more relaxed, the number of iterations increases during the solution process, and the convergence becomes slower, so the solution time becomes longer.

Figure 4-1 shows the proportion of ships using different energy supply methods in each category under 5 scenarios (Results for scenarios 6 are not shown since we did not obtain them). We can find that the proportion of ships using scrubber and shore power decreases in category I and II while increases in category III and IV when the

ratio of ships equipped with these devices increases. This suggests that when promoting scrubber and shore power in maritime industry, it is more cost-effective to implement on large ships.

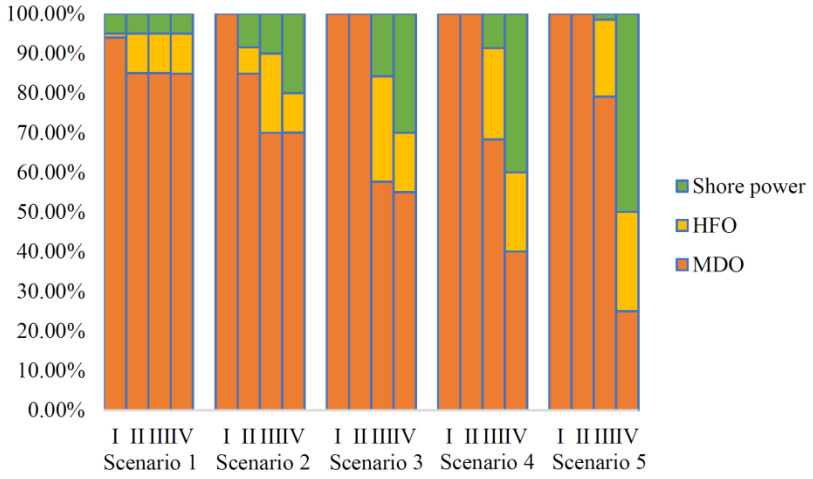

Figure 4-1: The proportion of ships using different energy supply methods in each category under 5 scenarios

4.5.3 Sensitivity Analysis

In this section, we investigated the impacts of some crucial parameters, such as α, β, and K_i^v. Since all scenarios should have the same trend, only with different key points, we conducted the sensitivity analysis on scenario 1.

In scenario 1, the ratios of ships equipped without any devices, with only scrubber, with only shore power devices, and with both equipment are 85%, 5%, 5%, and 5%, respectively. To study the impacts of α and β, we set one of them to 0 and the other from 1% to 10%. Figure 4-2 shows the proportion of ships using a certain energy supply method in different ship types with the change of α and β. I, II, III, and IV represent ship category, which were mentioned in Chapter 4.5.1. N, S, P, and B represent the equipment owned by ships, where N means ships have neither scrubber nor shore power devices, S means ships only have scrubber, P means ships only have shore power equipment, and B means ships have both devices. Therefore, we can obtain 16 ship types. Figure 4-2 (a) and Figure 4-2 (b) show the impacts of α, which means β was set to 0. Therefore, none of the ships chose shore power because of the expensive cost. With the increase of α, the proportion of scrubber-capable ships using MDO is on the decline, such as IS, IB, IIS, IIB, IIIS, IIIB, IVS, and IVB. While the proportion of using scrubbers is on the rise for these ship types. The ratio of category

IV changes first, until category I. Because the subsidy for ships of category IV to use scrubber is the cheapest while the most expensive for category I. The ratio for IVB remains at 0 for MDO utilization while 100% for HFO. Because all ship calls of this type represent less than 1% of the total number of ship calls. Therefore, to achieve 1% scrubber utilization, all ship calls of this type chose HFO. For ships belong to N and P, since they are not equipped with scrubber, they can only use MDO. The ratio for these ships remains at 100% for MDO utilization while 0 for HFO.

The same trend can be found for the impacts of β in Figure 4-2 (c) and Figure 4-2 (d), but for the different ship types. The proportion of ships belong to P and B using MDO declines, while increases for using shore power. For ships belong to N and S, since they do not have shore power equipment, they can only use MDO. The ratio for these ships remains at 100% for MDO utilization while 0 for shore power. The change for category I to IV also has a similar pattern.

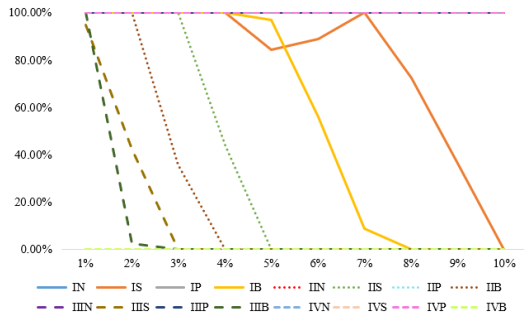

(a) The impact of α on the usage of MDO

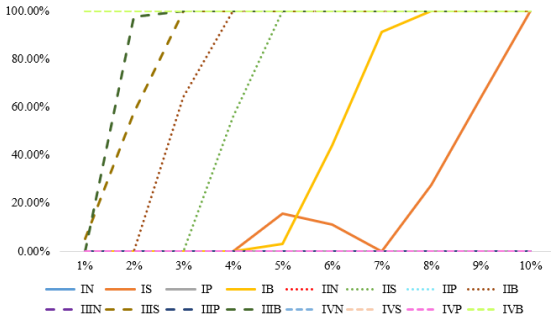

(b) The impact of α on the usage of HFO

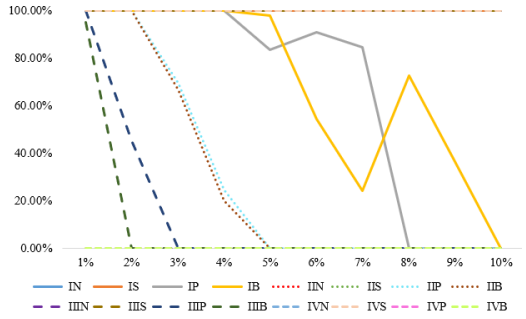

(c) The impact of β on the usage of MDO

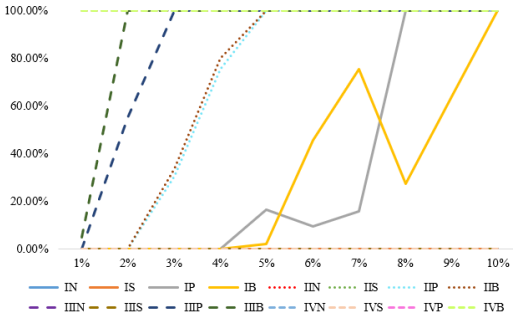

(d) The impact of β on the usage of shore power

Figure 4-2: The proportion of ships using different energy supply methods

The impacts of α and β on subsidy is shown in Figure 4-3. When we discuss the impacts of α, the subsidy for both MDO and shore power are 0. Therefore, we only show the trend for the subsidy for scrubber. This is the same for β, where we only

show the subsidy for shore power. We can see that with the increase of α and β, the subsidy for scrubber and shore power also increases. Because large ships require less subsidies, they are given priority.

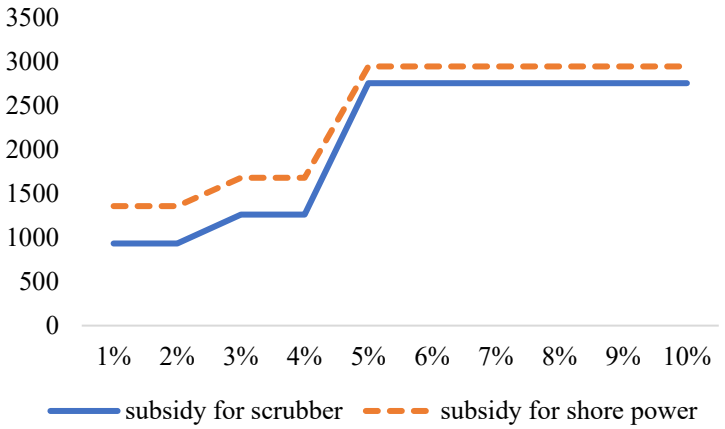

Figure 4-3: The impacts of α and β on subsidy

To investigate the impacts of K_i^v, we designed a new scenario where all ships are equipped with both scrubber and shore power devices. Because we want to figure out what the subsidy plan will be without equipment restriction. When all ships can choose among all the energy supply methods, they will choose the cheapest one. Table 4-6 shows the subsidy for scrubber and the range of α when only subsidy for scrubber is allowed. When no subsidy is given, all ship calls chose MDO. When the subsidy is 146, the cost of using MDO and HFO is the same for ship category IV. Therefore, all ship calls of category IV can choose between MDO and HFO. When the subsidy is 932, the cost of using MDO and HFO is the same for ship category III, while HFO is the cheapest in category IV. Therefore, all ship calls of category IV chose HFO while those of category III can choose between MDO and HFO. It is the same when subsidy is 1260 and 2750. Table 4-7 shows the subsidy for shore power and the range of β when only subsidy for shore power is allowed. Table 4-8 shows the subsidy for scrubber and shore power and the range of α and β. The calculation rule for subsidy and the range is the same as that in Table 4-6. Figure 4-4 compares the subsidy for scrubber and shore power under 7 scenarios when α and β are set to 5%. We can find that when more ships are equipped with scrubber and shore power devices, the subsidy can be reduced during promotion.

Table 4-6: The subsidy for scrubber and the range of α when only subsidy for scrubber is allowed

subsidy for scrubber	the range of α
0	0
146	0–9.6%
932	9.6%–23%
1260	23%–44.9%
2750	44.9%–100%

Table 4-7: The subsidy for shore power and the range of β when only subsidy for shore power is allowed

subsidy for shore power	the range of β
0	0
513	0–9.6%
1356	9.6%–23%
1677	23%–44.9%
2941	44.9%–100%

Table 4-8: The subsidy for scrubber and shore power and the range of α and β

subsidy for scrubber	subsidy for shore power	the range of α	the range of β	the range of $a+b$
0	0	0	0	0
146	513	0–a	0–b	0–9.6%
932	1356	0–a	9.6%–9.6%+b	0–13.4%
1260	1677	13.4%–13.4%+a	9.6%–9.6%+b	0–21.9%
2750	2941	44.9%–44.9%+a	0–b	0–55.1%

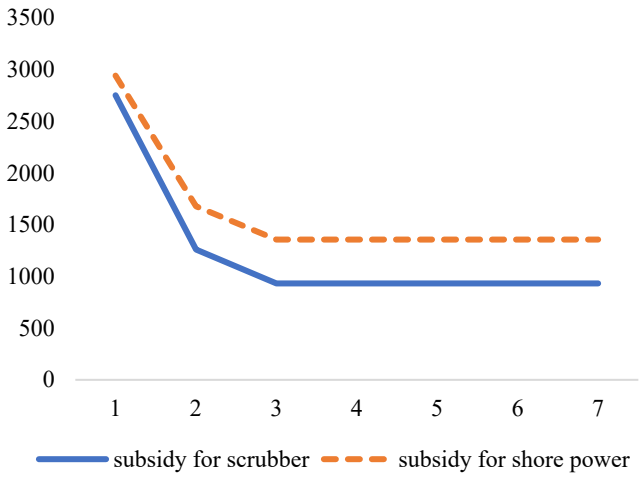

Figure 4-4: The subsidy for scrubber and shore power under 7 scenarios

We could also study the impacts of C_i^v. But it is obvious that reducing cost could reduce subsidy because the gap will become closer. When technology development makes the cost of using scrubber and shore power lower than MDO, no subsidy will need. All ships will actively choose these two supply methods.

From the analysis of Chapter 4.5.2 and Chapter 4.5.3, we can obtain the following managerial insights. First, in the initial stage of the promotion of scrubber or shore power, we should start with large ships. Because there is scale economy when installing scrubber or shore power for large ships. Besides, large ships consume more energy. The unit energy consumption cost of HFO and shore power is lower than MDO. Therefore, it is more cost-effective and easier to persuade large ships to use scrubber or shore power than small-size ships. Second, increasing the number of ships equipped with scrubber or shore power will reduce subsidy. Usually, the government chooses a one-time subsidy for ships willing to install the equipment. This research suggests that the government could also consider subsidizing ships for usage of scrubber or shore power. The more ships that are willing to install these devices, the less subsidy that the government will pay. Third, each subsidy corresponds to a utilization range. The government can choose the subsidy amount according to the target utilization level.

4.6 CONCLUSIONS

This research optimizes subsidy plan to promote the use of scrubber and shore power in maritime industry to reduce berth emissions. A bi-level optimization model is developed to formulate this problem where the government in the upper level minimizes total subsidy amount while ship operators in the lower level choose the cheapest available energy supply method. The problem is difficult to solve due to the interdependence and nonlinearity. We therefore convert the bi-level model into single-level model and linearize the nonlinear components to make it computationally tractable.

We conduct several numerical experiments using the data of Port of Shanghai to evaluate the performance of the model. Results suggest that in the initial stage of the promotion of scrubber or shore power, we should start with large ships. Besides, increasing the number of ships equipped with scrubber or shore power will reduce subsidy. Third, each subsidy corresponds to a utilization range. The government can

choose the subsidy amount according to the target utilization level. These results can provide guidance for the practical implementation of subsidies to promote the adoption of green technologies.

One limitation of this research is that we use average value of each ship category due to data limitation. It would be better if we could get more accurate data. For the future research, first, we can use machine learning to predict the parameter values for each ship category and use them as model input. Second, we can reformulate a more comprehensive model. For example, we can incorporate the emission reduction efficiency of different green technologies in the objective function. We take the sum of total subsidy and emission amount as a new objective function in the upper level. Also, for the lower-level problem, we can add ship operation cost in the model. For instance, different green technologies may have differences in fuel consumption, and we add the sum of bunkering cost in the objective function. Correspondingly, we need to add constraints regarding fuel consumption. Modifying the objective functions and constraints can make the model more comprehensive.

Chapter 5: A bi-level programming approach to optimize ship fouling cleaning[11]

This chapter focuses on cleaning the ship fouling that has significant adverse effect on both vessel performance and environmental sustainability. It involves two parties: cleaning service providers and shipping companies. The former decides the deployment of the cleaning equipment, while the latter decides when and where the fouling should be cleaned. The interaction between the two parties is formulated through a bi-level model. The computational complexity of the bi-level model is greatly simplified by transforming it into a single-level model. Numerical experiments are conducted using real-world data to evaluate the performance of the proposed models. Additionally, sensitivity analyses are performed to investigate the influence of key parameters.

5.1 INTRODUCTION

Maritime shipping is a crucial component of global logistics, responsible for delivering over 80% of global trade by volume in 2022 according to the United Nations Conference on Trade and Development (UNCTAD). During shipping voyages, various marine organisms, such as algae, plants, and small animals, attach to the surface of a ship's hull, leading to ship fouling. Such ship fouling has significant adverse effects on both vessel performance and environmental sustainability. First, it increases hydrodynamic drag, which in turn increases fuel consumption and greenhouse gas emissions. Utama and Nugroho (2018) provide an overview of the relationship between biofouling, ship drag, and fuel consumption. Hakim et al. (2017) conclude that fuel consumption in-creases by about 10% in a year due to marine fouling. Second, ship fouling can facilitate the transport and introduction of non-native species, leading to ecological disturbance and potential damage to marine ecosystems.

[11] Wang, W., Guo, H., Li, F., Zhen, L., & Wang, S. (2023). A bi-level programming approach to optimize ship fouling cleaning. Journal of Marine Science and Engineering, 11(12), 2324.

Fitridge et al. (2012) show that a conservative estimate of the direct economic losses caused by biofouling on the aqua-culture industry is 5%–10%. Therefore, it is imperative to regularly clean ship hulls to reduce the adverse impacts of biofouling. There are two main approaches to keeping a ship's hull clean: the first approach is to use antifouling coatings (Farkas et al., 2021), and the second is hull cleaning (Dinariyana et al., 2022; Farkas et al., 2022). Antifouling coatings, as the name suggests, involve the application of special coatings to the surface of a ship's hull to reduce the attachment of pollutants and marine organisms. These coatings typically contain additives that deter biofouling, making the surface of a ship's hull easier to clean than in the absence of such coatings. Conversely, hull cleaning involves the physical or chemical removal of pollutants and marine organisms that have already attached to the surface of a ship's hull. Methods used include scraping, high-pressure water cleaning, high-frequency ultrasonic cleaning, and chemical cleaning.

This chapter primarily focuses on the second approach, that is, the cleaning of a ship's hull when pollutants and marine organisms are already attached. Those interested in antifouling coatings can refer to references (Yebra, Kiil, and Dam-Johansen, 2004; Maan et al., 2020). Many countries have issued regulations on biofouling cleaning. For example, New Zealand and Australia require all vessels to carry out hull cleaning within 30 days of arrival in their ports 1. These regulations aim to prevent the spread of invasive species due to contaminated hulls and to maintain the ecological balance of marine ecosystems.

The hull cleaning process involves two parties: cleaning service providers and shipping companies. The former provide cleaning equipment and services, aiming to maximize their profits, whereas the latter decide whether and where to use the cleaning service such that their cost is minimized. To formulate the interaction between the two parties, a bi-level non-linear programming model was developed. In the upper level of the model, the service provider makes decisions regarding the deployment of equipment, considering factors such as service revenue and equipment costs. Meanwhile, in the lower level, shipping companies optimize their cleaning decisions by balancing the cost of fouling cleaning, the additional fuel cost caused by fouling, and the availability of cleaning equipment. The problem is challenging from a computational standpoint due to the interaction between the decisions at both levels

and the non-linearity of the lower-level problem. To address the complexity of the problem, the bi-level non-linear model is transformed into a single-level linear model using the big-M method, a mathematical technique used in linear programming to handle constraints with binary decision variables. The transformed problem can be easily solved by the off-the-shelf Gurobi solver, a widely used software package for linear programming (LP), mixed-integer linear programming (MILP), quadratic programming (QP), mixed-integer quadratic programming (MIQP), and other related optimization problems. Numerical experiments are conducted to compare the performance of the proposed solution method with a heuristic algorithm that iteratively solves the up-per-level and lower-level problems in sequence until the upper-level solution remains unchanged. The results demonstrate that the proposed method, which transforms the bi-level model into a single-level model, is well suited to the problem as it significantly speeds up computation compared with the heuristic algorithm. Furthermore, the results of the numerical experiments suggest that cleaning service providers engage in partial demand fulfillment to maximize profit. In addition, it is recommended that equipment procurement be prioritized in the first year. Sensitivity analyses are per-formed to explore the impact of key parameters. The findings reveal that requiring full demand satisfaction results in a USD 27 million loss in profit for the cleaning service providers. Increases in the purchase cost of equipment also decrease the providers' profits and potentially lead to some service providers exiting the market. However, in-creasing cleaning price will increase total profits at the expense of fulfilling only a portion of the demands.

5.2 RESEARCH GAP

While the literature has extensively examined the effects of fouling, cleaning methods, and cleaning schedules, there remains a gap in comprehensive research that simultaneously addresses the optimal locations and timing for ship cleaning, as well as the appropriate number of devices to be deployed. Also, the bi-level models have not been conducted to explore ship fouling cleaning when cleaning service providers and ships interact with each other. Therefore, the main contributions of this research are three folds. First, this study provides a quantitative approach to optimize the fouling cleaning process, which is a unique contribution compared to the existing literature. By applying mathematical techniques and optimization methods, the present

research offers a systematic framework for achieving efficient and effective foul cleaning. Second, the present research introduces a bi-level model that incorporates both service providers and demanders. In this model, the upper-level decision makers, who are the service providers, determine the optimal deployment of cleaning equipment, including location, quantity, and timing, in order to maximize total profits. On the other hand, the lower-level decision makers, which are the ships, decide when and where to clean fouling to minimize the total cost. It is important to note that the upper-level deployment decision influences the cleaning decisions of the lower-level ships, while the lower-level decisions also impact the upper-level deployment. This bi-level model allows for the simultaneous optimization of equipment deployment and service purchase decisions. By considering the interactions between these two groups, the study offers comprehensive solutions that address the needs and objectives of both service providers and demanders. Third, to enhance computational efficiency, the present research transforms the complex bi-level non-linear problem into a single-level linear problem through the big-M method, which converts the formulation of the lower-level problem into constraints for the upper-level problem. By doing so, the two problems are effectively merged into a single-level optimization problem, which can be solved using linear programming techniques. This transformation simplifies the optimization process and reduces the computational complexity, resulting in faster solution times.

5.3 PROBLEM DESCRIPTION AND FORMULATION

This section presents problem description and the model formulation. The main nomenclature is summarized in Table 5-1, and additional ones will be introduced whenever necessary.

Table 5-1: Nomenclature

Sets	
R	Set of container shipping routes, indexed by r, $r \in R$
P	Set of all ports on shipping routes, indexed by p, $p \in P$
S	Set of homogenous ships, indexed by s, $s \in S$
N	Planning period, indexed by n, $n \in \{1, \dots, \lvert N \rvert\}$
Φ_s	An ordered set of port–time pairs of ship s
Φ_{sk}	Set of all port–time pairs of ship s at the kth year
Ω_s	Set of all port–time pairs of ship s that have $y^*_{spt} = 1$
Ω_{sk}	Set of all port–time pairs of ship s that have $y^*_{spt} = 1$ and $365(k-1) < t \leq 365k$
V_{spt}	Set of ships that are in service at port p when ship s arrives at this port at the port–time pair (p, t)
$\mathbb{Z}_0^+$	Set of non-negative integers
Parameters	
C^f	The unit fuel cost (USD/nautical mile)
C^p	The cleaning price (USD) at port p
C^e	The amortized purchasing cost (USD/year) of cleaning equipment
L_{sp}	The distance (nautical mile) of the next leg for ship s after visiting port p
D_{sp}	The dwell time (days) of ship s at port p
α	The increase in the rate of fouling (kg/m^2·day)
β	The coefficient between fuel consumption growth rate and ship fouling level
π_{spt}	The position of port–time pair (p, t) at set Φ_s
τ_{spt}	The position of port–time pair (p, t) at set Ω_s
Decision variables	
x_{pn}	The amount of equipment to be deployed at port p at the beginning of the nth year
y_{spt}	Binary variable which equals 1 if the ship s cleans fouling at the port–time pair (p, t) or 0 otherwise
F_{spt}	The fouling accumulation (kg) on a ship s at port–time pair (p, t)

The present research designs the plan for cleaning equipment deployment and ship fouling cleaning in a liner shipping network with a set of shipping routes, with the set indicated by R. Let N be the set of the planning horizon consisting of $|N|$ time periods, each corresponding to a year. In this context, the route $r \in R$ is defined as a closed loop, serving $|P_r|$ ports of call and $|A_r|$ legs, where $|A_r| = |P_r| - 1$. For instance, the route r can be described by (a, b, c, d, a) where port a, b, c, d, and a are the first, second, third, fourth, and fifth port of call, respectively. The voyage from the i^{th} port of call to the $(i+1)^{\text{th}}$ port of call is the i^{th} leg. The collection of all ports within these routes forms the set P. A fleet of homogeneous ships, denoted as S, sails along

these routes. Each ship $s \in S$ operates exclusively and repeatedly on a single route, as illustrated in Figure 5-1. In contrast, a route may accommodate multiple ships with diverse schedules, as depicted in Figure 5-2. When ship s arrives at port p, its time of arrival is recorded as t (measured in days), creating a port–time pair denoted as (p, t). These pairs are arranged in the order of the ship's ports of call. For any $n \in N$, there is an ordered set Φ_{sn} including all the port–time pairs of ship s in which the time t satisfies $365(n-1) < t \leq 365n$. All port–time pairs of ship s during planning period N are combined to form the ordered set Φ_s, where $\Phi_s = \bigcup_{n \in N} \Phi_{sn}$. It is important to note that all ships accumulate fouling during their voyages. It is assumed that biofouling does not increase while a ship is in motion due to its high speed. However, when a ship remains stationary, such as when floating or at berth, fouling accumulates linearly with time at a rate of α. The extent of fouling accumulation on ship s when arriving at a given port–time pair (p, t) is denoted as F_{spt} (kg/m^2). For instance, in Figure 5-1, ship s departs from port a without any fouling on the first day. After three days of sailing, it arrives at port b with no fouling accumulation ($F_{sb4} = 0$). However, after spending two days berthed at port b, the fouling on the ship increases to 2α ($F_{sb4} + 2\alpha = 2\alpha$). Furthermore, it is assumed that the growth rate of fuel consumption is linearly related to fouling, with a coefficient of β. For example, considering the fouling of ship s before departing from port b as 2α, fuel consumption will increase by the proportion of $2\alpha\beta$ when the ship travels from port b to port c.

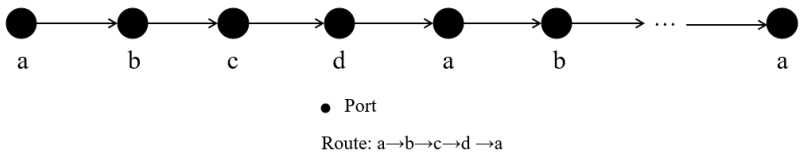

Figure 5-1: An example of a ship sailing repeatedly on a route

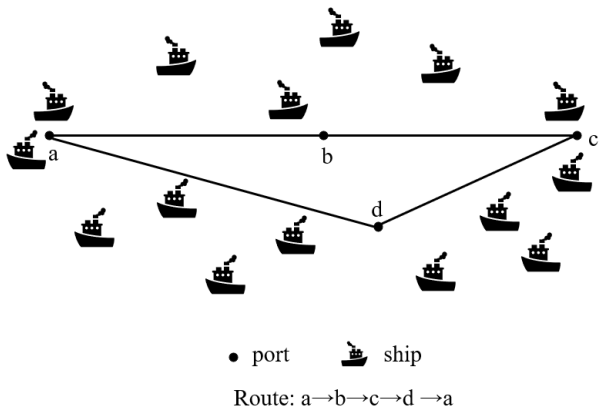

Note: Each of the ships may have a different schedule, and their positions along the route vary based on their individual schedules.

Figure 5-2: An example of a route accommodating multiple ships with diverse schedules

5.3.1 Bi-level Decisions

Two parties are involved in the present research: cleaning service providers and ships. The service providers provide fouling cleaning services at different ports with different prices, while ships arriving at a port of call decide whether to purchase the fouling cleaning service from the service providers. The research problem is formulated as a bi-level model. In the upper level, service providers optimize their service deployment strategies. In the lower level, ships, as the customers of fouling cleaning services, optimize their cleaning decisions.

Before introducing the bi-level problem, it should be mentioned that ships are cost-driven, which means that regardless of the deployment plans proposed by service providers, each ship s has its own optimal decisions as to where to use the cleaning service. The decisions are exclusively determined by total costs, as shown in the following model:

[P1] Minimize $\sum_{(p,t)\in\Phi_s}\left[\left(F_{spt}+\alpha D_{sp}\right)\beta\left(1-y_{spt}\right)C^f L_{sp}+C^p y_{spt}\right]$ (5-1)

subject to

$$F_{spt}=\left(F_{sp't'}+\alpha D_{sp'}\right)\left(1-y_{sp't'}\right),\ \forall(p,t),(p',t')\in\Phi_s:\pi_{spt}-\pi_{sp't'}=1 \quad (5\text{-}2)$$

$$y_{spt}\in\{0,1\},\ \forall(p,t)\in\Phi_s. \quad (5\text{-}3)$$

The objective Function (5-1) minimizes total costs which consist of additional fuel costs incurred by biofouling and cleaning costs. Constraints (5-2) are a state

transition function between two consecutive states. Constraints (5-3) define y_{spt} to be binary.

Since P1 is deterministic, the optimal solutions $y^*_{spt}, \forall(p,t) \in \Phi_s, s \in S$ can be easily obtained. For each $y^*_{spt} = 1$, it means that ship s requires a cleaning service when arriving at port–time pair (p,t). Let Ω_s and Ω_{sk} be the set for ship s that includes all port–time pairs (p,t) that have $y^*_{spt} = 1$ and the port–time pairs that have $y^*_{spt} = 1$ and $365(k-1) < t \leq 365k$, respectively. Therefore, Ω_s can be regarded as the demand for cleaning services for ship s. Having ship demands, the bi-level decision problem can be formulated.

The service providers collectively act as the leader, whose main goal is to maximize profits by designing an optimal deployment plan for cleaning equipment. Their profits are derived from service revenue minus equipment costs. It is worth noting that different prices for cleaning services exist at different ports, while the equipment costs remain the same. Since fouling accumulation occurs over a period of time, the service providers are not required to purchase all the equipment in the first year. Instead, they determine the amount of equipment to be purchased at the beginning of each year (nth year) for each port, denoted as x_{pn}. Deploying more equipment allows for the servicing of a greater number of ships, thus increasing service revenue. However, it also leads to higher equipment costs. Hence, the service providers need to carefully design the deployment plan to balance between revenue and costs.

On the other hand, the ships, as the followers, determine whether and where to utilize the cleaning service under the given the deployment plan $\vec{x}$. To maximize the total profits, the deployment plan made by service providers may not be able to serve all demands. Consequently, the ships that cannot be served will not use the cleaning service on the subsequent voyages and instead turn to other techniques, such as antifouling painting. Because ship demands are the best choice based on total costs, any violation will increase total costs, and it is assumed that ships do not accept cost increases. The total demands when ship s arrives at port p at port–time pair (p,t) is denoted as $|\mathrm{V}_{spt}|$. Given the deployment plan $\vec{x}$, the choices of ship s can be modeled as follows:

$$[\mathrm{P2}]\ Y_s(\vec{x}) = \operatorname{argmin} \sum_{k \in N} \sum_{(p,t) \in \Omega_{sk}} \left(\left|\mathrm{V}_{spt}\right| + 1 - \sum_{n=1}^{k} x_{pn} \right) y_{spt} \tag{5-4}$$

subject to

$$y_{spt} \leq y_{sp't'}, \forall (p,t), (p',t') \in \Omega_s : \tau_{spt} - \tau_{sp't'} = 1 \quad (5\text{-}5)$$

$$y_{spt} \in \{0,1\}, \forall (p,t) \in \Omega_s. \quad (5\text{-}6)$$

Let $(p,t) \in \Omega_s$ be the first pair at which the equipment supply is insufficient to satisfy demands, i.e., $\left|V_{spt}\right| + 1 > \sum_{n=1}^{k} x_{pn}$. In the optimal solution, there will be $y_{sp't':\tau_{sp't'} < \tau_{spt}} = 1$ and $y_{sp't':\tau_{sp't'} \geq \tau_{spt}} = 0$. This means that when the port can provide sufficient equipment, the ship s will use the service. Conversely, if the port cannot meet requirements, the ship s will not use the service. Constraints (5-5) state that the ship will leave the market and turn to other techniques once it cannot be served. Constraints (5-6) define y_{spt} to be binary.

5.3.2 Model Formulation

Given the lower-level solution $Y_s(\vec{x})$, $\forall s \in S$, the service providers can maximize total profits by designing the equipment deployment plan as follows:

[P3] Maximize $\sum_{s \in S} \sum_{(p,t) \in \Omega_s} C^p y_{spt} - \sum_{p \in P} \sum_{n \in N} C^e x_{pn} (|N| - n + 1)$ (5-7)

subject to

$$x_{pn} \in \mathbb{Z}_0^+, \forall p \in P, n \in N \quad (5\text{-}8)$$

$$\vec{y}_s \in Y_s(\vec{x}), \forall s \in S \quad (5\text{-}9)$$

where Constraints (5-8) impose non-negativity conditions on the decision variables of service providers. Constraints (5-9) indicate that y_{spt} depends on the decisions of ship s at the lower-level problem, denoted by $Y_s(\vec{x})$. The optimal decisions of ship s are determined by P2. If there exists more than one optimal solution to the lower-level problem, the ships will select the one that benefits upper-level decision makers.

5.4 SOLUTION METHOD

Bi-level problems are known for their computational complexity due to their hierarchical structure and the requirement to solve both an upper-level and a lower-level problem simultaneously. Furthermore, the presence of non-linearity in the lower-level problem adds to the computational challenge. However, there is a method to alleviate this complexity by transforming the bi-level non-linear problem into a single-

level linear programming problem, which is shown in Figure 5-3. The reason for this transformation is that the lower-level problem involves a trade-off between demand and supply, which can be represented by binary decision variables. By substituting this trade-off with binary decision variables, we can then use binary variables to convert the objective function of the lower-level problem (P2) into constraints for the upper-level problem (P3). By doing so, the two problems are effectively merged into a single-level optimization problem, which can be solved using linear programming techniques. This transformation simplifies computational complexity and allows for the utilization of efficient linear programming algorithms. P2 requires that if $\left|\mathrm{V}_{spt}\right| \geq \sum_{n=1}^{k} x_{pn}$, $y_{spt} = 0$, and if $\left|\mathrm{V}_{spt}\right| + 1 \leq \sum_{n=1}^{k} x_{pn}$, y_{spt} can be a value of zero or one depending on the decision made at the last port–time pair, which means that if the existing equipment is insufficient to cover the demand, the ship will not use cleaning services any more even if it can be served in the subsequent ports of call. Therefore, let y_{spt} and $y_{sp't'}$ denote the decision at the current and the last port–time pair, respectively, where $\tau_{spt} - \tau_{sp't'} = 1$. When $\left|\mathrm{V}_{spt}\right| + 1 \leq \sum_{n=1}^{k} x_{pn}$, if $y_{sp't'} = 1$, $y_{spt} = 1$, and if $y_{sp't'} = 0$, $y_{spt} = 0$. To transform the bi-level problem into a single-level problem, the binary variable w_{spt}, $\forall (p,t) \in \Omega_s$ is defined to indicate the relationship between $\left|\mathrm{V}_{spt}\right|$ and $\sum_{n=1}^{k} x_{pn}$. If $w_{spt} = 1$, $\left|\mathrm{V}_{spt}\right| + 1 \leq \sum_{n=1}^{k} x_{pn}$, and if $w_{spt} = 0$, $\left|\mathrm{V}_{spt}\right| \geq \sum_{n=1}^{k} x_{pn}$. When $w_{spt} = 0$, it is necessary to ensure $y_{spt} = 0$, and when $w_{spt} = 1$, we should obtain $y_{spt} = y_{sp't'}$. The transformation from a bi-level problem to a single-level problem using the big-M method is as follows:

$$[\mathrm{P4}]\ \left|\mathrm{V}_{spt}\right| \geq \sum_{n=1}^{k} x_{pn} - M w_{spt},\ \forall (p,t) \in \Omega_{sk},\ k \in N \tag{5-10}$$

$$\left|\mathrm{V}_{spt}\right| + 1 \leq \sum_{n=1}^{k} x_{pn} + M\left(1 - w_{spt}\right),\ \forall (p,t) \in \Omega_{sk},\ k \in N \tag{5-11}$$

$$y_{spt} - y_{sp't'} \leq 1 - w_{spt},\ \forall (p,t),(p',t') \in \Omega_s : \tau_{spt} - \tau_{sp't'} = 1 \tag{5-12}$$

$$y_{sp't'} - y_{spt} \leq 1 - w_{spt},\ \forall (p,t),(p',t') \in \Omega_s : \tau_{spt} - \tau_{sp't'} = 1 \tag{5-13}$$

$$y_{spt} \leq w_{spt},\ \forall (p,t) \in \Omega_s \tag{5-14}$$

where M is the total number of ships in the network plus one. The inequalities in P4 are equivalent to (5-4) and (5-5).

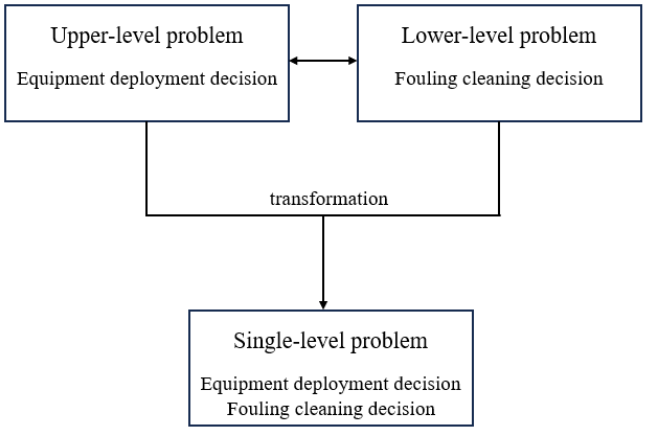

Figure 5-3: The flowchart of the solution method

5.5 NUMERICAL EXPERIMENTS

In this section, the performance of the solution method is evaluated using real-world data. The proposed approach, which transforms the bi-level problem into a single-level problem, is compared with a heuristic algorithm that sequentially solves the upper-level and lower-level problems. This comparison demonstrates the superiority of the proposed method. Furthermore, the optimal decisions of both service providers and ships are determined using the proposed method, and the interaction between these two parties is analyzed. Additionally, sensitivity analysis is conducted to assess the influence of key parameters. All the experiments were carried out on a laptop with 6 CPU cores, 2.6 GHz processing speed, and 24 GB of memory. The model is coded in Python and solved by Gurobi 9.5.0.

5.5.1 Parameter Setting

Five routes, listed in Table 5-2, were selected from the Asia–Europe network of a global liner shipping company to evaluate the performance of the proposed model. These routes contain 18 ports, as shown in Figure 5-4. A total of 250 ships travels on these routes, with 100 ships sailing on each of the first four routes and 50 ships sailing on the last route. The departure time of ships on the five routes is randomly generated from the ranges [1, 75], [1, 80], [1, 90], [1, 85], and [1, 40], respectively. The second numbers in the brackets are the duration required for a ship to complete the corresponding route. The sailing speed is 12 knots, and the planning period is set to five years. The dwell time at each port of call is randomly generated from the range [5, 15]. Having the departure time from the first port of call, the distance between ports

of call, ship dwell time, and sailing speed, the set of port–time pairs of each ship can be calculated. The unit fuel cost is USD 110.6/nautical mile according to Meng, Du, and Wang (2016) and Wu et al. (2023). The ship cleaning price is randomly generated from [26808, 40549] according to Schultz et al. (2011). The amortized purchasing cost is set to USD 100,000/year. According to Bryers and Characklis (1981) and Hakim et al. (2017), α and β are estimated to be 6.72 and 0.0001, respectively.

Table 5-2: Ship routes

Index	Route
1	Ningbo → Xiamen → Yantian → Tanjung Pelepas → Rotterdam → Port Tanger Med → Hong Kong → Ningbo
2	Shanghai → Yantian → Tanjung Pelepas → Colombo → Port Tanger Med → Hamburg → Antwerp → Port Tanger Med → Singapore → Laem Chabang → Ningbo → Shanghai
3	Antwerp → Rotterdam → Algeciras → Singapore → Hong Kong → Shanghai → Qingdao → Busan → Ningbo → Shanghai→ Yantian → Tanjung Pelepas → Sines → Antwerp
4	Busan → Ningbo → Tanjung Pelepas→ Rotterdam → Tanjung Pelepas → Shanghai → Qingdao → Ningbo → Busan
5	Shanghai → Tanjung Pelepas → Chittagong → Tanjung Pelepas → Singapore → Laem Chabang → Ningbo → Shanghai

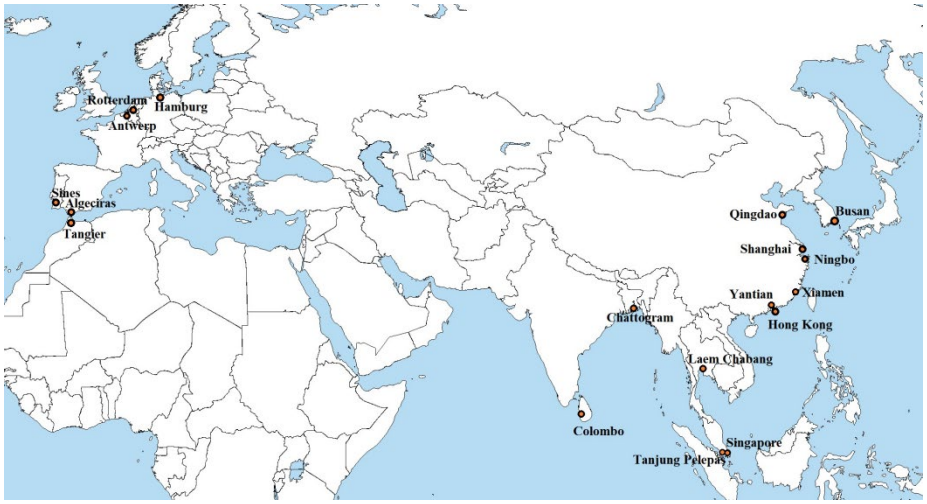

Figure 5-4: All ports of the selected routes

5.5.2 Computational Performance

To test the performance of the solution method, it is compared with an algorithm described in Algorithm 1. This algorithm iteratively solves the upper-level and lower-level problem in sequence until the upper-level solution stays unchanged. A comparison between the proposed solution method and Algorithm 1 is shown in Table 5-3. Since the planning period will influence total demand, the computation times of the different methods under different planning periods are shown. Results show that

transforming the bi-level model to a single level speeds up computation, and the proposed method is therefore suitable for our problem.

Algorithm 1. The heuristic for solving bi-level problems

1 **Initialization**: Regard all $y_{spt} = 1$ in Problem (1), denoted by y^*_{spt}, as the input of P3
2 **Repeat** until x^*_{pn} stays unchanged:
3 Solve P3 with y^*_{spt} and obtain x^*_{pn}
4 Solve P2 with x^*_{pn} and obtain y^*_{spt}
5 **Return** x^*_{pn} and y^*_{spt}

Table 5-3: Comparison between the proposed solution method and Algorithm 1

Planning Period	Computation Time	
	Single Level	Algorithm
5	17.1	390.8
10	19.7	430.8
20	20.3	480.5

Before solving the bi-level problem, the optimal solution for P1 is first obtained as the input of the bi-level problem. The time consumption is 89.4 s. Every port–time pair with $y_{spt} = 1$ is regarded as a cleaning demand. The demand distribution on each port over five years is shown in Figure 5-5. It shows that the demand is concentrated in only six ports, with only slight variations in demand from year to year at each port.

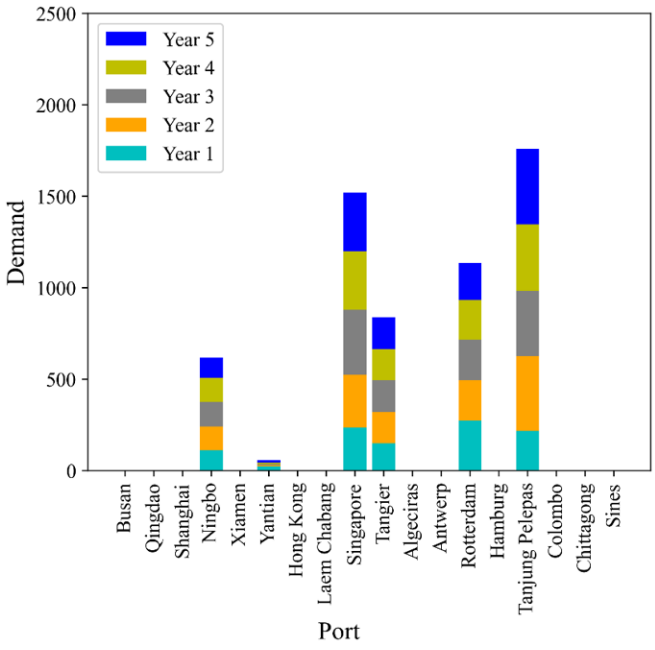

Figure 5-5: Demand distribution over the planning period

Having the demand, the bi-level problem can be solved, which takes 17.1 s. The deployment plan of the cleaning equipment is shown in Figure 5-6. Only four ports are deployed with equipment considering the revenue earned by providing service and the equipment purchase costs. It is worth noting that most of the equipment is purchased in the first year, with a small number of purchases in the second and third year. The reason can be found from Figure 5-7, which presents the maximal daily demand of the four ports in each year. The maximal demand is roughly the same each year, explaining why procurement is concentrated in the first year. However, there is a slight increase in demand in the second and third year, resulting in additional purchases. The total profit earned for providing cleaning services over the planning period is around USD 45.7 million.

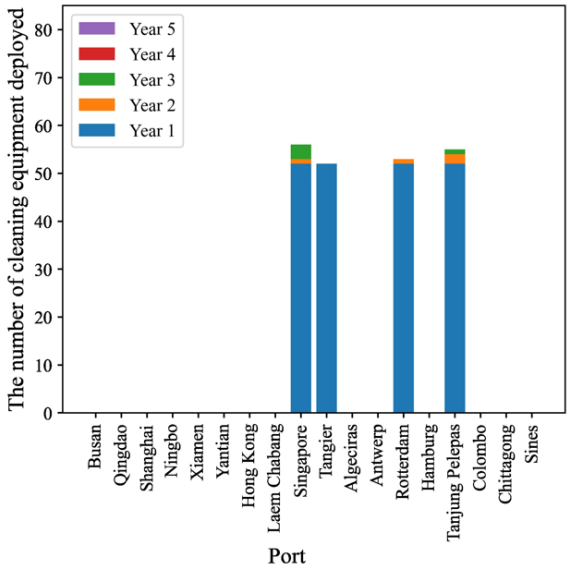

Figure 5-6: The deployment plan of the cleaning equipment

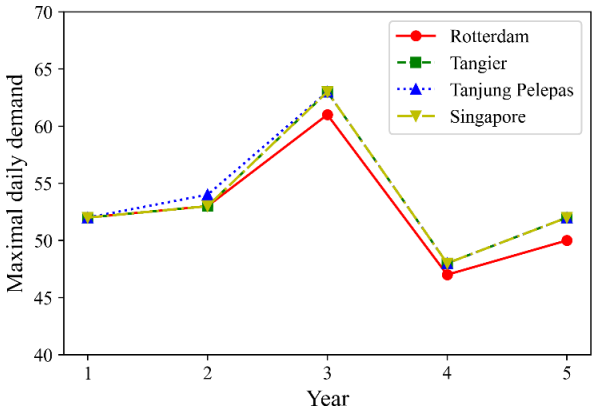

Figure 5-7: The maximal daily demand of the four ports in each year

For ships, due to the deployment plan of devices, not all demands can be satisfied. Figure 5-8 shows a comparison between initial demand and satisfied demand. The lighter bars on the left represent initial demand, while the darker bars on the right represent satisfied demand. Since the Shanghai and Ningbo ports are not equipped with cleaning devices, the demand for these two ports is lost. Similarly, the Singapore and Tanjung Pelepas ports see demand lost due to insufficient equipment supply.

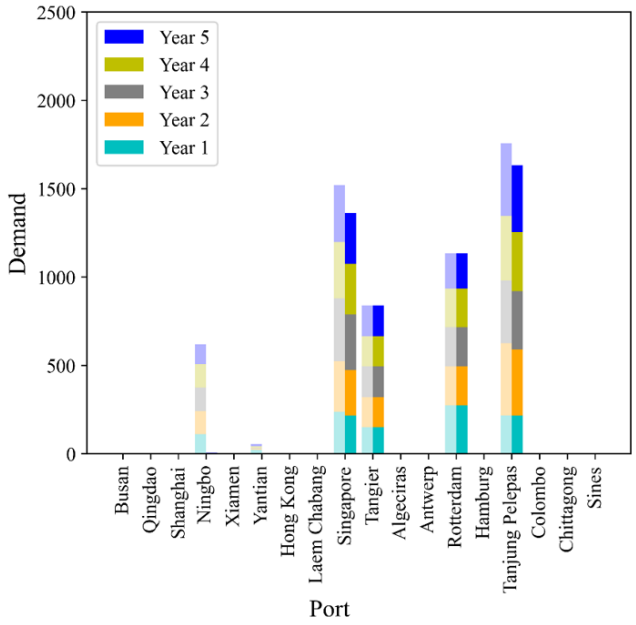

Figure 5-8: The comparison between initial demand and satisfied demand

5.5.3 Sensitivity Analysis

In this chapter, the impacts of some key parameters are analyzed, such as the demand satisfaction requirements, the cleaning price, and the purchase costs.

It can be seen from the above analysis that some demand is lost due to the lack of cleaning equipment. What if we require all demand be satisfied? The answers are shown in Table 5-4. When requiring all demand be satisfied, the service providers can earn USD 34 million more in revenue but spend USD 61 million more on equipment, resulting in a USD 27 million loss in profit. The equipment deployment plan also changes, as shown in Figure 5-9. The lighter bars on the left represent results without the full demand satisfaction requirement, while the darker bars on the right represent the results of full demand satisfaction. It shows that the ports that previously had no equipment, i.e., Ningbo and Yantian, are now equipped with cleaning devices. The other four ports that previously provided services are now equipped with more

equipment, especially in the third year. It suggests that in order for service providers to maintain a loyal customer base, they may need to make a trade-off by sacrificing a portion of their profits.

Table 5-4: The comparison between partial satisfaction and full satisfaction of demand

	Revenue (USD, Millions)	Cost (USD, Millions)	Profit (USD, Millions)
Partial satisfaction	153	107	46
Full satisfaction	187	168	19
Change	34	61	−27

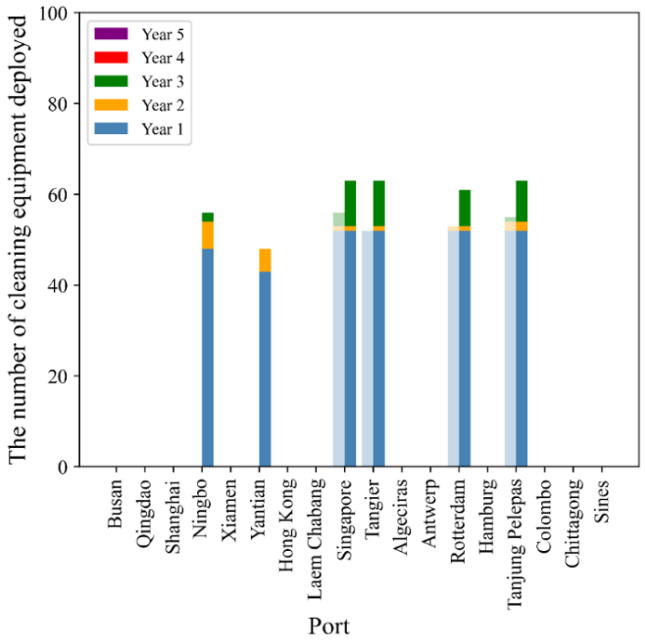

Figure 5-9: Comparison of equipment deployment plans before and after the full demand satisfaction requirement

Second, the impact of cleaning price is explored. The cleaning price in each port is changed in proportion from 0.1 to 10. The influences on demand, equipment deployment, and profits are shown in Figure 5-9 and elaborated below.

Figure 5-10 (a) shows total port demand before (referred to as initial demand) and after (referred to as actual demand) the ship is affected by the equipment deployment plan. It shows that when cleaning price is too low, even with very high demand, service providers are reluctant to provide service because the revenue cannot cover the cost. With the increase in cleaning price, the initial demand continues to decline because expensive cleaning costs discourage ships from cleaning for longer

periods of time until the additional fouling costs become prohibitively high. As a result, cleaning frequency decreases, which is reflected in the initial demand. The actual satisfied demand follows a broadly similar trend to the initial demand, except for a slight increase when price increases by 2 to 2.5 times. The slight increase can be explained by Figure 5-10 (b), which depicts the total demand in each year when the price is 2 and 2.5 times the original price. It is worth noting that when price increases by 2 to 2.5 times, there is only a slight drop in demand. Because the revenue from each demand is increasing, service providers will serve as many demands as possible, so the actual demand will increase slightly. When the price continues to increase because the initial demand is falling, the actual demand is also falling, though the gap between the two will become smaller and smaller.

The total amount of purchased equipment in each year is shown in Figure 5-10 (c). When the cleaning price is too low, service providers will not purchase any equipment. When prices continue to increase, equipment purchases generally show a downward trend. However, there is an exception. The reason can be found in Figure 5-11, which shows the annual equipment deployment of the five ports (because other ports have no equipment deployment). When cleaning price increases, the initial demand may shift between different ports. For example, the ships sailing on route 1 in Table 5-2 may change their cleaning port from Rotterdam to Ningbo because the rising cleaning price allows ships to sail a longer distance before cleaning. The demand change may result in previously unequipped ports such as Ningbo now having equipment, previously equipped ports such as Rotterdam now without equipment, and changes in deployment between ports.

Overall, increasing cleaning price can increase profits, as shown in Figure 5-10 (d). However, in extreme cases when there is no demand, service providers will exit the market.

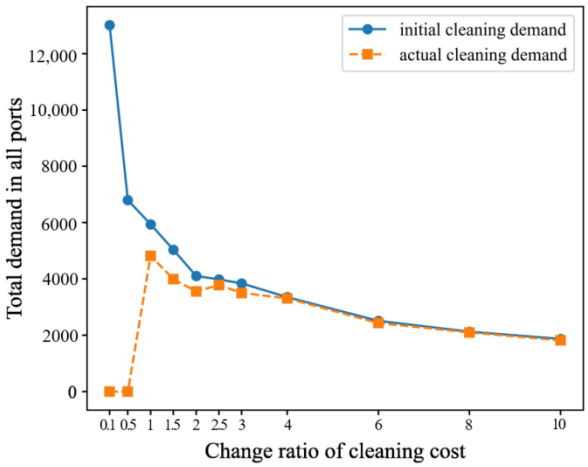

(a) Total demand in all ports

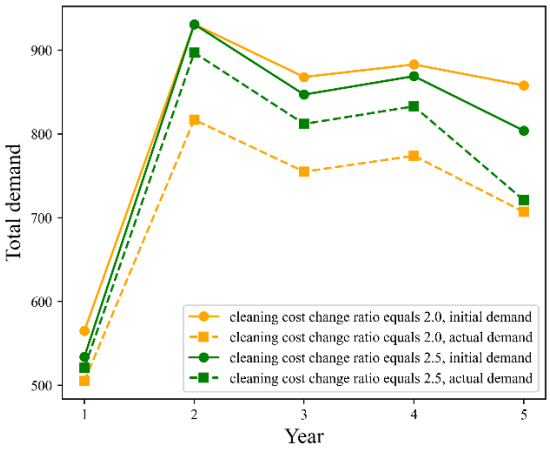

(b) Annual demand in all ports

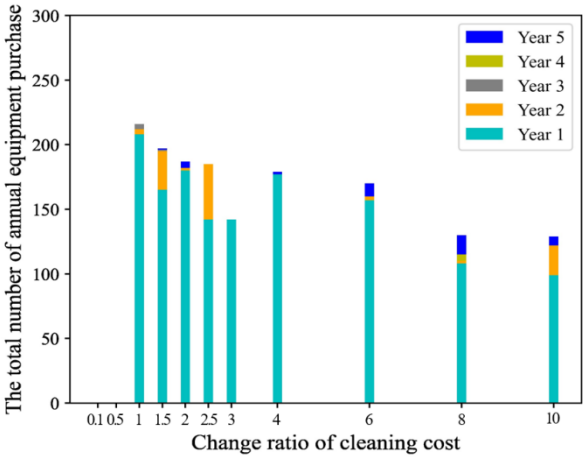

(c) The total amount of annual purchased equipment

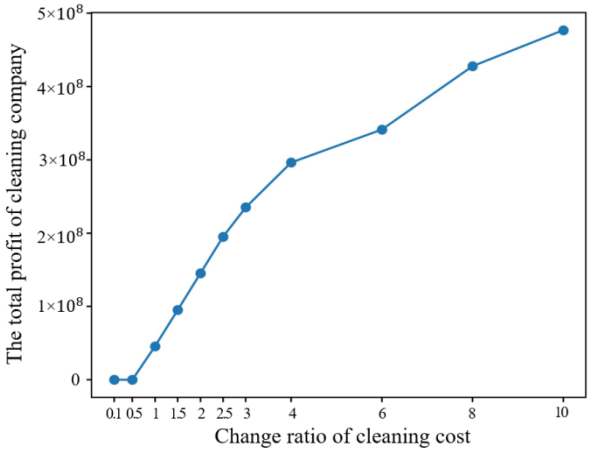

(d) Total profit of service providers

Figure 5-10: The influences of cleaning price

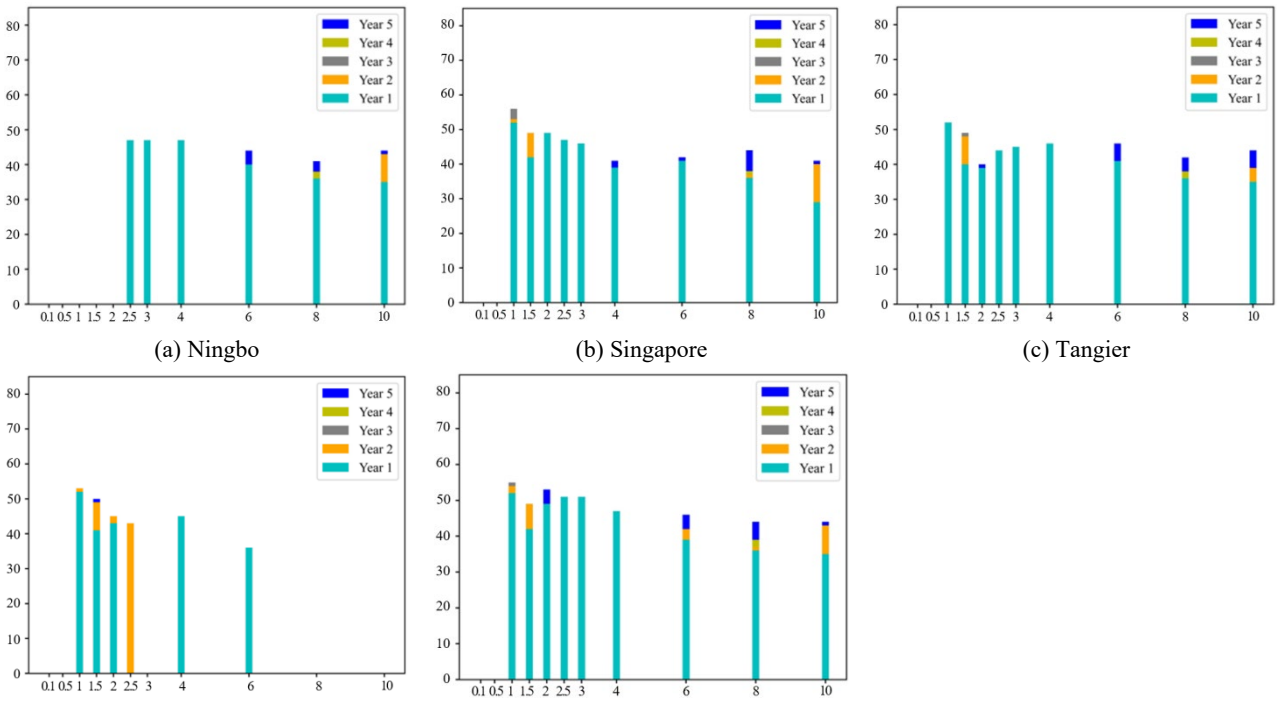

(a) Ningbo (b) Singapore (c) Tangier

(d) Rotterdam (e) Tanjung Pelepas

Figure 5-11: The amount of annual equipment deployed at five ports

Finally, the impact of purchase cost was investigated. Purchase cost was changed in proportion from 0.5 to 2.0 with a step size of 0.1, as shown in Figure 5-12. Figure 5-12 (a), (b) present the variation in equipment deployment plans and total profit. Changing purchase cost does not affect initial demand because purchase cost does not appear in the model of P1, so with the increase in purchase cost the potential revenue stays the same while the cost of equipment increases, resulting in a profit loss and therefore resulting in a reduction in the total amount of purchased equipment. When profit reaches zero, service providers will exit the market, which means no fouling cleaning service can be found in the market.

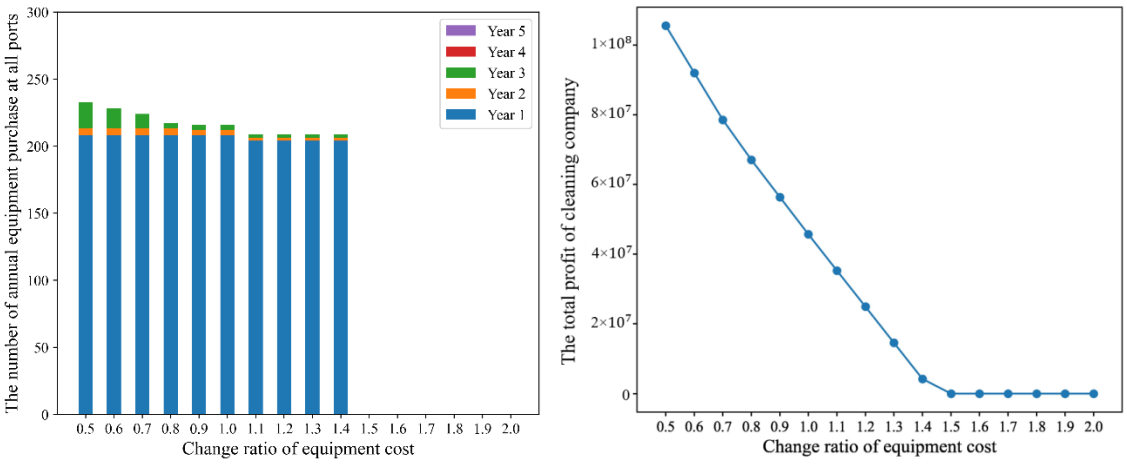

(a) The impact on equipment deployment (b) The impact on service profit

Figure 5-12: The influences of purchase cost

5.6 DISCUSSIONS

There are three main limitations to be acknowledged in this study. Firstly, the assumption that ships that cannot be served will not use the cleaning service on subsequent voyages and will opt for alternative techniques like antifouling painting may have practical implications. Under this assumption, if a ship decides to clean fouling during a port visit but cannot find available cleaning equipment, it will never use the cleaning service again. This means that the service providers lose this customer permanently. This assumption has an impact on the demand for cleaning services, as well as the equipment procurement and deployment decisions made by service providers. If delayed cleaning is allowed, the ship may decide to use the cleaning service at the next port of call, thereby maintaining demand. With increased demand, the revenue of service providers may increase. Future research could consider this aspect and modify the formulation of the model accordingly. Instead of pre-calculating the cleaning demand in P1, the objective function of P1 can become the lower-level objective function. The decision-making process will be constrained by the deployment of cleaning equipment in the upper level, taking into account the possibility of delayed cleaning.

Secondly, the present study assumes that cleaning demands are primarily driven by cost considerations. While cost is an important factor, there are situations where ships are obliged to undergo fouling cleaning irrespective of its cost-effectiveness. For instance, certain countries may enforce regulations mandating the cleaning of fouling

before a ship's entry into their ports. This regulatory requirement significantly influences the demand for cleaning services. To incorporate this realistic situation, future research could introduce a binary parameter for each port that indicates cleaning requirements. If the parameter is set to 1, it signifies that cleaning before the visit is re-quired, otherwise there is no such requirement. This parameter can then be incorporated into the constraints of the lower-level problem to restrict the cleaning decisions accordingly.

Thirdly, this study is based on the assumption that biofouling does not increase while a ship is in motion due to its high speed. However, this assumption may not be universally applicable and can be influenced by various factors, including the specific marine environment, vessel design, and the duration of ship operation. These factors can affect the extent of biofouling settlement during ship motion. To address this limitation and enhance the model's applicability to a wider range of scenarios, we will consider incorporating fouling accumulation while ships are in motion into the accumulation function in future research. This addition will provide a more comprehensive and accurate representation of biofouling dynamics, accounting for the influence of ship motion on fouling accumulation.

These modifications will address the limitations of the current study and provide a more comprehensive and realistic understanding of the fouling cleaning decision-making process. By considering the possibility of delayed cleaning and incorporating regulatory requirements, research can offer practical insights for decision makers in the industry and enhance the applicability of findings.

5.7 CONCLUSIONS

This research develops a bi-level model to optimize the hull cleaning process. To overcome computational complexity, an efficient approach leveraging the big-M method is employed to convert the problem into a computationally tractable single-level formulation. Comprehensive numerical experiments are conducted to assess the performance of the developed models. The findings highlight several important insights. Firstly, the results indicate that service providers may choose to sacrifice a portion of the demand in order to maximize profits. Additionally, there is a notable concentration of equipment procurement in the initial year due to high demand during that period. Sensitivity analyses are additionally conducted to investigate the impact

of key parameters on the system. Notably, the results elucidate that pursuing complete demand satisfaction may yield a substantial USD 27 million loss in profit. Furthermore, manipulating the cleaning price exerts a direct influence on demand levels and equipment purchases, thereby affecting overall profitability. Additionally, variations in purchase costs directly impact profits, resulting in corresponding adjustments to the total number of equipment purchases. Finally, the study reveals that market exit becomes a likely outcome in scenarios where service providers fail to generate profits.

These findings provide valuable insights into optimization of the hull cleaning process and offer practical implications for decision makers in the industry. For service providers, understanding the trade-off between demand satisfaction and profit maximization can help them make strategic decisions on how to best allocate their resources and prioritize their operations. By strategically sacrificing a portion of the demand, service providers can optimize their profitability and resource utilization. Furthermore, the observed concentration of equipment procurement in the initial year due to high demand highlights the need for proactive planning and allocation of resources. Understanding this pattern can assist service providers in effectively managing their equipment inventory and optimizing their procurement strategies to meet the fluctuating demand. Additionally, this study reveals that service providers can directly in-fluence demand levels and equipment purchases by manipulating cleaning prices, thereby affecting their overall profitability. These findings provide valuable guidance for decision makers in formulating pricing strategies to maximize profitability. For ship operators, the insights gained from this study can help them develop cost-effective cleaning strategies. By considering factors such as pricing strategies, equipment procurement patterns, and cost considerations, ship operators can minimize expenses while maintaining the desired level of cleanliness. Importantly, the practical implications of this study extend beyond financial considerations. By optimizing the hull cleaning process, decision makers can significantly reduce the environmental impact associated with marine fouling and improve operational efficiency.

Chapter 6: Conclusions and Future Research

6.1 CONCLUSIONS

As sustainability becomes a widely acknowledged and shared goal, the shipping industry, a cornerstone of global trade, has been actively exploring diverse avenues to achieve this objective. This thesis delves into three approaches for realizing sustainability: autonomous vessels, cleaner energy generation, and fouling cleaning.

Autonomous ships, with their numerous advantages, are poised to emerge as a potential trend in the future. Nevertheless, there is a notable dearth of research examining the influence of autonomous ships on traditional vessels and the shipping industry concerning routes, fleet composition, fleet assignment, and demand fulfillment. Consequently, the initial study in this thesis develops a two-stage stochastic programming model to delve into these impacts. The overarching objective is to maximize the expected service profit. The computational complexity is addressed by both sample average approximation and a two-phase Benders-based branch-and-cut algorithm. Additional acceleration strategies, including column generation and variable fixing, are employed to expedite computations. Through extensive numerical experiments, the performances of various solution methods are rigorously compared and validated. The results indicate that regarding each scenario as an independent subproblem yields superior performance compared to aggregating all scenarios. Furthermore, the modified two-phase algorithm outperforms the original one, and the implementation of acceleration techniques substantially reduces computation time. Additionally, the sensitivity analysis yields valuable managerial insights. It underscores that autonomous ships, in general, exhibit greater competitiveness, and strategically sacrificing partial demand can be a beneficial approach.

The second study delves into the subsidy design for energy generation methods at berths, aiming to meet targeted emissions goals. Three distinct methods, i.e., heavy fuel oil with scrubber, marine diesel oil, and shore power, entail varying costs and emission levels. The objective is to attain the desired utilization level of these methods

with the minimal subsidy. While the government provides the subsidy, ship operators make the crucial decision regarding the energy generation method. Consequently, a bi-level optimization model is devised to encapsulate the intricate interaction between these two stakeholders. The complexity of the problem, arising from interdependence and nonlinearity, presents a significant challenge. However, a solution method incorporating model transformation and linearization proves instrumental in simplifying the computational process. Numerical experiments are conducted to validate the model, revealing insightful results. It becomes evident that providing subsidies to larger vessels is more advantageous in the initial stages. Moreover, an increase in the adoption of scrubbers or shore power-equipped ships results in reduced subsidies, and varying subsidy amounts correspond to different adoption levels.

The third study focuses on cleaning the ship fouling to minimize adverse effects on both vessel performance and environmental sustainability. This process involves two key entities: cleaning service providers and shipping companies. The former is responsible for determining the strategic deployment of cleaning equipment, while the latter decides the timing and location for fouling removal. A bi-level model has been formulated to capture the intricate interdependence between these two parties. The computational complexity of this bi-level model has been effectively addressed through a transformative approach. The study employs comprehensive numerical experiments that yield valuable managerial insights. These insights establish a clear correlation between demand fulfillment and profits, offering guidance to service providers regarding optimal equipment deployment strategies over time. Furthermore, sensitivity analysis highlights the significant impact that adjustments to cleaning prices and purchase costs can have on fouling cleaning demand and equipment deployment.

6.2 FUTURE RESEARCH

Future research can be extended in two main directions. Firstly, there is a need to explore additional methods that contribute to sustainability. Secondly, optimization efforts should be directed towards the three approaches discussed in the paper.

The pursuit of sustainability in the maritime industry has given rise to numerous solution methods. One notable development is the implementation of new international regulations by various maritime organizations, imposing restrictions on maritime operations. A compelling avenue for future research lies in delving into how shipping

companies will respond to and navigate these evolving policies, exploring the dynamic interactions and adaptations within the industry.

In addition to regulatory measures, the adoption of cleaner and renewable fuels presents a pivotal strategy. Fuels such as low-sulfur alternatives, liquefied natural gas (LNG), and the integration of wind-assisted propulsion systems and solar panels offer substantial promise in reducing harmful emissions. However, the widespread adoption of these fuels faces challenges related to accessibility and costs, necessitating a nuanced examination. A pertinent research direction involves the redesign of the shipping network to accommodate different propulsion fuels, considering the diverse operational implications and economic feasibility.

Further exploration into technological advancements forms another crucial dimension of sustainable maritime practices. For instance, the emergence of electricity-powered or hydrogen-fueled ships presents unique operational characteristics. A research approach that incorporates these distinctive features into the analysis could significantly enhance our understanding of their operational dynamics and concurrently improve both operational and environmental efficiency.

In summary, the multifaceted nature of achieving sustainability in the maritime sector demands a comprehensive research agenda. Investigating industry responses to evolving regulations, optimizing shipping networks for diverse propulsion fuels, and understanding the operational intricacies of advanced technologies are key areas that promise valuable insights and advancements toward a more sustainable future for maritime operations.

Expanding further on optimization possibilities, a nuanced exploration of the modeling assumptions is essential. Investigating how to incorporate real-world complexities into the models can enhance their accuracy and applicability. For instance, considering varying environmental conditions, market dynamics, and regulatory changes in the modeling framework would contribute to a more comprehensive understanding of the system.

Moreover, the efficiency of solving these optimized models can be a focal point for improvement. Exploring advanced computational techniques, optimization algorithms, or machine learning approaches may streamline the solving process,

making it more scalable and adaptable to complex scenarios. This avenue of research could lead to faster and more accurate decision-making tools for stakeholders in the maritime industry.

In addition to the static nature of data, the temporal aspect of the shipping industry poses a challenge. Optimizing models to incorporate dynamic data, such as real-time weather conditions, market trends, and geopolitical events, can provide a more realistic representation of the operational environment. This dynamic approach enables decision-makers to respond promptly to changing circumstances, contributing to increased operational resilience and efficiency.

Furthermore, a critical aspect to consider is the integration of sustainability metrics into the optimization models. Assessing the environmental impact of different operational decisions and incorporating eco-friendly criteria can align with the industry's growing focus on sustainable practices.

Lastly, exploring ways to enhance the collaboration between stakeholders in the maritime sector is another avenue for improvement. Developing models that facilitate effective communication and coordination between cleaning service providers, shipping companies, and regulatory bodies could lead to more harmonized and sustainable industry practices.

In summary, optimization possibilities extend beyond refining modeling assumptions and include advancements in computational efficiency, incorporation of dynamic data, integration of sustainability metrics, and fostering collaborative frameworks among industry stakeholders. These areas present exciting opportunities for researchers and practitioners alike to contribute to the ongoing development of sustainable and efficient practices in the maritime sector.

References

Abareshi, M., & Zaferanieh, M. (2019). A bi-level capacitated P-median facility location problem with the most likely allocation solution. *Transportation Research Part B: Methodological*, 123, 1-20.

Accorsi, L., & Vigo, D. (2021). A fast and scalable heuristic for the solution of large-scale capacitated vehicle routing problems. *Transportation Science*, 55(4), 832-856.

Adulyasak, Y., Cordeau, J.-F., & Jans, R. (2015). Benders decomposition for production routing under demand uncertainty. *Operations Research*, 63(4), 851-867.

Archetti, C., Bianchessi, N., & Speranza, M. G. (2014). Branch-and-cut algorithms for the split delivery vehicle routing problem. *European Journal of Operational Research*, 238(3), 685-698.

Archetti, C., Savelsbergh, M. W. P., & Speranza, M. G. (2008). To split or not to split: That is the question. *Transportation Research Part E: Logistics and Transportation Review*, 44(1), 114-123.

Authority, D. M. (2017). Analysis of regulatory barriers to the use of autonomous ships final report. *Kopenhag: Danish Maritime Authority*.

Bianchessi, N., & Irnich, S. (2019). Branch-and-cut for the split delivery vehicle routing problem with time windows. *Transportation Science*, 53(2), 442-462.

Branchini, R. M., Armentano, V. A., & Morabito, R. (2015). Routing and fleet deployment in liner shipping with spot voyages. *Transportation Research Part C: Emerging Technologies*, 57, 188-205.

Bryers, J., & Characklis, W. (1981). Early fouling biofilm formation in a turbulent flow system: overall kinetics. *Water Research*, 15(4), 483-491.

Cai, L., Wu, Y., Zhu, S., Tan, Z., & Yi, W. (2020). Bi-level programming enabled design of an intelligent maritime search and rescue system. *Advanced Engineering Informatics*, 46, 101194.

Callow, M. (1990). Ship fouling: problems and solutions. *Chemistry and Industry* (London), (5), 123-127.

Camacho-Vallejo, J. F., González-Rodríguez, E., Almaguer, F. J., & González-Ramírez, R. G. (2015). A bi-level optimization model for aid distribution after the occurrence of a disaster. *Journal of Cleaner Production*, 105, 134-145.

Casas-Ramírez, M. S., Camacho-Vallejo, J. F., Díaz, J. A., & Luna, D. E. (2020). A bi-level maximal covering location problem. *Operational Research*, 20, 827-855.

Chang, C. H., Kontovas, C., Yu, Q., & Yang, Z. (2021). Risk assessment of the operations of maritime autonomous surface ships. *Reliability Engineering & System Safety*, 207, 107324.

Chang, J. S., & Mackett, R. L. (2006). A bi-level model of the relationship between transport and residential location. *Transportation Research Part B: Methodological*, 40(2), 123-146.

Cheng, H. H., & Ouyang, K. (2021). Development of a strategic policy for unmanned autonomous ships: a study on Taiwan. *Maritime Policy & Management*, 48(3), 316-330.

Coelho, V. N., Grasas, A., Ramalhinho, H., Coelho, I. M., Souza, M. J., & Cruz, R. C. (2016). An ILS-based algorithm to solve a large-scale real heterogeneous fleet VRP with multi-trips and docking constraints. *European Journal of Operational Research*, 250(2), 367-376.

Coraddu, A., Oneto, L., Baldi, F., Cipollini, F., Atlar, M., & Savio, S. (2019). Data-driven ship digital twin for estimating the speed loss caused by the marine fouling. *Ocean Engineering*, 186, 106063.

Dantzig, G. B., & Ramser, J. H. (1959). The truck dispatching problem. *Management Science*, 6(1), 80-91.

Degiuli, N., Farkas, A., Martić, I., & Grlj, C. G. (2023). Optimization of maintenance schedule for containerships sailing in the Adriatic Sea. *Journal of Marine Science and Engineering*, 11(1), 201.

Demirel, Y. K., Song, S., Turan, O., & Incecik, A. (2019). Practical added resistance diagrams to predict fouling impact on ship performance. *Ocean Engineering*, 186, 106112.

Demirel, Y. K., Uzun, D., Zhang, Y., Fang, H. C., Day, A. H., & Turan, O. (2017). Effect of barnacle fouling on ship resistance and powering. *Biofouling*, 33(10), 819-834.

Desaulniers, G. (2010). Branch-and-price-and-cut for the split-delivery vehicle routing problem with time windows. *Operations Research*, 58(1), 179-192.

Despaux, F., & Basterrech, S. (2016). Multi-trip vehicle routing problem with time windows and heterogeneous fleet. *International Journal of Computer Information Systems and Industrial Management Applications*, 8, 355-363.

de Vos, J., Hekkenberg, R. G., & Banda, O. A. V. (2021). The impact of autonomous ships on safety at sea–a statistical analysis. *Reliability Engineering & System Safety*, 210, 107558.

Dinariyana, A. A. B., Deva, P. P., Ariana, I., & Handani, D. W. (2022). Development of model-driven decision support system to schedule underwater hull cleaning. *Brodogradnja*, 73(3), 21-37.

Dror, M., & Trudeau, P. (1990). Split delivery routing. *Naval Research Logistics*, 37(3), 383-402.

Erol, E., Cansoy, C. E., & Aybar, O. Ö. (2020). Assessment of the impact of fouling on vessel energy efficiency by analyzing ship automation data. *Applied Ocean Research*, 105, 102418.

Evans, L. V. (1981). Marine algae and fouling: A review, with particular reference to ship-fouling. Botanica Marina, XXIV, 167–17

Fadda, P., Mancini, S., Serra, P., & Fancello, G. (2023). The heterogeneous fleet vehicle routing problem with draft limits. *Computers & Operations Research*, 149, 106024.

Fan, C., Wróbel, K., Montewka, J., Gil, M., Wan, C., & Zhang, D. (2020). A framework to identify factors influencing navigational risk for Maritime Autonomous

Surface Ships. *Ocean Engineering*, 202, 107188.
Farkas, A., Degiuli, N., & Martić, I. (2020). An investigation into the effect of hard fouling on the ship resistance using CFD. *Applied Ocean Research*, 100, 102205.
Farkas, A., Degiuli, N., & Martić, I. (2021a). The impact of biofouling on the propeller performance. *Ocean Engineering*, 219, 108376.
Farkas, A., Degiuli, N., & Martić, I. (2021b). Assessment of the effect of biofilm on the ship hydrodynamic performance by performance prediction method. *International Journal of Naval Architecture and Ocean Engineering*, 13, 102-114.
Farkas, A., Degiuli, N., Martić, I., & Ančić, I. (2022). Energy savings potential of hull cleaning in a shipping industry. *Journal of Cleaner Production*, 374, 134000.
Farkas, A., Degiuli, N., Martić, I., & Dejhalla, R. (2020). Impact of hard fouling on the ship performance of different ship forms. *Journal of Marine Science and Engineering*, 8(10), 748.
Farkas, A., Degiuli, N., Martić, I., & Vujanović, M. (2021). Greenhouse gas emissions reduction potential by using antifouling coatings in a maritime transport industry. *Journal of Cleaner Production*, 295, 126428.
Fitridge, I., Dempster, T., Guenther, J., & De Nys, R. (2012). The impact and control of biofouling in marine aquaculture: A review. *Biofouling*, 28(7), 649-669.
François, V., Arda, Y., Crama, Y., & Laporte, G. (2016). Large neighborhood search for multi-trip vehicle routing. *European Journal of Operational Research*, 255(2), 422-441.
Gang, J., Tu, Y., Lev, B., Xu, J., Shen, W., & Yao, L. (2015). A multi-objective bi-level location planning problem for stone industrial parks. *Computers & Operations Research*, 56, 8-21.
Georgiev, P., & Garbatov, Y. (2021). Multipurpose vessel fleet for short black sea shipping through multimodal transport corridors. *Brodogradnja*, 72(4), 79-101.
Ghaderi, H. (2019). Autonomous technologies in short sea shipping: trends, feasibility and implications. *Transport Reviews*, 39(1), 152-173.
Goerlandt, F. (2020). Maritime autonomous surface ships from a risk governance perspective: Interpretation and implications. *Safety Science*, 128, 104758.
Gschwind, T., Bianchessi, N., & Irnich, S. (2019). Stabilized branch-price-and-cut for the commodity-constrained split delivery vehicle routing problem. *European Journal of Operational Research*, 278(1), 91-104.
Gu, Y., Goez, J. C., Guajardo, M., & Wallace, S. W. (2021). Autonomous vessels: state of the art and potential opportunities in logistics. *International Transactions in Operational Research*, 28(4), 1706-1739.
Gutierrez, A., Dieulle, L., Labadie, N., & Velasco, N. (2018). A multi-population algorithm to solve the VRP with stochastic service and travel times. *Computers & Industrial Engineering*, 125, 144-156.
Hakim, M. L., Utama, I. K. A. P., Nugroho, B., Yusim, A. K., Baithal, M. S., & Suastika, I. K. (2017, December). Review of correlation between marine fouling and fuel consumption on a ship. *In Proceeding of SENTA: 17th Conference on Marine*

Technology (pp. 122-129).

Jin, J., Zhang, J., & Liu, D. (2018). Design and verification of heading and velocity coupled nonlinear controller for unmanned surface vehicle. *Sensors*, 18(10), 3427.

Jin, M., Liu, K., & Eksioglu, B. (2008). A column generation approach for the split delivery vehicle routing problem. *Operations Research Letters*, 36(2), 265-270.

Kretschmann, L., Burmeister, H. C., & Jahn, C. (2017). Analyzing the economic benefit of unmanned autonomous ships: An exploratory cost-comparison between an autonomous and a conventional bulk carrier. *Research in Transportation Business & Management*, 25, 76-86.

Lee, M. C., Wee, H. M., Wu, S., Wang, C. E., & Chung, R. L. (2015). A bi-level inventory replenishment strategy using clustering genetic algorithm. *European Journal of Industrial Engineering*, 9(6), 774-793.

Li, F., Yang, D., Wang, S., & Weng, J. (2019). Ship routing and scheduling problem for steel plants cluster alongside the Yangtze River. *Transportation Research Part E: Logistics and Transportation Review*, 122, 198-210.

Lin, Y., Wang, X., Hu, H., & Zhao, H. (2020). Research on feeder network design: a case study of feeder service for the port of Kotka. *European Transport Research Review*, 12(1), 1-13.

Liu, Z., Zhang, Y., Yu, X., & Yuan, C. (2016). Unmanned surface vehicles: An overview of developments and challenges. *Annual Reviews in Control*, 41, 71-93.

Maan, A. M., Hofman, A. H., de Vos, W. M., & Kamperman, M. (2020). Recent developments and practical feasibility of polymer‐based antifouling coatings. *Advanced Functional Materials*, 30(32), 2000936.

Makhsoos, A., Mousazadeh, H., Mohtasebi, S. S., Abdollahzadeh, M., Jafarbiglu, H., Omrani, E., Salmani, Y., & Kiapey, A. (2018). Design, simulation and experimental evaluation of energy system for an unmanned surface vehicle. *Energy*, 148, 362-372.

Mendoza, J. E., Castanier, B., Guéret, C., Medaglia, A. L., & Velasco, N. (2010). A memetic algorithm for the multi-compartment vehicle routing problem with stochastic demands. *Computers & Operations Research*, 37(11), 1886-1898.

Meng, Q., Du, Y., & Wang, Y. (2016). Shipping log data based container ship fuel efficiency modeling. *Transportation Research Part B: Methodological*, 83, 207-229.

Monty, J. P., Dogan, E., Hanson, R., Scardino, A. J., Ganapathisubramani, B., & Hutchins, N. (2016). An assessment of the ship drag penalty arising from light calcareous tubeworm fouling. *Biofouling*, 32(4), 451-464.

Munim, Z. H. (2019). Autonomous ships: A review, innovative applications and future maritime business models. *Supply Chain Forum: An International Journal*, 20(4), 266-279.

Notteboom, T., & Cariou, P. (2013). Slow steaming in container liner shipping: is there any impact on fuel surcharge practices? *The International Journal of Logistics Management*, 24(1), 73-86.

Oliveira, D. R., & Granhag, L. (2020). Ship hull in-water cleaning and its effects on fouling-control coatings. *Biofouling*, 36(3), 332-350.

Paradiso, R., Roberti, R., Laganá, D., & Dullaert, W. (2020). An exact solution framework for multitrip vehicle-routing problems with time windows. *Operations Research*, 68(1), 180-198.

Pecin, D., Pessoa, A., Poggi, M., & Uchoa, E. (2017). Improved branch-cut-and-price for capacitated vehicle routing. *Mathematical Programming Computation*, 9, 61-100.

Peng, C., Delage, E., & Li, J. (2020). Probabilistic envelope constrained multiperiod stochastic emergency medical services location model and decomposition scheme. *Transportation Science*, 54(6), 1471-1494.

Pessoa, A., Sadykov, R., Uchoa, E., & Vanderbeck, F. (2020). A generic exact solver for vehicle routing and related problems. *Mathematical Programming*, 183, 483-523.

Poggi, M., & Uchoa, E. (2014). New exact algorithms for the capacitated vehicle routing problem. *Vehicle Routing: Problems, Methods, and Applications* (pp. 59-86).

Qi, J., Wang, S., & Psaraftis, H. (2021). Bi-level optimization model applications in managing air emissions from ships: A review. *Communications in Transportation Research*, 1, 100020.

Şahin, M. K., & Yaman, H. (2022). A branch and price algorithm for the heterogeneous fleet multi-depot multi-trip vehicle routing problem with time windows. *Transportation Science*, 56(6), 1636-1657.

Schiaretti, M., Chen, L., & Negenborn, R. R. (2017a). Survey on autonomous surface vessels: Part I-a new detailed definition of autonomy levels. In *International Conference on Computational Logistics* (pp. 219-233). Springer, Cham.

Schiaretti, M., Chen, L., & Negenborn, R. R. (2017b). Survey on autonomous surface vessels: Part II-categorization of 60 prototypes and future applications. In *International Conference on Computational Logistics* (pp. 234-252). Springer, Cham.

Schultz, M. P., Bendick, J. A., Holm, E. R., & Hertel, W. M. (2011). Economic impact of biofouling on a naval surface ship. *Biofouling*, 27(1), 87-98.

Song, S., Demirel, Y. K., Muscat-Fenech, C. D. M., Tezdogan, T., & Atlar, M. (2020). Fouling effect on the resistance of different ship types. *Ocean Engineering*, 216, 107736.

Stoilova, K., & Stoilov, T. (2022). Model predictive traffic control by bi-level Optimization. *Applied Sciences*, 12(9), 4147.

Taillard, E. D., Laporte, G., & Gendreau, M. (1996). Vehicle routeing with multiple use of vehicles. *Journal of the Operational Research Society*, 47(8), 1065-1070.

Tan, Z., Liu, Q., Song, J., Wang, H., & Meng, Q. (2021). Ship choice and shore-power service assessment for inland river container shipping networks. *Transportation Research Part D: Transport and Environment*, 94, 102805.

Torres, F., Gendreau, M., & Rei, W. (2022). Crowdshipping: An open VRP variant with stochastic destinations. *Transportation Research Part C: Emerging*

Technologies, 140, 103677.
Townsin, R. L. (2003). The ship hull fouling penalty. *Biofouling*, 19(S1), 9-15.
Tribou, M., & Swain, G. (2015). Grooming using rotating brushes as a proactive method to control ship hull fouling. *Biofouling*, 31(4), 309-319.
Utama, I. K. A. P., & Nugroho, B. (2018). Biofouling, ship drag, and fuel consumption: A brief overview. *Journal of Ocean Technology*, 13(2), 42-48.
Wang, K., Li, J., Yan, X., Huang, L., Jiang, X., Yuan, Y., Ma, R., & Negenborn, R. R. (2020). A novel bi-level distributed dynamic optimization method of ship fleets energy consumption. *Ocean Engineering*, 197, 106802.
Wang, L., Kinable, J., & Van Woensel, T. (2020). The fuel replenishment problem: A split-delivery multi-compartment vehicle routing problem with multiple trips. *Computers & Operations Research*, 118, 104904.
Wang, W., Wang, S., & Zhen, L. (2023). Optimal subsidy design for energy generation in ship berthing. *Maritime Policy & Management*, 1-14.
Wang, Y., Yu, X., Liang, X., & Li, B. (2018). A COLREGs-based obstacle avoidance approach for unmanned surface vehicles. *Ocean Engineering*, 169, 110-124.
Wu, Y., Huang, Y., Wang, H., & Zhen, L. (2023). Nonlinear programming for fleet deployment, voyage planning and speed optimization in sustainable liner shipping. *Electronic Research Archive*, 31(1), 147-168.
Yang, D., Pan, K., & Wang, S. (2018). On service network improvement for shipping lines under the one belt one road initiative of China. *Transportation Research Part E: Logistics and Transportation Review*, 117, 82-95.
Yang, X., Gu, W., Wang, W., & Wang, S. (2023). Optimal scheduling of autonomous vessel trains in a hub-and-spoke network. *Ocean & Coastal Management*, 231, 106386.
Yang, Y. (2022). An exact price-cut-and-enumerate method for the capacitated multitrip vehicle routing problem with time windows. *Transportation Science*, 57(1), 230-251.
Yebra, D. M., Kiil, S., & Dam-Johansen, K. (2004). Antifouling technology—past, present and future steps towards efficient and environmentally friendly antifouling coatings. *Progress in Organic Coatings*, 50(2), 75-104.
Yoshizaki, H. T. Y. (2009). Scatter search for a real-life heterogeneous fleet vehicle routing problem with time windows and split deliveries in Brazil. *European Journal of Operational Research*, 199(3), 750-758.
Zhong, X., Dong, J., Liu, M., Meng, R., Li, S., & Pan, X. (2022). Experimental study on ship fouling cleaning by ultrasonic-enhanced submerged cavitation jet: A preliminary study. *Ocean Engineering*, 258, 111844.
Zhu, L., & Xing, W. (2021). Policy-oriented analysis on the navigational rights of unmanned merchant ships. *Maritime Policy & Management*, 49(3), 447-462.
Zhu, M., Shen, S., & Shi, W. (2023). Carbon emission allowance allocation based on a bi-level multi-objective model in maritime shipping. *Ocean & Coastal Management*, 241, 106665.
Zhuge, D., Wang, S., Zhen, L., & Laporte, G. (2021). Subsidy design in a vessel speed reduction incentive program under government policies. *Naval Research*

Logistics, 68(3), 344-358.

Ziajka-Poznańska, E., & Montewka, J. (2021). Costs and benefits of autonomous shipping—a literature review. *Applied Sciences*, 11(10), 4553.

Ziar, E., Seifbarghy, M., Bashiri, M., & Tjahjono, B. (2023). An efficient environmentally friendly transportation network design via dry ports: a bi-level programming approach. *Annals of Operations Research*, 322(2), 1143-1166.

Zolich, A., Palma, D., Kansanen, K., Fjørtoft, K., Sousa, J., Johansson, K.H., Jiang, Y., Dong, H. (2018). Survey on communication and networks for autonomous marine systems. *Journal of Intelligent & Robotic Systems*, 95, 789-813.

Appendices

Appendix A: Generating feasible routes in Chapter 2

Label setting algorithm is a common approach used to solve minimum-cost network flow problems. The efficiency of label setting in this research is mainly affected by two main factors. The first is the number of ports. The second is two types of constraints used during sequence and route generation process, namely the ship type constraint and the duration constraint. To speed up the computation process, we first group feeder ports by vessel type. Each port p can be visited by a ship in ship type set V_p. For each vessel type $v \in V$, we have a set of feeder ports $P_v = \{1, \dots, |P_v|\}$, where $v \in V_p, \forall p \in P_v$. This grouping procedure has two main benefits. First, it can make the number of ports in each group less than total number of ports, hence reducing the computation time. Second, it eliminates the procedure to judge whether ship type constraint is satisfied.

We define a forward path $f_v = (0, i_1, \dots, i_n)$ for each vessel type v, which is a sequence or part of a sequence. It starts at the hub port p_0 (denoted by 0), visits a set of feeder ports $P^{f_v} = \{i_1, \dots, i_{n-1}\} \subseteq P_v$, and ends at port $i_n \in \{0\} \cup P_v \backslash P^{f_v}$. If it ends at port $\{0\}$, it is a complete sequence, otherwise it is part of a sequence. We associate a label $L^{f_v} = (P^{f_v}, i_n, T^{f_v})$ with each path $f_v = (0, i_1, \dots, i_n)$, where P^{f_v} is the set of feeder ports that this path has already visited, i_n is the last port of the path, T^{f_v} is the duration of the path, including the sailing time and the dwell time. Because of duration constraints, a label is feasible only if $T^{f_v} \leq \alpha$. Clearly, each feasible path $f_v = (0, i_1, \dots, i_n)$, where $i_n = 0$ corresponds to a feasible sequence. To generate a feasible sequence set, we initialize a label with $P_v^f = \emptyset$, $i_n = 0$, $T^{f_v} = 0$. This means that this path has just started from the hub port. In the first extension, the path must visit a feeder port $i_n' \in P_v$. In the next extensions, it can either visit a feeder port $i_n' \in P_v$ or back to hub port $i_n' = 0$. For the sake of clarity, we explain the first and next iterations separately as follows:

First iteration: Let $L^{f_v'}$ represents the label generated by extending L^{f_v} with $i_n' \in P_v$. It is constructed as follows:

- $P^{f_v'} = P^{f_v} \cup \{i_n'\}$;

- $T^{f_v'} = T^{f_v} + t_{i_n} + t_{i_n,i_n'}$;

where t_{i_n} is the dwell time at port i_n, $t_{i_n,i_n'}$ is the travel time from port i_n to port i_n'.

Next iterations:

(1) If $i_n' \in P_v \backslash P^{f_v}$, the label $L^{f_v'}$ is constructed the same as the first iteration.

(2) If $i_n' = 0$, the label $L^{f_v'}$ is constructed as follows:

- $P^{f_v'} = P^{f_v}$;
- $T^{f_v'} = T^{f_v} + t_{i_n} + t_{i_n,0}$.

To speed up the solution process and reduce the number of labels generated, the following dominance rule can be applied. Given two labels $L^{f_v^1} = \left(P^{f_v^1}, i_n^1, T^{f_v^1}\right)$ and $L^{f_v^2} = \left(P^{f_v^2}, i_n^2, T^{f_v^2}\right)$, $L^{f_v^1}$ dominates $L^{f_v^2}$ if (i) $P^{f_v^1} = P^{f_v^2}$, (ii) $i_n^1 = i_n^2$, (iii) $T^{f_v^1} < T^{f_v^2}$.

Proof: If relations (i)–(iii) hold for $L^{f_v^1}$ and $L^{f_v^2}$, then for any port $i_n' \in P_v \backslash P^{f_v^2}$ such that $L^{f_v^2}$ can be extended toward i_n' to form a feasible label $L^{f_v^{2'}} = \left(P^{f_v^{2'}}, i_n', T^{f_v^{2'}}\right)$, $L^{f_v^1}$ can be extended toward j to form a feasible label $L^{f_v^{1'}} = \left(P^{f_v^{1'}}, i_n', T^{f_v^{1'}}\right)$ with relations (i)–(iii) still holding for $L^{f_v^{1'}}$ and $L^{f_v^{2'}}$.

Thus, by applying the above argument repeatedly until $i_n' = 0$, $L^{f_v^2}$ can be extended toward $i_n' = 0$ to form a feasible label $L^{f_v^{2'}} = \left(P^{f_v^{2'}}, 0, T^{f_v^{2'}}\right)$, $L^{f_v^1}$ can be extended toward $i_n' = 0$ to form a feasible label $L^{f_v^{1'}} = \left(P^{f_v^{1'}}, 0, T^{f_v^{1'}}\right)$ with relations (i)–(iii) still holding for $L^{f_v^{1'}}$ and $L^{f_v^{2'}}$.

Since $i_n' = 0$, both $L^{f_v^{1'}}$ and $L^{f_v^{2'}}$ are feasible and complete labels and feasible sequences. We can conclude that for every feasible and complete label $L^{f_v^{2'}}$ extending from $L^{f_v^2}$, there exists a feasible and complete label $L^{f_v^{1'}}$ extending from $L^{f_v^1}$ that has an equal or smaller duration. Therefore, $L^{f_v^1}$ dominates $L^{f_v^2}$.

The dominance rule can delete dominated subsequences and sequences during sequence generating process, which improves solution efficiency. Using a label setting algorithm augmented by dominance rules, we obtain all feasible sequences for each

vessel type $v \in V$. We then use sequences of the same vessel type as an input to the dynamic programming model in order to generate feasible routes. Finally, we obtain all feasible routes.

Appendix B: Proof that SP is feasible and bounded in Chapter 2

It is easy to show that $y_s^p(\omega) = 0, \forall p \in P_s, s \in S, \omega \in \Omega$ is feasible solution regardless of first-stage solution $\boldsymbol{x}$, which proves the feasibility. We construct two expressions $\sum_{s\in S}\sum_{p\in P_s}(F_p - C_p^h)D^p(\omega)$ and $\frac{1}{|\Omega|}\sum_{\omega\in\Omega}\sum_{p\in P}(F_p - C_p^h)D^p(\omega)$, which are the maximum value that SP (13) and (15) can achieve, respectively. This proves the boundness.

Appendix C: Proof of Proposition 1 in Chapter 2

Proof. Given a feasible solution $\boldsymbol{x}'$ and $\boldsymbol{y}'$ and the optimal solution $\boldsymbol{x}^*$ and $\boldsymbol{y}^*$ of $\boldsymbol{P}$, and a feasible dual solution $\boldsymbol{\omega}$ of the linear relaxation of $\boldsymbol{P}$, we deduct:

$$z(\boldsymbol{P}) = \sum_{i=1}^{n_1} c_i x_i^* + \sum_{j=1}^{n_2} d_j y_j^* \quad (1)$$

$$z(\boldsymbol{P}) \leq \sum_{i=1}^{n_1} c_i x_i^* + \sum_{j=1}^{n_2} d_j y_j^* + \boldsymbol{\omega}\left(\boldsymbol{h} - \sum_{i=1}^{n_1} a_i x_i^* - \sum_{j=1}^{n_2} b_j y_j^*\right) \quad (2)$$

$$z(\boldsymbol{P}) \leq \sum_{i=1}^{n_1} (c_i - \boldsymbol{\omega} a_i) x_i^* + \sum_{j=1}^{n_2} (d_j - \boldsymbol{\omega} b_j) y_j^* + \boldsymbol{\omega h}, \quad (3)$$

where a_i (resp. b_j) is the i^{th} (resp. j^{th}) column coefficient vector of matrix $\boldsymbol{A}$ (resp. $\boldsymbol{B}$) and c_i (resp. d_j) is the i^{th} (resp. j^{th}) coefficient of vector $\boldsymbol{c}$ (resp. $\boldsymbol{d}$). Since $\boldsymbol{\omega}$ is a feasible dual solution, we have $d_j - \boldsymbol{\omega} b_j \leq 0$ for all $j \in \{1, \dots, n_2\}$. Therefore,

$$z(\boldsymbol{P}) \leq \sum_{i=1}^{n_1} (c_i - \boldsymbol{\omega} a_i) x_i^* + \boldsymbol{\omega h} \quad (4)$$

after transformation, and we have $(c_i - \boldsymbol{\omega} a_i) x_i^* \geq \sum_{i=1}^{n_1} (c_i - \boldsymbol{\omega} a_i) x_i^* \geq z(\boldsymbol{P}) - \boldsymbol{\omega h}$ for all $i \in \{1, \dots, n_1\}$. Since $z(\boldsymbol{P}) \geq \boldsymbol{c x'} + \boldsymbol{d y'}$, it holds that $(c_i - \boldsymbol{\omega} a_i) x_i^* \geq \boldsymbol{c x'} + \boldsymbol{d y'} - \boldsymbol{\omega h}$ for all $i \in \{1, \dots, n_1\}$, which completes the proof.